

WAR 17150



RESEARCH MEMORANDUM

AIR-FLOW AND THRUST CHARACTERISTICS OF SEVERAL CYLINDRICAL
COOLING-AIR EJECTORS WITH A PRIMARY TO SECONDARY
TEMPERATURE RATIO OF 1.0

By W. K. Greathouse and D. P. Hollister

Lewis Flight Propulsion Laboratory
Cleveland, Ohio

CLASSIFICATION CHANGED

UNCLASSIFIED

To

By authority of *NASA PA 3* Date *10-31-58*
1-7-59 NBS

CLASSIFIED DOCUMENT

This material contains information affecting the National Defense of the United States within the meaning of the espionage laws, Title 18, U.S.C., Secs. 793 and 794, the transmission or revelation of which in any manner to an unauthorized person is prohibited by law.

**NATIONAL ADVISORY COMMITTEE
FOR AERONAUTICS**

WASHINGTON

March 6, 1953

NACA LIBRARY

CONFIDENTIAL

ERRATA

NACA RM E52L24

By W. K. Greathouse and D. P. Hollister

March 1953

It has been recently ascertained that, whereas the pumping characteristics data of this report appear to be reliable (accurate to ± 1.0 percent), the thrust coefficient data may be in error by as much as 7.0 percent. In general, the excessive inaccuracies occur for all data at primary pressure (P_p/p_0) ratios below about 2.30 or 2.50 and for most data obtained at secondary pressure ratios (P_s/p_0) of 3.0 and 4.0. A summary of the findings is included in the accompanying table.

If the cylindrical ejector thrust performance for any of the conditions listed in the table is desired, it may be computed from the pumping characteristics given in the report (as previously mentioned, they are accurate to within ± 1.0 percent). This calculation is made by summing up the total momentum ($MV + pA$) of the primary and secondary streams in the plane of the primary-nozzle exit and assuming that the total momentum at the exit of the secondary shroud is equal to this sum. The jet (or gross thrust is then computed from the total momentum as follows:

$$F_j = 0.997 \left\{ (M_p V_p + p_p A_p) + [M_s V_s + p_s (A_s - A_p)] - p_0 A_s \right\}$$

where

A cross-sectional area

M mass flow

p static pressure

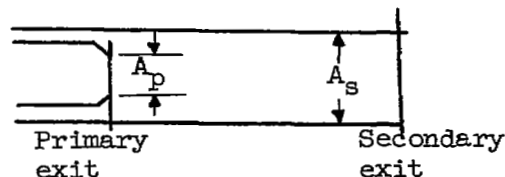
V velocity

and subscripts:

O ambient

p primary

s secondary



ESTIMATE OF ACCURACY OF THRUST DATA

[In general, the thrust data presented in RM ES2L24 are estimated to be accurate to ± 2.0 percent except for the conditions noted herein.]

Configuration		Primary pressure ratio below which scatter is excessive, P_p/P_0	Secondary pressure ratio for which thrust coefficient is more than 2 percent too high, P_s/P_0	Amount thrust coefficient is too high, percent	Remarks regarding remainder of data
Shroud diameter ratio, D_s/D_p	Spacing ratio, L/D_p				
1.06	0.19	2.5	3.0 ^a , 4.0 ^a	2.0 to 4.0	} Level of data correct
	.40	2.3	3.0 ^a , 4.0 ^a and points between $P_p/P_0 = 4.5$ and 5.5 for 2.0	2.0 to 4.0	
	.59	2.5	3.0 ^a , 4.0 ^a	2.0 to 4.0	
	.78	2.3	3.0 ^a , 4.0 ^a	2.0 to 5.0	
1.11	0.41	2.3	3.0 ^a , 4.0 ^a	2.0 to 5.0	Level of data correct
	.81	2.3	2.0, 3.0 ^a , 4.0 ^a	2.0 to 7.0	Level of data appears 1.0 percent high
	1.22	2.3	3.0 ^a , 4.0 ^a and points below $P_p/P_0 = 4.0$ for 2.0	2.0 to 5.0	Level correct
	1.65	2.5	3.0 ^a , 4.0 ^a	1.0 to 6.0	Level correct
1.21	0.38	2.5	3.0 ^a , 4.0 ^a	3.0 to 7.0	} Level appears 1.5 percent too high Level correct
	.80	2.5	3.0 ^a , 4.0 ^a	2.0 to 7.0	
	1.20	2.5	3.0 ^a , 4.0 ^a and points below $P_p/P_0 = 4.0$ for 2.0	2.0 to 4.0	
	1.60	2.3	2.0, 3.0 ^a , 4.0 ^a	2.0 to 4.0	
1.41	0.42	2.5	All ratios	-2.0	} Level appears 2.0 percent too low Level appears 3.0 percent too low Level correct
	.85	2.5	} $W_a = 0$ below P_p/P_s = 5.0 (too low)	-2.0 to -4.0	
	1.22	2.5		-2.0 to -4.0	
	1.59	4.0	-----	-----	

^aMaximum error at P_s/P_0 of 3.0 and 4.0 occurs at P_p/P_0 of about 4.0 and decreases to minimum indicated in fifth column at P_p/P_0 of 10.0.

UNCLASSIFIED

W
NACA RM E52L24

NATIONAL ADVISORY COMMITTEE FOR AERONAUTICS

3 1176 01359 5369

RESEARCH MEMORANDUM

AIR-FLOW AND THRUST CHARACTERISTICS OF SEVERAL CYLINDRICAL
COOLING-AIR EJECTORS WITH A PRIMARY TO SECONDARY
TEMPERATURE RATIO OF 1.0

By W. K. Greathouse and D. P. Hollister

SUMMARY

2799
An investigation was made to determine the performance of 17 cooling-air ejectors operating at primary-jet pressure ratios from 1 to 10, secondary pressure ratios to 4.0, and a temperature ratio of unity. This phase of the investigation was limited to cylindrical ejectors having shroud-exit to primary-nozzle-exit diameter ratios of 1.06, 1.11, 1.21, and 1.41 with several spacing ratios for each.

Ejector thrust and pumping characteristics were strongly influenced by variation in diameter ratio, and thus it would be desirable to control the shroud diameter of an ejector used in conjunction with a variable-area exhaust nozzle. At high primary pressure ratios, the amount of pumping for the small diameter-ratio ejector was practically independent of spacing ratio. Maximum variation in ejector gross thrust with spacing ratio was less than 6 percent for any diameter-ratio ejector operating at constant primary and secondary pressure ratios. Maximum pumping and maximum thrust occurred at slightly different spacing ratios for the small diameter-ratio ejectors, and thus indicated that maximum thrust and maximum pumping could not both be realized at take-off conditions with a small diameter-ratio ejector of fixed spacing ratio. The results show that if sufficient cooling air were supplied to maintain secondary pressure ratios above 1.0, a cylindrical ejector would produce a greater gross thrust over a range of flight conditions than would the convergent primary nozzle alone. Comparison of cylindrical and conical ejector characteristics showed that the cylindrical ejector pumped secondary-air flow over a wider range of operating primary pressure ratios and generally attained thrust values equal to or slightly higher than those of a conical ejector having the same diameter ratio, spacing ratio, and secondary pressure ratio.

INTRODUCTION

The air ejector is currently being used to pump afterburner and tail-pipe cooling air for turbojet-engine installations. Increased

UNCLASSIFIED

flight speed, and improved engine performance have expanded the range of conditions over which an ejector must operate. Emphasis on thrust has required that the cooling air be supplied with a minimum loss or, if possible, a gain in thrust over that of a bare engine. It is therefore necessary to have both thrust and pumping performance of many ejector configurations operating over a wide range of conditions in order to select the proper ejector. Two basic types of ejector, one having a conical shroud and the other a cylindrical shroud, have been the subject of numerous investigations, but the information available on cylindrical ejectors generally is limited to a low range of pressure ratios or does not include adequate thrust data. The pumping and thrust characteristics of conical ejectors are presented in references 1 and 2 for operational pressure ratios simulating flight conditions up to a Mach number of about 2.0. Reference 3 presents pumping characteristics of small model cylindrical ejectors but does not include thrust data. Both thrust and pumping performance of three full-scale cylindrical ejector configurations are reported in reference 4 over a limited range of operating conditions.

In order to extend the range of existing cooling-air-flow and thrust performance data, the NACA Lewis laboratory is conducting an experimental investigation of cooling-air ejectors. This report presents experimental data for several cylindrical-ejector configurations operating over a wide range of simulated flight conditions, and points out the performance differences between a cylindrical and a conical ejector. Also a limited comparison is made between ejector characteristics of this investigation and those previously reported in references 3 and 4.

Thrust and pumping characteristics over a range of primary pressure ratios P_p/p_0 from 1 to 10 and secondary pressure ratios P_s/p_0 to 4.0 are presented for cylindrical ejectors having diameter ratios D_s/D_p of 1.06, 1.11, 1.21, and 1.41 with several spacing ratios L/D_p for each. Data are in terms of secondary to primary weight-flow ratio and gross ejector thrust to gross primary-nozzle thrust ratio. The investigation was conducted with a convergent primary nozzle surrounded by a shroud having a cylindrical mixing section. Dry air (-20°F dew point) at a temperature of approximately 80°F was used for both the primary and secondary flows.

APPARATUS

Nomenclature used for the cylindrical ejector investigation is listed in figure 1, and the apparatus is schematically shown in figure 2. The ejector setup was the same as that for references 1 and 2, except that, of course, the ejector models and ejector instrumentation were different. The ejector consisted of a convergent primary-jet nozzle within a concentric shroud that had a cylindrical mixing section, all

of which extended into an exhaust chamber connected to the laboratory exhaust system. Primary- and secondary-air flows were introduced into concentric pipes and passed through the ejector into the exhaust chamber. The capacity of the system was such that the total pressure could be varied to a maximum of 72 inches of mercury absolute for the primary air and to 56 inches for the secondary air, while the exhaust pressure could be reduced from atmospheric to 4 inches of mercury absolute. The air was passed through a drier and supplied at 80° F with a water content of 2 grains of moisture per pound of dry air.

Primary- and secondary-air flows were measured by means of standard A.S.M.E. sharp-edged orifices. Total pressures and temperatures were measured by total-pressure tubes and iron-constantan thermocouples.

Primary pressure and temperature measuring stations were $17\frac{1}{4}$ inches and $4\frac{3}{4}$ inches, respectively, upstream of the primary-nozzle exit. For the secondary system, the pressure and temperature measuring stations were both located $4\frac{1}{2}$ inches upstream of the primary-nozzle exit, except for the 1.06-diameter-ratio ejector, which also had total-pressure tubes that measured the secondary pressure at the entrance of the cylindrical mixing section. Exhaust pressure was measured by static-pressure taps located on the outside of the shroud-exit lip. The net axial force acting on the ejector ducts was transmitted to a balanced-pressure-diaphragm, null-type thrust-measuring cell, which produced an output pressure directly proportional to the applied force. The ejector ducts were connected to the laboratory air system by flexible diaphragms and pivoted to a steel frame in a pendulum-type arrangement. A counterweight was connected to the ejector rig by large pulleys and steel tapes, so that an axial preload force could be applied to the thrust cell. The labyrinth seal between the ejector ducts and exhaust chamber had adequate clearance to prevent metal-to-metal contact.

The primary nozzle had a half-cone angle of 8°, an exit diameter of 4 inches, and a 5-inch-inside-diameter approach pipe. The shroud consisted of a cylindrical mixing section attached to a conical approach passage. An angle of approximately 45° was maintained between the ejector axis and a line through the perimeter of the primary-nozzle exit and the entrance to the cylindrical mixing section.

PROCEDURE

Performance of each ejector configuration was investigated over a range of primary pressure ratios from 1 to about 10 with various constant secondary pressure ratios up to 4.00. Additional tests were performed for zero secondary-air flow with the upstream secondary-flow passage blocked. Also, a calibration of the primary nozzle with the shroud removed was made to determine flow coefficients and primary-nozzle thrust over the range of primary pressure ratios.

Four shrouds of different diameters were used to provide diameter ratios of 1.06, 1.11, 1.21, and 1.41. The spacing ratio was varied as shown in the following table by cutting off portions of the cylindrical shroud:

Diameter ratio, D_s/D_p	Spacing ratio, L/D_p						
	0.19	0.40	0.59	0.78	0.98	----	----
1.06	0.19	0.40	0.59	0.78	0.98	----	----
1.11	----	.41	----	.81	----	1.22	1.65
1.21	----	.385	----	.796	----	1.20	1.60
1.41	----	.418	----	.855	----	1.22	1.59

The axial force transmitted to the thrust cell was composed of (1) the ejector-thrust force, (2) the axial preload force, and (3) the labyrinth-seal forces acting on the ejector ducts. The labyrinth-seal forces were determined by calibration over the range of exhaust pressures. The preload was kept at a value such that the net force on the thrust cell was always in the same direction. The ejector thrust was obtained by subtracting the force acting on the thrust cell from the sum of the preload and labyrinth-seal forces. In order to assure accurate and consistent thrust data, the labyrinth-seal-force calibration was checked daily throughout the investigation.

RESULTS AND DISCUSSION

Performance of a cooling-air ejector for turbojet-engine installations can be evaluated in terms of the ability of the ejector to pump air and of the effect it has upon thrust. These performance parameters are affected by both design and operational variables. Principal design variables are diameter ratio D_s/D_p and mixing length L , while principal operational variables are primary pressure ratio P_p/p_0 and secondary pressure ratio P_s/p_0 . Nozzle and shroud convergence angles, cooling-air-passage size in the plane of the jet-nozzle exit, and variations in configuration due to use of a variable nozzle producing only moderate changes in flow passages would be expected to have only a second-order effect on ejector performance.

Performance of the primary-jet nozzle without the ejector shroud is shown in figure 3 for the range of pressure ratios investigated. Primary-nozzle thrust can be calculated by using presented values of the thrust coefficient so that a numerical value of ejector thrust can in turn be computed.

Pumping Characteristics

The effect of primary pressure ratio on secondary pressure ratio with no secondary flow is presented in figure 4 in order to indicate operational limits of the cylindrical ejectors investigated. The ejector will pump a secondary-air flow at any combination of primary and secondary pressure ratios that lies above the corresponding zero secondary-flow curve. For example, if the available secondary pressure ratio from ram scoops, boundary-layer scoops, and so forth, were 1.20 at a particular flight Mach number, the ejector with a spacing ratio L/D_p of 0.19 (fig. 4(a)) could pump a secondary-air flow only up to a primary pressure ratio of 6.0 (the cut-off point). Operation beyond this point would result in a backflow from the primary-jet stream into the secondary system.

Ejectors do not normally operate at zero secondary flow, but it is nevertheless helpful in gaining an understanding of ejector performance characteristics to note the flow phenomenon at such a condition. Typical ejector characteristics with no secondary flow (fig. 4(a), $L/D_p = 0.19$) show a reduction in secondary pressure ratio to a minimum as primary pressure ratio is increased, and a linear relation between the two ratios beyond this minimum region. The reduction in secondary pressure ratio down to point A resulted from the shearing forces between the subsonic primary jet and the relatively still air in the shroud. At point A the primary jet expanded sufficiently to fill the exit area of the secondary shroud, and thus the secondary pressure ratio became a function of the primary-jet velocity, the primary-jet static pressure, and the amount of turbulence set up in the secondary passage. From A to B the ejector acted as a convergent-divergent nozzle, in that the flow became supersonic after leaving the primary nozzle and through a shock system was reduced to subsonic conditions so that it emerged from the shroud exit at exhaust pressure. The secondary pressure was, of course, subject to conditions upstream of the shock and thus dropped to the low value at B. Beyond B, a stable supersonic flow was maintained upstream of the shock system (as in the case of a convergent-divergent nozzle) and the secondary pressure became a linear function of the primary total pressure as shown from B to C.

Cylindrical-ejector characteristics with zero secondary flow are changed considerably by changes in both diameter ratio and spacing ratio, as indicated in figure 4. For a given diameter ratio, ejector characteristics became practically independent of spacing ratio for the higher spacing-ratio configurations, because the jet apparently filled the shroud of each long ejector at practically the same primary pressure ratio and distance downstream of the jet nozzle. Thus, any increase in shroud length beyond that for which the shroud was filled had only moderate effect (such as frictional losses) on ejector performance with zero secondary flow. At low spacing ratios, however, ejector characteristics changed greatly with spacing ratio, because a different value of

[REDACTED]

primary pressure ratio (different expansion angle of primary jet) was required to fill the exit area of each shroud length. For ejectors having long shrouds for which the effect of spacing ratio was small, the performance with zero secondary flow showed a marked change with a change in diameter ratio. As shown by comparison of figures 4(a) to 4(d), the linear portions of the curves at 0.80 spacing ratio have less slope for the larger diameter ratios. The reason for this effect may be surmised directly from the fact that a larger diameter ratio permits the primary jet to expand to a higher Mach number and thus results in a lower pressure in the secondary passage for a given primary pressure ratio.

The largest diameter ratio investigated, $D_s/D_p = 1.41$, exhibited a hysteresis effect, as indicated by dashed lines in figure 4(d). The primary jet "popped out" to fill the ejector shroud at a specific value of increasing primary pressure ratio; while for a decreasing primary pressure ratio the jet had a tendency to remain attached to the shroud even at lower values of primary pressure ratio, and thus hysteresis was produced. Hysteresis is not uncommon for large diameter-ratio ejectors and is reported in reference 3.

Profiles of static pressure along the shroud wall of a cylindrical ejector having a long spacing ratio are shown in figure 5 for zero secondary-flow conditions. For values of primary pressure ratio above 2.0, the pressure profile upstream of the shock system remained unchanged because of stable supersonic flow ahead of the shock. Location of the shock front (represented by dashed lines) moved downstream as primary pressure ratio was increased, but the region at which the primary jet impinged on the shroud wall (between stations 3 and 5) remained the same. At the primary pressure ratio of 7.696, internal shock was no longer present, and the expansion to exhaust pressure occurred after the flow was discharged from the shroud exit, as in the case of an underexpanded convergent-divergent nozzle.

The pumping characteristics with secondary flow in figures 6 to 9 show the effect of primary pressure ratio on ejector weight-flow ratio for several constant values of secondary pressure ratio. The same general trends are exhibited for all configurations investigated; but, of course, the weight-flow-ratio values varied in magnitude with each ejector. For secondary pressure ratios less than 1.0, weight-flow ratio increased with primary pressure ratio to a maximum and then decreased to zero; while for secondary pressure ratios greater than 1.0, the weight-flow ratio progressively decreased to zero as primary pressure ratio was raised. It should be noted that the largest diameter-ratio ejector (fig. 9) pumped a very large quantity of air as compared with the smallest diameter-ratio ejector (fig. 6) at the same operating conditions. This characteristic is in direct contrast to those desirable for an after-burner installation equipped with a variable-area primary nozzle and fixed ejector shroud in that either an excess cooling-air flow would

occur for the nonafterburning condition (nozzle closed, large diameter ratio) or insufficient cooling air would be pumped for the afterburning condition (nozzle open, small diameter ratio). Some current conical-ejector installations are being designed with a variable-area ejector shroud linked to the variable-area primary nozzle in such a manner as to control the diameter ratio of the ejector shroud as primary-nozzle area is varied.

2799 The static-pressure profile along the shroud wall of a cylindrical ejector operating at a weight-flow ratio of approximately 0.03 is shown in figure 10. At low pumping pressure ratios (curves a, b, and c), the secondary stream was entrained by and mixed with the subsonic primary stream, with the result that both streams were diffused to exhaust pressure at the shroud exit. The mixing at these conditions must have been nearly complete, because the secondary air was moved from a region of low pressure to a region of higher pressure, that is, secondary pressure ratios less than 1.0. Also, the shapes of the three curves (a to c) appear to be the same as those for zero secondary flow and low primary pressure ratios in figure 5. The curves marked d indicate that the secondary stream was accelerated by the primary jet and that a shock system (represented by dashed lines) occurred near the exit of the shroud. The static-pressure profile upstream of the shock became independent of primary pressure ratio for the constant weight-flow ratio of 0.03 (fig. 10), as did the pressure profile for zero secondary flow in figure 5.

Effect of Spacing Ratio on Pumping

Effects of spacing ratio on pumping characteristics of the various ejectors are shown in figures 11 to 14. The plots represent the variation of weight-flow ratio with spacing ratio for ejectors operating with constant primary pressure ratio, constant secondary pressure ratio, and a fixed diameter ratio. All four diameter-ratio ejectors indicated a larger variation in weight-flow ratio at low values of primary pressure ratio than at higher values. For supersonic flight conditions ($P_p/P_0 = 6.0$ and 9.0), the amount of ejector pumping was almost independent of spacing ratio for the two smaller diameter-ratio ejectors ($D_s/D_p = 1.06$ and 1.11) investigated; but for the larger ejectors ($D_s/D_p = 1.21$ and 1.41), the amount of pumping varied considerably with shroud length, especially over the lower range of spacing ratios. At take-off conditions ($P_p/P_0 = 2.0$), however, parts (a) of figures 11 to 14 show that ejector pumping was dependent on spacing ratio. Spacing ratio is therefore indicated to be an important ejector design variable at take-off conditions, although at high flight speeds it may warrant less consideration.

Effect of Diameter Ratio on Pumping

The variation of weight-flow ratio with diameter ratio is shown in figure 15 for the intermediate spacing ratio of 0.80 at selected primary pressure ratios of 2.0, 3.5, and 6.0. Weight-flow ratio continuously increased with diameter ratio for constant values of secondary pressure ratio above 1.0, because a smaller percentage of the shroud-exit area was filled by the primary jet at larger shroud diameters, and thus the restriction to secondary flow was decreased. For secondary pressure ratios less than 1.0, where ejector pumping is dependent upon mixing, the weight-flow ratio maximized (except for fig. 15(c)) as diameter ratio increased to values such that the mixed jet could just fill the exit area of the ejector shroud. For larger diameter ratios, the jet could not completely fill the shroud exit, and thus weight-flow ratio decreased, because an inflow occurred from the exhaust chamber into the relatively low pressure region within the shroud. For the primary pressure ratio of 6.0 (fig. 15(c)), the maximum region appeared to be beyond the range of diameter ratios investigated.

Thrust Characteristics

In order to determine the effect of the ejector shroud on thrust performance, ejector gross thrust was measured simultaneously with the preceding weight-flow data and at zero secondary-flow conditions. The thrust ratio was defined as the ratio of ejector thrust F_{ej} to the previously measured thrust F_j of the convergent primary nozzle without a shroud operating at the same over-all primary pressure ratio. This method, of course, does not charge either stream for inlet momentum of the air flow.

The variation in thrust ratio with over-all primary pressure ratio of the four diameter-ratio ejectors is presented in figures 16 to 19 for several constant secondary pressure ratios and for zero secondary-flow conditions. In general, the thrust-ratio curves at constant secondary pressure ratio meet the zero secondary-flow thrust curve at the same primary pressure ratio for which the weight-flow ratio becomes zero. However, for several ejector configurations having small spacing ratios (figs. 16(a), 17(a), and 18(a)), a few thrust-ratio curves intersected and fell below the zero secondary-flow thrust curve at low values of primary pressure ratio (P_p/p_0 less than 2.0). This effect occurred because at a low pressure ratio across the ejector, the mass flow through the unchoked primary nozzle was dependent upon the pressure existing within the shroud at the primary-nozzle exit. Therefore, the primary nozzle at zero secondary flow and low shroud pressures produced a greater thrust (because of greater mass flow) than was produced with a finite secondary flow, and consequent higher shroud pressures. Fortunately, actual ejector installations are seldom required to operate in this low range of primary pressure ratios.

For the largest diameter ratio investigated ($D_s/D_p = 1.41$), the effect of hysteresis is exhibited by the zero secondary-flow thrust curves of figure 19 and is similar to the effect of hysteresis on secondary pressure ratio in figure 4(d), previously discussed. The low values of thrust ratio obtained with decreasing primary pressure ratio (represented by dashed lines) resulted from overexpansion of the primary jet and the accompanying shock losses in the cylindrical shroud. Hysteresis either did not occur with secondary flow or its effects were negligible, for it could not be detected from performance curves or from operational characteristics of the ejector setup.

Thrust characteristics were similar for all four diameter-ratio ejectors investigated. In general, thrust ratios greater than 1.0 were obtained with secondary pressure ratios above 1.0, and thrust ratios less than 1.0 resulted with secondary pressure ratios below 1.0. The larger diameter-ratio ejectors produced a greater gain in thrust at high secondary pressure ratios and a greater thrust loss at low secondary pressure ratios than did the smaller diameter-ratio ejectors, as may be surmised from the fact that ejector thrust behaves much like that of a convergent-divergent nozzle, and because higher weight-flow ratios are attained with larger diameter-ratio ejectors. The lowest value of thrust ratio for each configuration, of course, occurred at zero secondary-flow conditions (except as previously discussed). Thus, the zero secondary-flow thrust curve indicates the maximum loss (or minimum gain) in gross thrust that can occur for a specific operating primary pressure ratio. When compared with the gross thrust of the convergent primary nozzle, the ejector gross thrust losses with zero secondary flow were as great as 8.5, 14.0, 25.0, and 40.0 percent for the respective diameter ratios of 1.06, 1.11, 1.21, and 1.41.

For an ejector operating with a constant secondary pressure ratio of 1.0, the thrust ratio remained relatively close to the value of 1.0 over a wide range of primary pressure ratios, as shown in figures 16 to 19. Thus, if sufficient cooling air were supplied to a cylindrical-ejector installation to maintain secondary pressure ratios close to 1.0, the ejector would produce practically the same gross thrust over a range of flight conditions as would the convergent primary nozzle. At secondary pressure ratios greater than 1.0, the ejector can, of course, produce considerably more gross thrust than can the primary nozzle alone. In terms of net thrust, the losses and gains in thrust with the ejector discussed previously will be changed by an amount dependent on the inlet momentum of both the engine and the cooling-air flows. The ejector installation is also ordinarily charged with the losses in taking cooling air aboard the aircraft.

As previously stated, the thrust parameters used herein represent gains or losses of ejector gross thrust relative to the gross thrust of

a convergent nozzle. Reference 5, however, presents the thrust of various conical ejectors in terms of nozzle efficiency (ratio of measured thrust to theoretical thrust with isentropic expansion) and indicates that ejectors with optimum diameter and spacing ratios can maintain a relatively high nozzle efficiency (96 to 98 percent) over a wide range of nozzle pressure ratios when operating with secondary to primary weight-flow ratios between 3 and 7 percent.

Effect of Spacing Ratio on Thrust

The variation of gross thrust ratio with spacing ratio is shown in figures 20 to 23 for the four diameter-ratio ejectors investigated. The plots are presented for several constant values of secondary pressure ratio at primary pressure ratios of 2.0, 3.5, 6.0, and 9.0. The maximum variation in thrust ratio at constant secondary pressure ratio was less than 6 percent for any diameter-ratio ejector over the range of spacing ratios investigated and conditions presented. A larger change in thrust ratio occurred at the primary pressure ratio of 2.0 (as was the case for weight-flow ratio) than at the higher primary pressure ratios. Comparison of thrust and weight-flow variation with spacing ratio at the primary pressure ratio of 2.0 [figs. 20(a) and 21(a) compared with figs. 11(a) and 12(a), respectively] indicates that regions of maximum thrust occurred at smaller spacing ratios than did regions of maximum pumping for the two smaller diameter-ratio ejectors ($D_s/D_p = 1.06$ and 1.11) investigated. Consequently, at take-off conditions a small diameter-ratio cylindrical ejector of fixed spacing ratio can produce maximum thrust only with some sacrifice in pumping (or vice versa). Regions of maximum thrust and maximum pumping for the two larger diameter-ratio ejectors were not defined over the range of spacing ratios investigated, although the trends were similar to those of the smaller diameter-ratio ejectors.

Effect of Diameter Ratio on Thrust

Gross ejector thrust ratio is presented as a function of diameter ratio in figure 24 for several constant values of primary pressure ratio and secondary pressure at the intermediate spacing ratio of 0.80. These curves exhibit thrust characteristics similar to the pumping characteristics previously described and shown in figure 15. The continuous rise in thrust ratio with increasing diameter ratio for high values of secondary pressure ratio is a result of both the greater mass flow through the ejector and the greater expansion ratio. For low values of secondary pressure ratio the thrust ratio decreased with an increase in diameter ratio (fig. 24(b)), even though the total mass flow through the ejector (see fig. 15(b)) was in some cases increasing. The decrease in thrust ratio must have resulted from overexpansion of the primary stream at the pressure ratios encountered.

Comparison of Cylindrical and Conical Ejectors

Comparison of cylindrical and conical ejectors can be made by direct comparison of these data with those of references 1 and 2. Two such comparisons are made in figures 25 and 26 for ejectors having approximately the same diameter ratio or spacing ratio. A desirable characteristic of the cylindrical ejector is its ability to pump over a wider operating range of primary pressure ratios than that of a conical ejector at a specific secondary pressure ratio. In general, it may be said that a cylindrical ejector will produce equal or better thrust than a conical ejector of comparable diameter and spacing ratios. At some operating conditions the cylindrical ejector attained a greater thrust ratio, even though it was pumping less secondary-air flow than the conical ejector. As an example, at a primary pressure ratio of 5.0 and a secondary pressure ratio of 2.0, the cylindrical ejector of figure 25 had a thrust ratio of 1.060 and a weight-flow ratio of 0.04, while the conical ejector had a thrust ratio of 1.035 and a weight-flow ratio of 0.06. Because thrust is a function of total mass flow and velocity at the shroud exit, the larger thrust produced by the cylindrical ejector can be logically attributed to a higher average discharge velocity. Therefore, the flow process through the cylindrical-ejector mixing section must produce weaker shock losses and more nearly approach an isentropic expansion than the flow through a conical-ejector mixing section. It is therefore, desirable, with respect to thrust, to use cylindrical ejectors whenever possible.

Comparison of Performance with Small Model Ejectors

Performance data of small model cylindrical ejectors from reference 3 are presented along with performance data from the present investigation in figure 27(a), which compares ejectors having approximately the same diameter ratios, and in figure 27(b), which compares ejectors having about the same spacing ratio. The ejectors of reference 3 had a 1.40-inch-diameter cylindrical shroud with changeable primary nozzles as compared with the ejectors of the present investigation, which had a 4.0-inch-diameter primary nozzle with changeable cylindrical shrouds. Ejectors of the present investigation served as a better pump than those of reference 3, in that a lower secondary pressure ratio was needed for the present ejectors to pump a given weight-flow ratio at the same primary pressure ratio (fig. 27). For a specific diameter ratio, the difference between performance curves of the two ejector investigations (fig. 27(a)) was of the same order for either zero secondary flow

$$\left(\frac{W_S}{W_P} \sqrt{\frac{T_S}{T_P}} = 0 \right) \text{ or for constant weight-flow ratio } \left(\frac{W_S}{W_P} \sqrt{\frac{T_S}{T_P}} = 0.083 \right).$$

However, the difference between comparable performance curves of figure 27(b) was less for the larger diameter ratios than for the small

diameter ratios. Figure 27(b) also shows that the 1.20-diameter-ratio ejectors of reference 3 performed much like the 1.11-diameter-ratio ejector of the present investigation.

The reason for the differences in data from the two investigations is not apparent but could possibly be the effect of (1) boundary-layer or scale effects, (2) the primary-jet velocity profile, or (3) the humidity of the air supply. Atmospheric air was used in the ejectors of reference 3, and dry air (-20° F dew point) was used in the present investigation. The effect of humidity (ref. 6) is such that the data from the two investigations would tend to agree more closely if the air supplies had been of the same moisture content.

Comparison of Performance with Full-Scale Installation

The performance of two full-size cylindrical ejectors is compared with that of model cylindrical ejectors of this investigation in figure 28. The dashed lines are full-scale data as cross-plotted from reference 4 with no correction for gas temperature, and the solid lines represent the same data multiplied by a temperature-ratio correction

factor $\left(\sqrt{\frac{T_s}{T_p}}\right)$ in an attempt to generalize the weight-flow parameter.

The model-ejector performance curves have about the same shape and magnitude as the full-scale corrected curves but occur over a higher range of primary pressure ratios. It should be noted that the full-scale ejectors employed a variable-area clam-shell primary nozzle which had a noncircular and nonplanar exit. Because of this exit configuration, the diameter and spacing ratios of the full-scale ejectors were not explicitly defined, and thus a geometric dissimilarity existed between the models and the full-scale ejectors. Also, the velocity distribution and temperature gradient of the primary jet were undoubtedly quite different for the two investigations. The comparison indicates the desirability of more extensive ejector tests (with model and full-scale similarity) to determine the exact cause of discrepancies among such data.

Application of Data

The data and comparisons contained herein are based on experimental results of model ejectors as determined with an unheated primary jet. As pointed out in reference 1, a final choice of ejector geometry must be based on the cooling-air supply-duct characteristics and the flight plan of a specific aircraft after the model-ejector performance parameters are considered in terms of a full-size ejector operating hot. Reference 4 shows that a full-scale ejector with a hot primary jet had a greater weight-flow ratio than that which is indicated for a cold model ejector. The ejector pumping data herein are thus conservative.

2700

The weight-flow parameter of model ejector $\frac{W_s}{W_p} \sqrt{\frac{T_s}{T_p}}$ may be partially corrected for temperature by multiplying by the square root of primary total to secondary total temperature ratio $\left(\frac{W_s}{W_p} \sqrt{\frac{T_s}{T_p}} \times \sqrt{\frac{T_p}{T_s}} = \frac{W_s}{W_p} \right)$ as described in reference 7. This correction factor is only approximate; until more complete high-temperature data are available, the performance of full-size-ejector installations can only be estimated. It is believed that the effect of temperature on ejector gross thrust ratio is slight.

CONCLUDING REMARKS

The experimental results contained herein showing pumping and thrust characteristics of 17 cylindrical cooling-air ejectors indicate a direct contrast between the cooling-air requirements and pumping characteristics of an afterburner installation having a variable-area jet nozzle and fixed ejector configuration, in that excessive cooling air could result with nonafterburning. Thus, it would be desirable with respect to ejector performance to use also a variable-area ejector shroud, so that cooling-air flow could be regulated to give the best net thrust. However, for some aircraft the weight penalty imposed by a variable ejector may dictate that cooling air be regulated by some other means or not regulated at all.

The amount of ejector pumping was practically independent of spacing ratio for the smaller diameter-ratio ejectors but was changed considerably for the large diameter-ratio ejectors, especially over the low range of spacing ratios. Maximum variation in gross thrust ratio with spacing ratio was less than 6 percent for any diameter-ratio ejector operating at constant secondary pressure ratio over the range of spacing ratios investigated and conditions presented.

Spacing ratio was indicated to be an important design variable at take-off conditions and a secondary consideration at high-speed flight conditions. At take-off conditions the smaller diameter-ratio ejector produced maximum thrust at a smaller spacing ratio than that for maximum pumping. Consequently, a small diameter-ratio ejector with fixed spacing ratio can provide maximum thrust at take-off conditions only with some sacrifice in pumping ability or vice versa.

Comparison of typical cylindrical- and conical-ejector characteristics indicates that it is desirable to use cylindrical ejectors whenever possible, because the cylindrical ejector pumps secondary-air flow over a wider operating range of primary pressure ratios than does a

[REDACTED]

conical ejector having the same diameter ratio, the same spacing ratio, and the same constant secondary pressure ratio. The cylindrical ejector attained thrust ratios that were generally equal to or better than those of the conical ejector. In fact, at some operating conditions the cylindrical ejector produced the greater thrust, even though its total mass flow was less than that of the conical ejector.

A limited amount of experimental data from this investigation was compared with both model cylindrical-ejector data and full-scale cylindrical-ejector data from other investigations. Similar trends were observed for the pumping characteristics, but the values of performance parameters were shifted somewhat with respect to operating pressure ratios. Further ejector tests on both model and full-scale setups are necessary in order to determine whether the discrepancies are the effect of ejector size or operating temperatures. No appreciable effect of temperature on ejector thrust is expected.

Lewis Flight Propulsion Laboratory
National Advisory Committee for Aeronautics
Cleveland, Ohio

REFERENCES

1. Greathouse, W. K., and Hollister, D. P.: Preliminary Air-Flow and Thrust Calibrations of Several Conical Cooling-Air Ejectors with a Primary to Secondary Temperature Ratio of 1.0. I - Diameter Ratios of 1.21 and 1.10. NACA RM E52E21, 1952.
2. Greathouse, W. K., and Hollister, D. P.: Preliminary Air-Flow and Thrust Calibrations of Several Conical Cooling-Air Ejectors with a Primary to Secondary Temperature Ratio of 1.0. II - Diameter Ratios of 1.06 and 1.40. NACA RM E52F26, 1952.
3. Kochendorfer, Fred D., and Rousso, Morris D.: Performance Characteristics of Aircraft Cooling Ejectors Having Short Cylindrical Shrouds. NACA RM E51E01, 1951.
4. Wallner, Lewis E., and Jansen, Emmert T.: Full-Scale Investigation of Cooling Shroud and Ejector Nozzle for a Turbojet Engine - Afterburner Installation. NACA RM E51J04, 1951.
5. Fleming, William A.: Internal Performance of Several Types of Jet-Exit Configuration for Supersonic Turbojet Aircraft. NACA RM E52K04, 1953.

6. Ellis, C. W., Hollister, D. P., and Sargent, A. F., Jr.: Preliminary Investigation of Cooling-Air Ejector Performance at Pressure Ratios from 1 to 10. NACA RM E51H21, 1951.
7. Wilsted, H. D., Huddleston, S. C., and Ellis, C. W.: Effect of Temperature on Performance of Several Ejector Configurations. ✓
NACA RM E9E16, 1949.

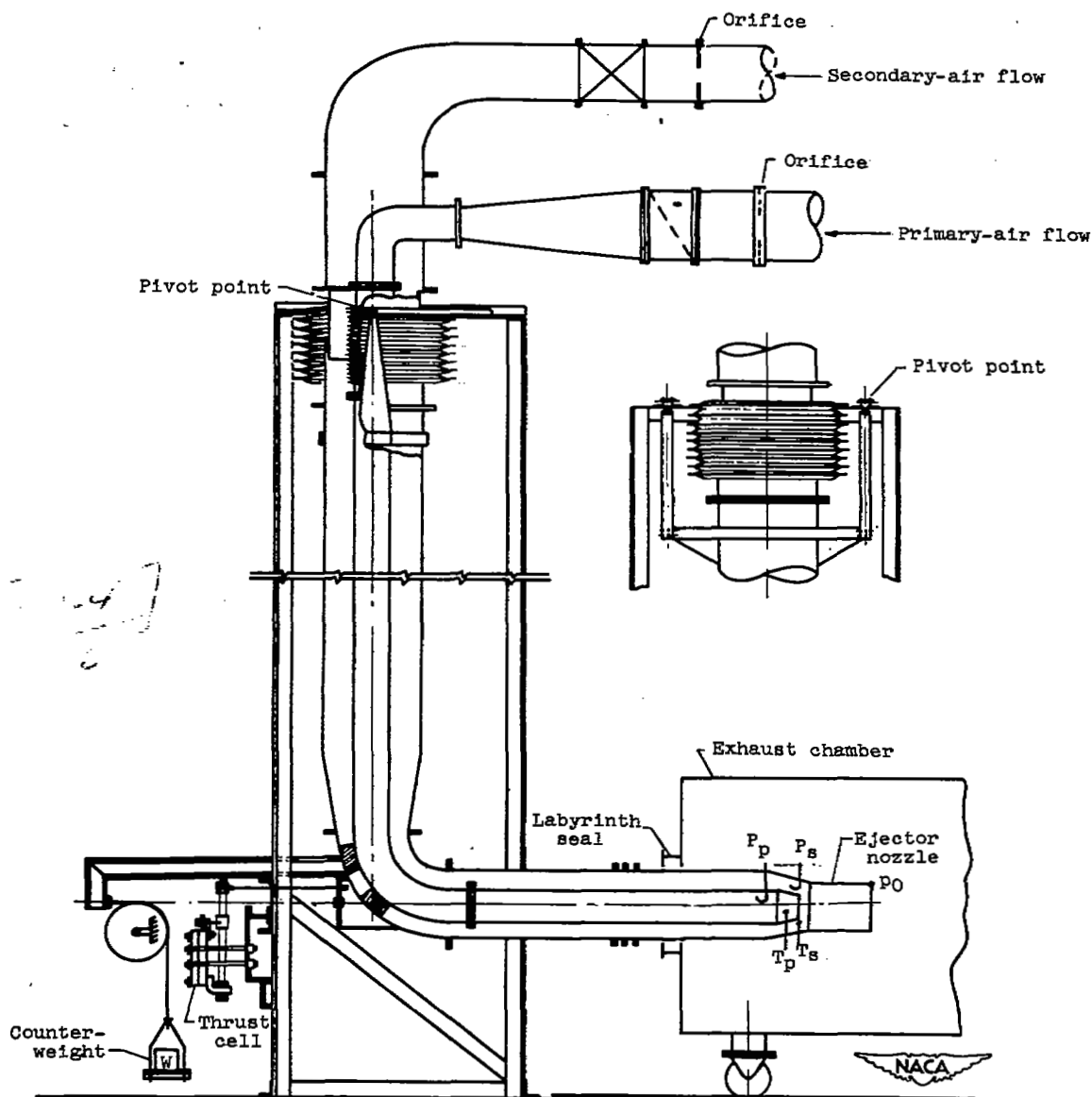


Figure 2. - Schematic diagram of model setup for ejector investigation.

$$\frac{L}{D_j} = .385$$

$$L = .385 \times$$

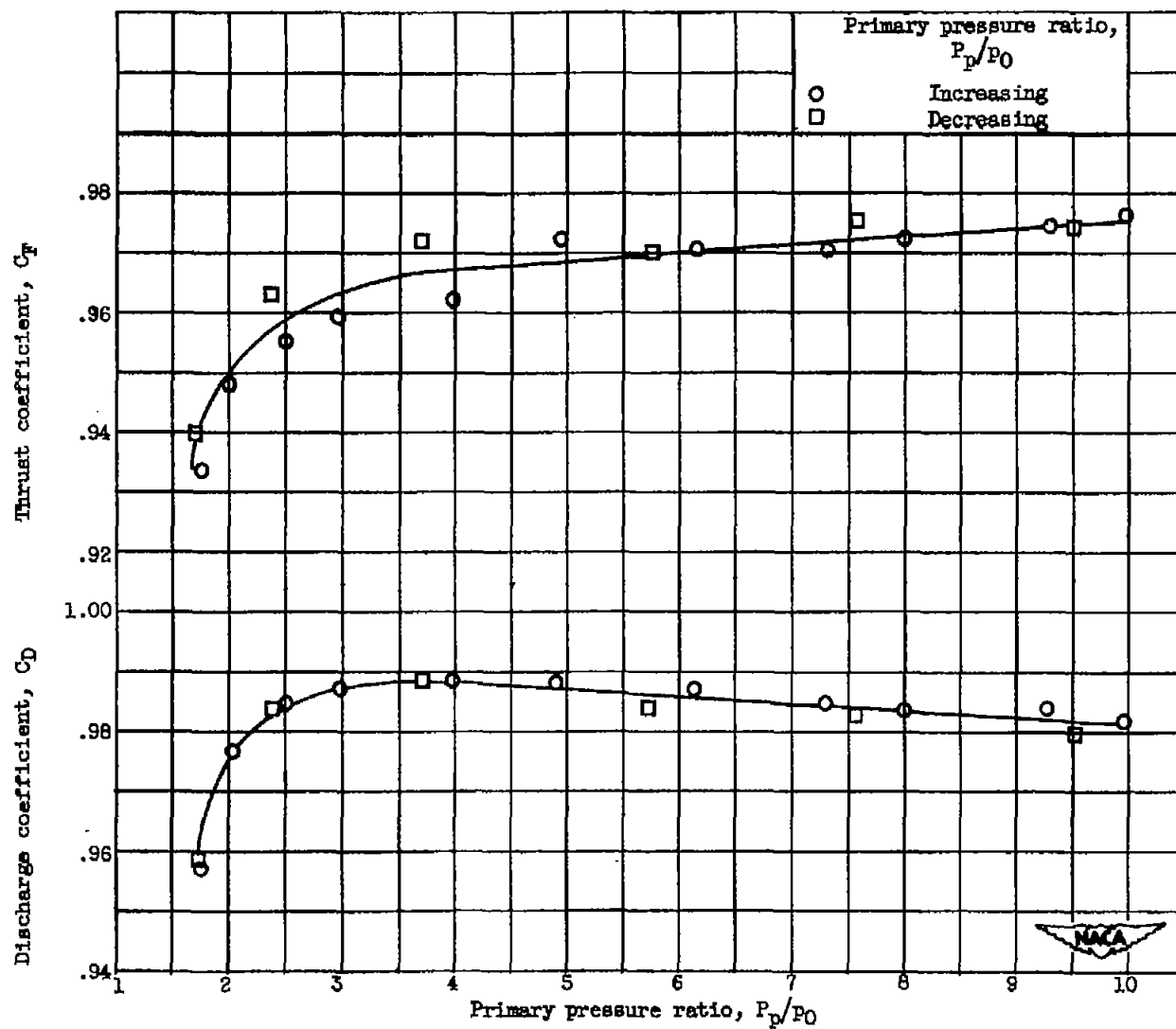


Figure 3. - Primary-nozzle flow coefficients.

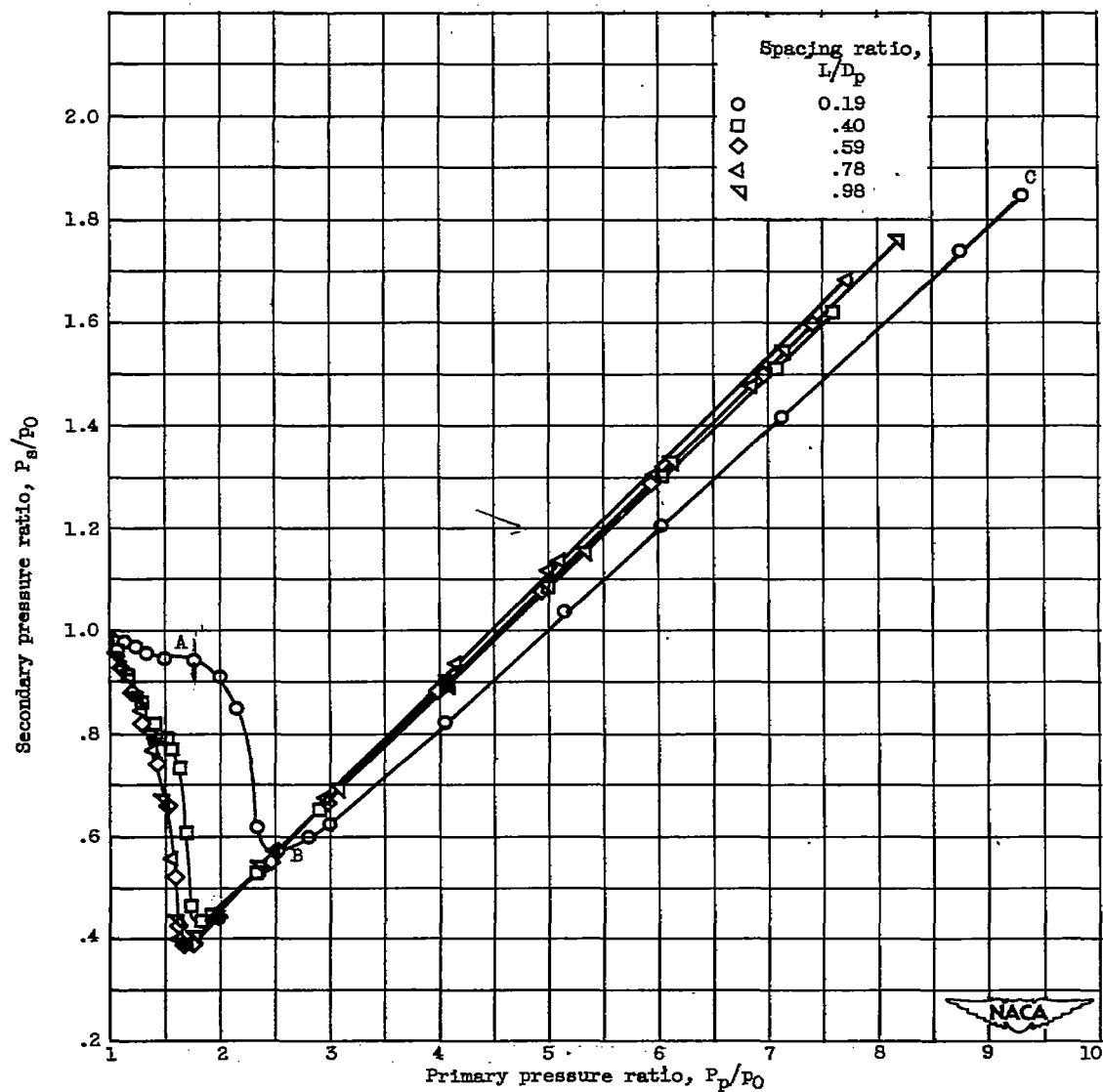


Figure 4. - Performance characteristics of cylindrical ejectors with several spacing ratios operating with zero secondary flow.

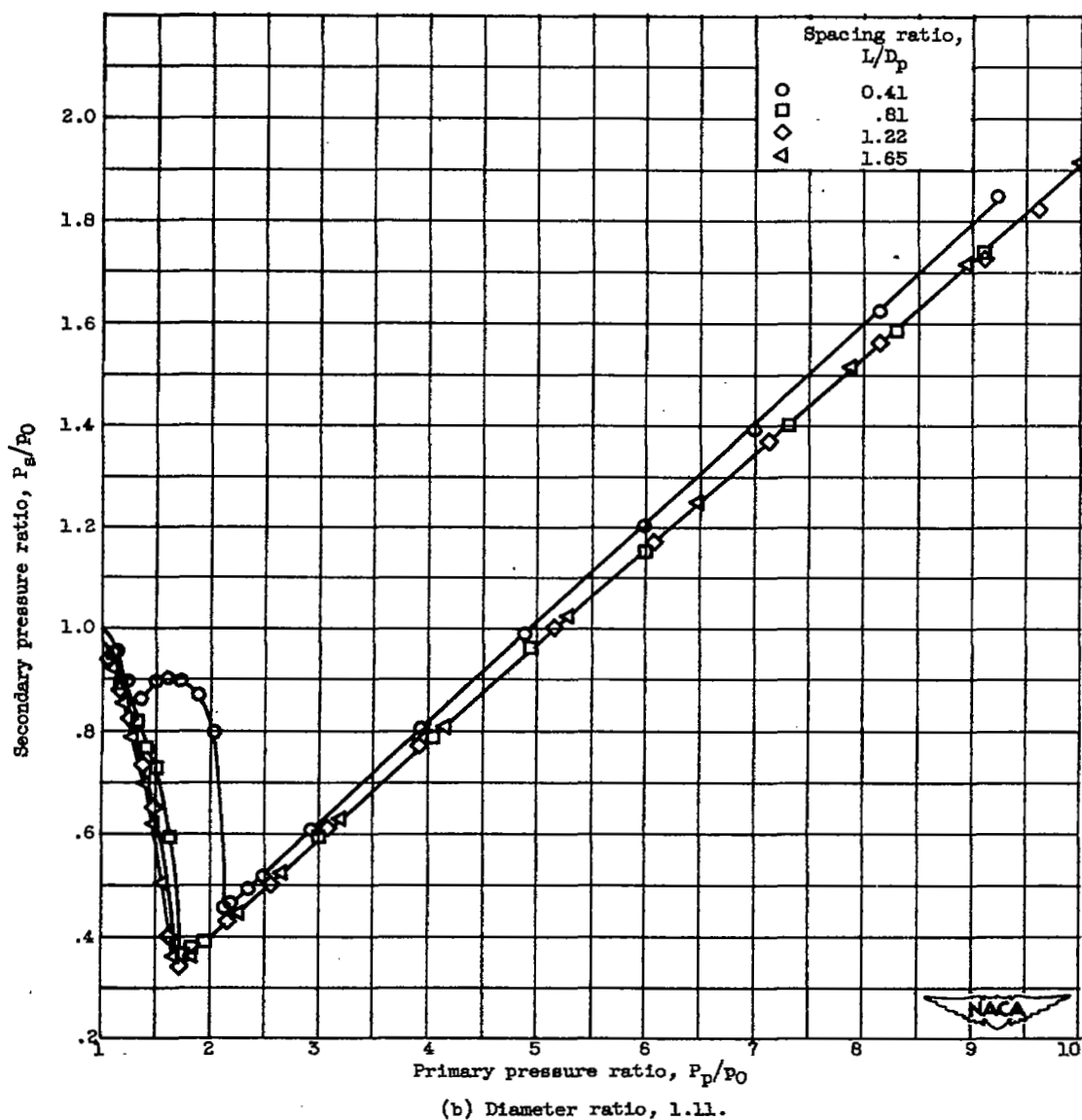


Figure 4. - Continued. Performance characteristics of cylindrical ejectors with several spacing ratios operating with zero secondary flow.

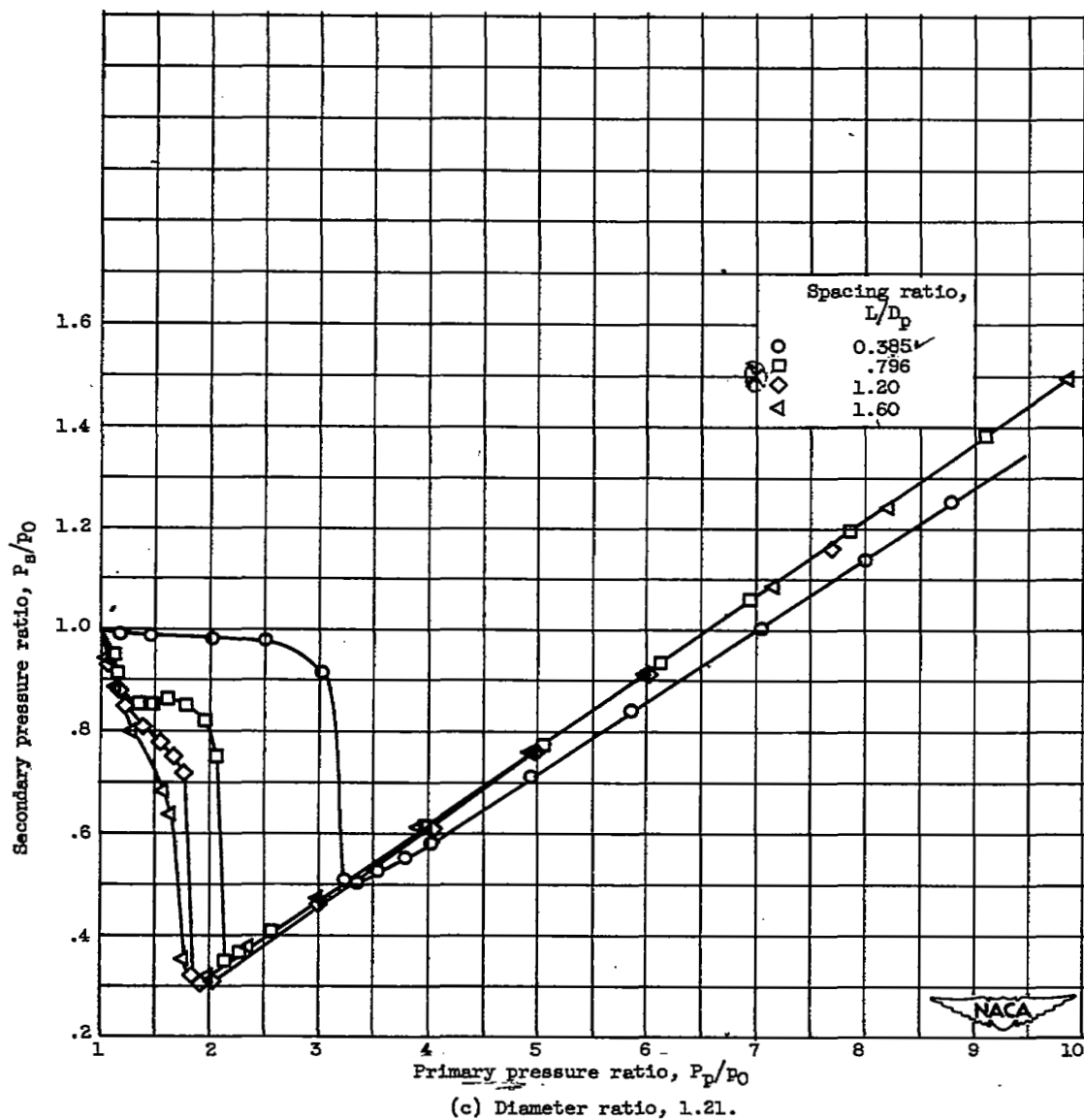


Figure 4. - Continued. Performance characteristics of cylindrical ejectors with several spacing ratios operating with zero secondary flow.

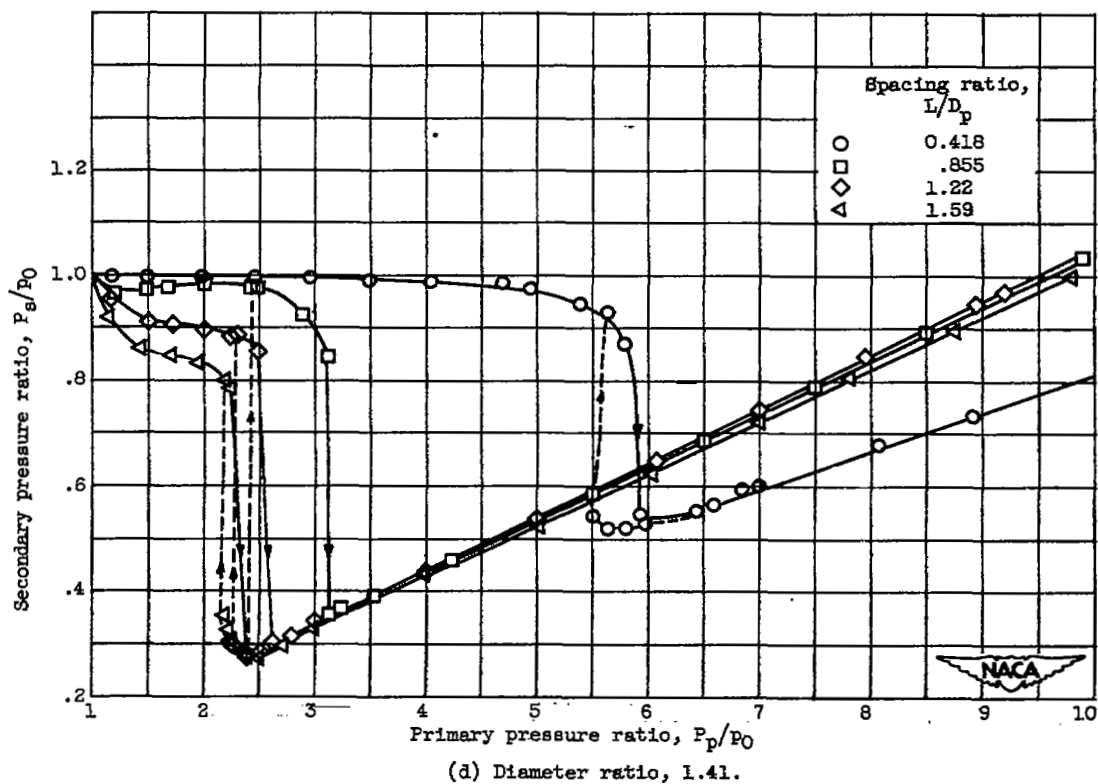


Figure 4. - Concluded. Performance characteristics of cylindrical ejectors with several spacing ratios operating with zero secondary flow.

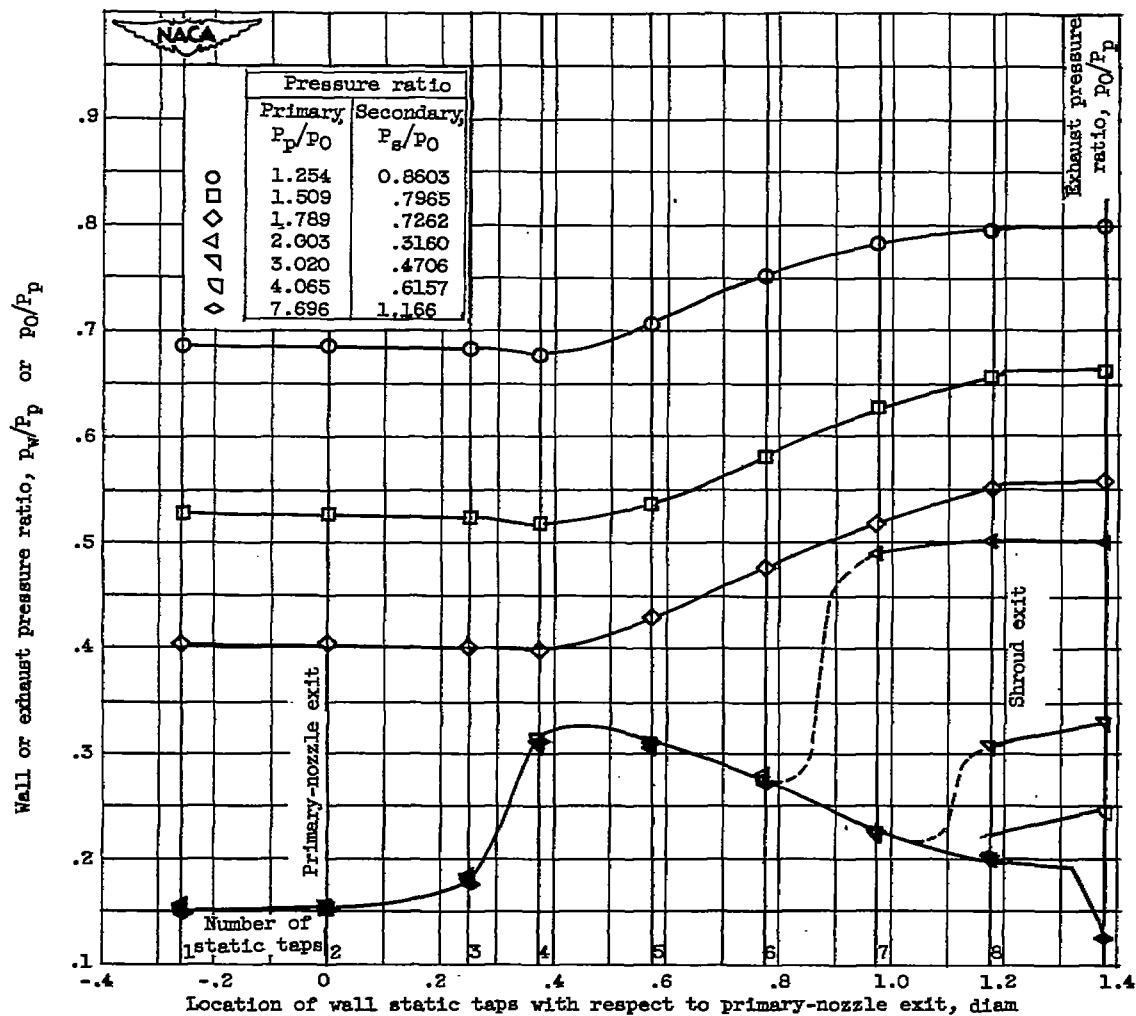
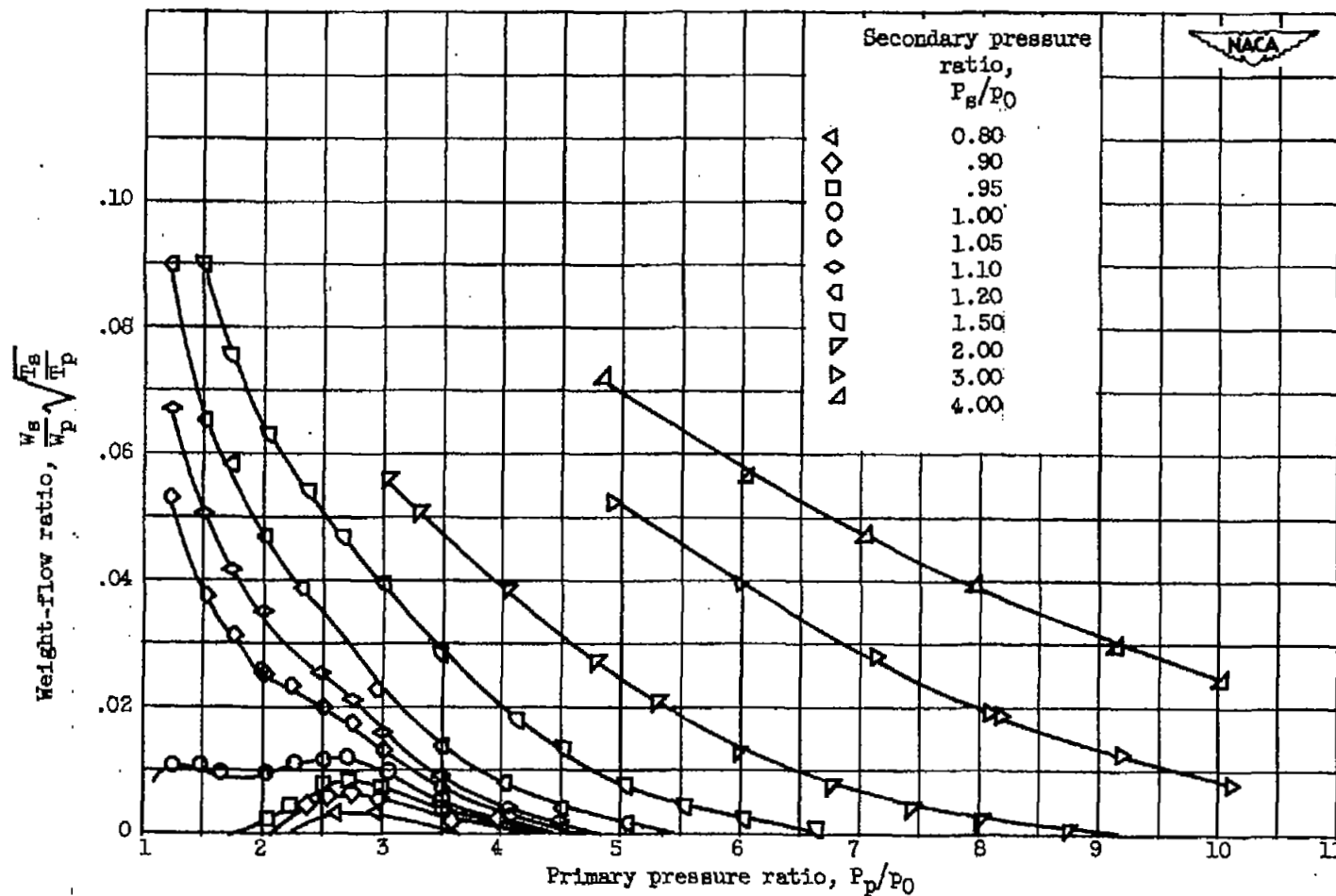


Figure 5. - Static-pressure profiles along ejector shroud wall for zero secondary-flow conditions. Cylindrical shroud; diameter ratio, 1.21; spacing ratio, 1.20.



(a) Spacing ratio, 0.19.

Figure 6. - Effect of primary pressure ratio on ejector weight-flow ratio at diameter ratio of 1.06.

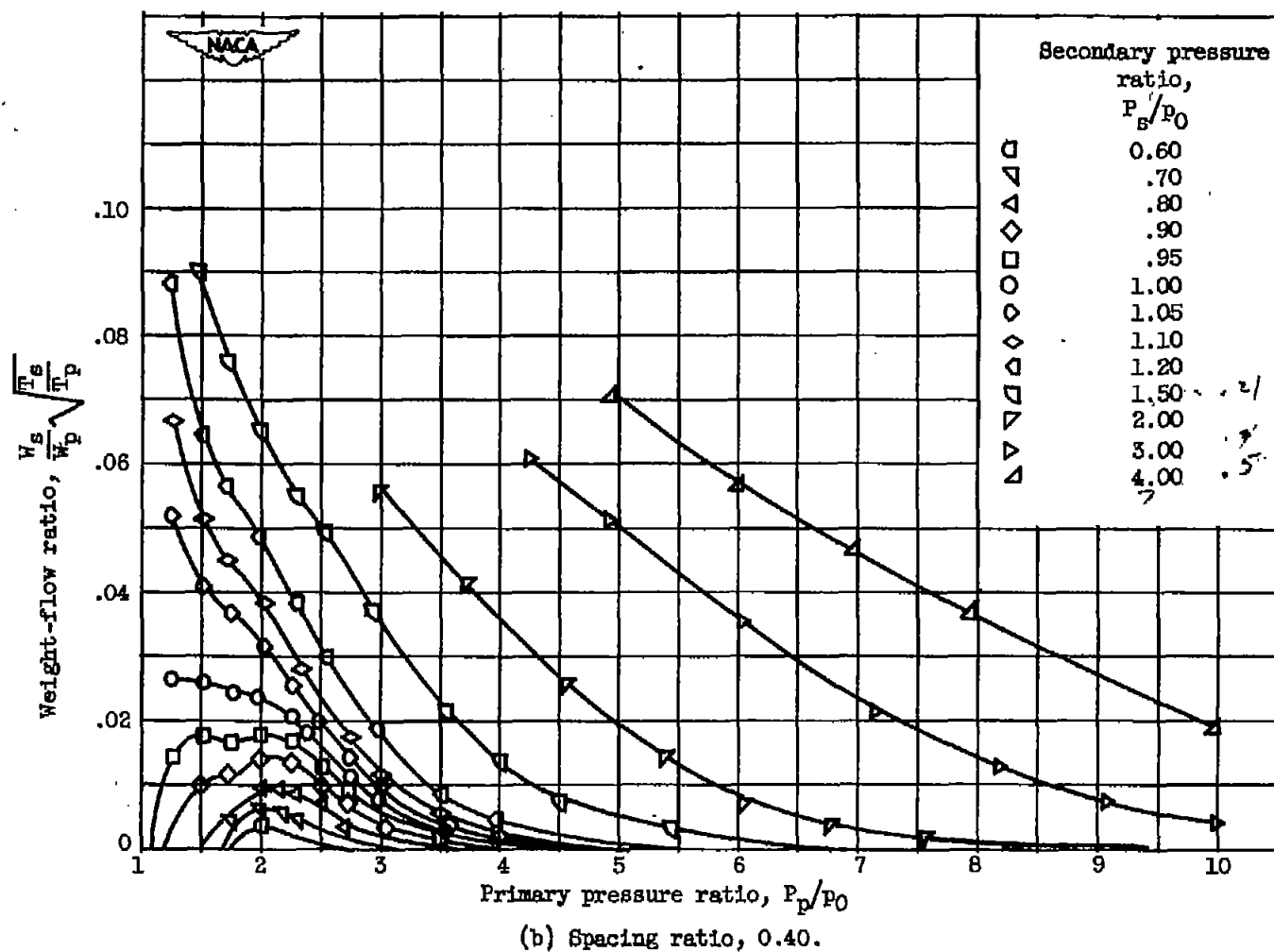


Figure 6. - Continued. Effect of primary pressure ratio on ejector weight-flow ratio at diameter ratio of 1.06.

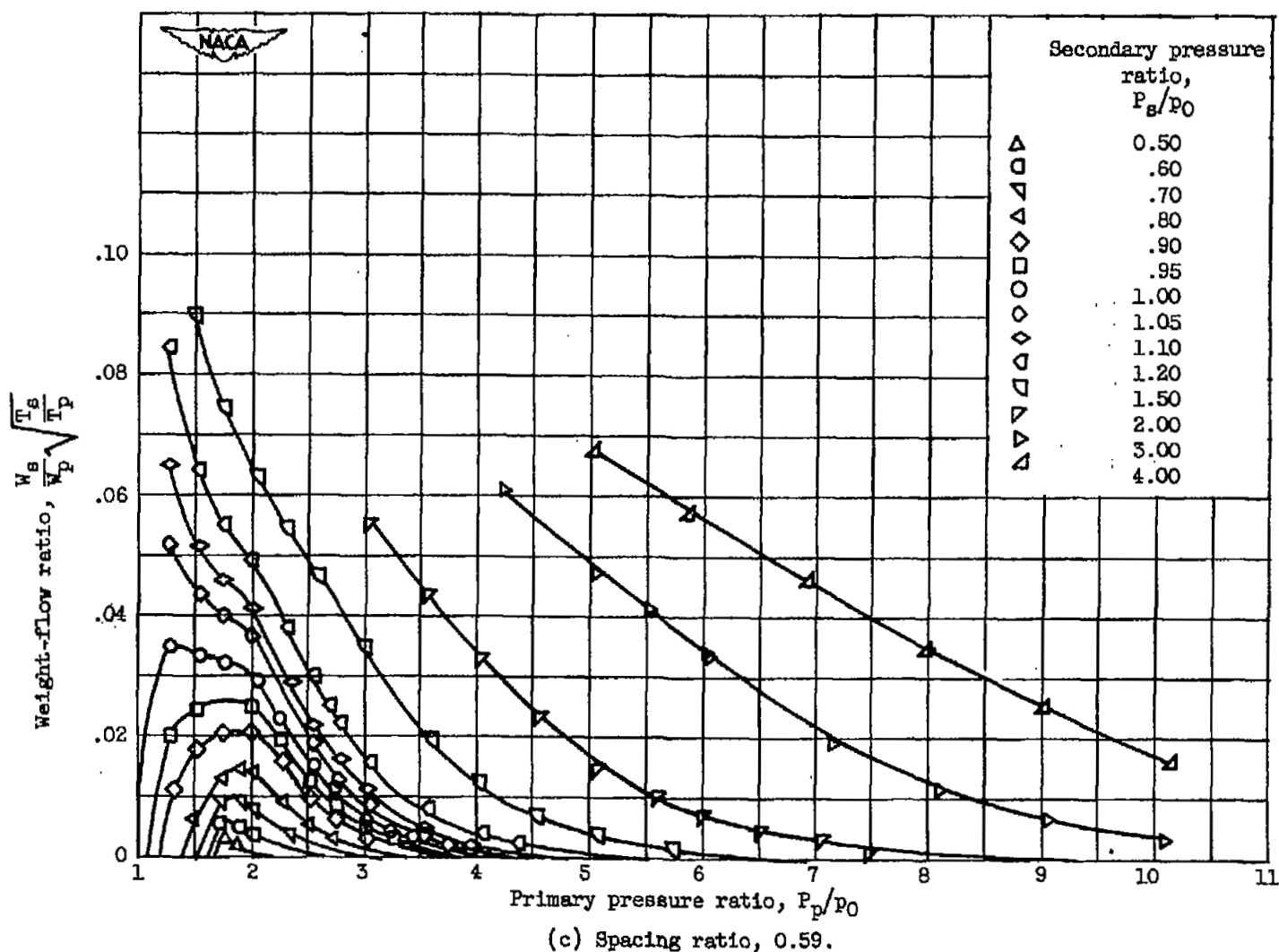
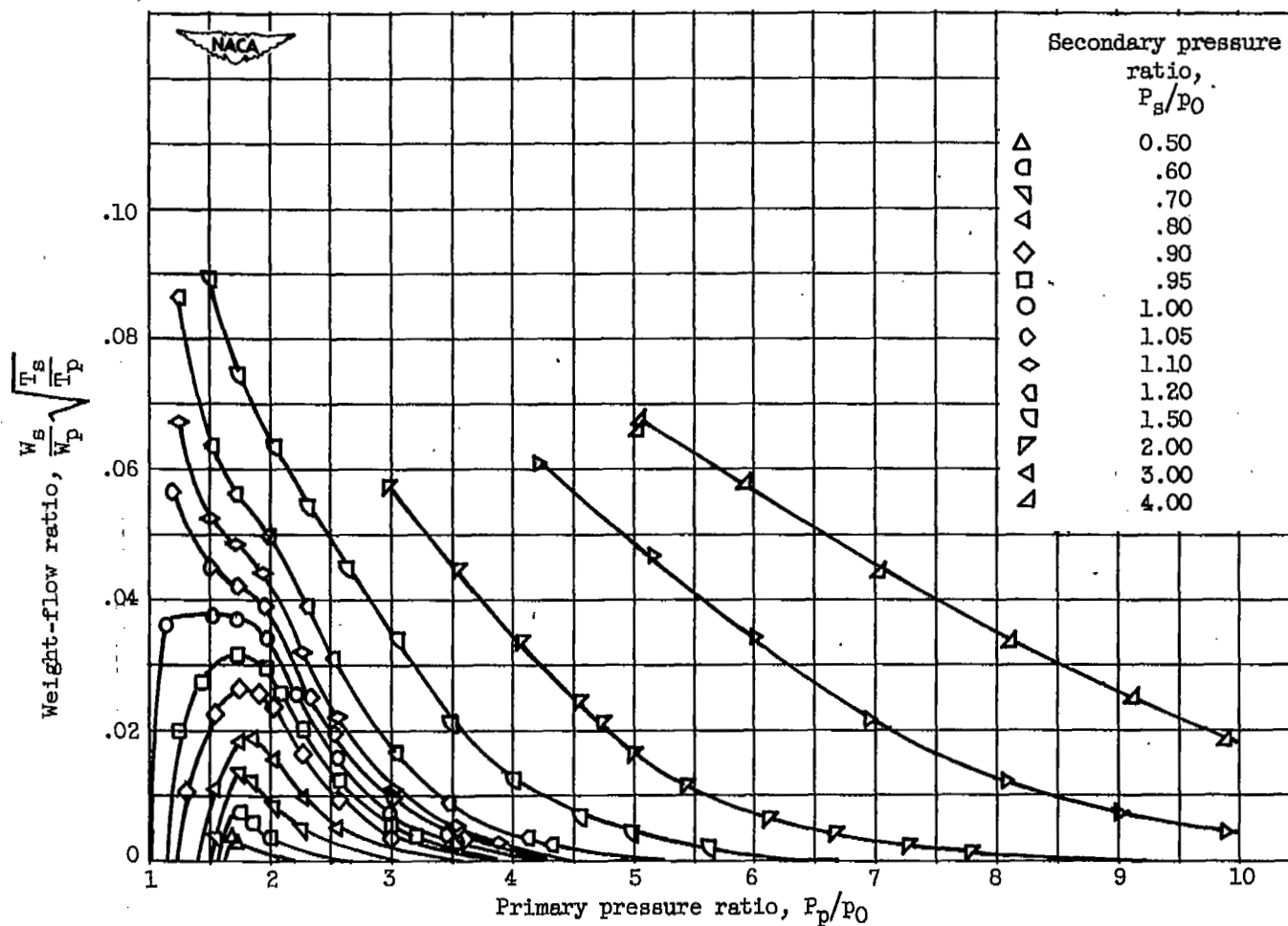
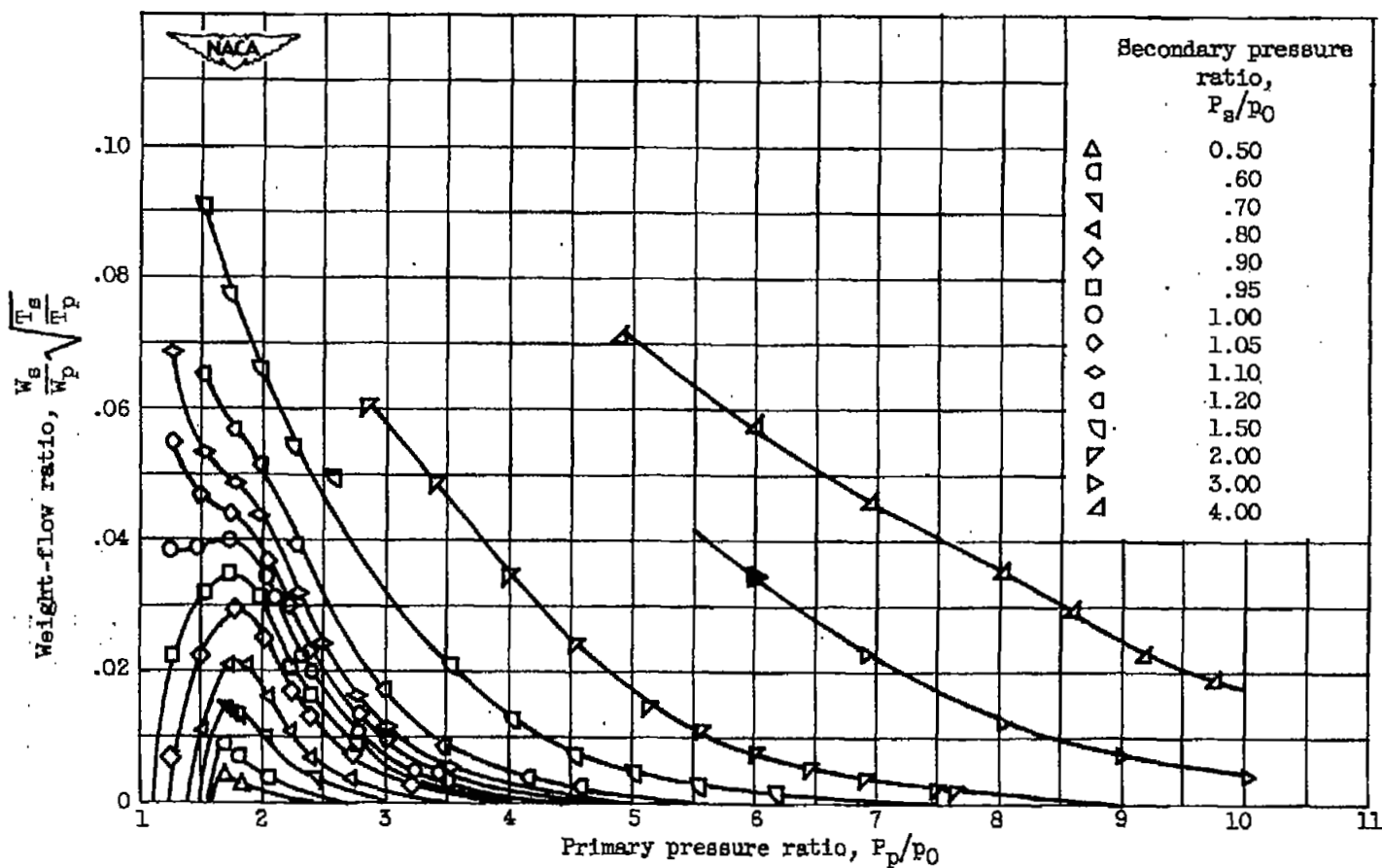


Figure 6. - Continued. Effect of primary pressure ratio on ejector weight-flow ratio at diameter ratio of 1.08.



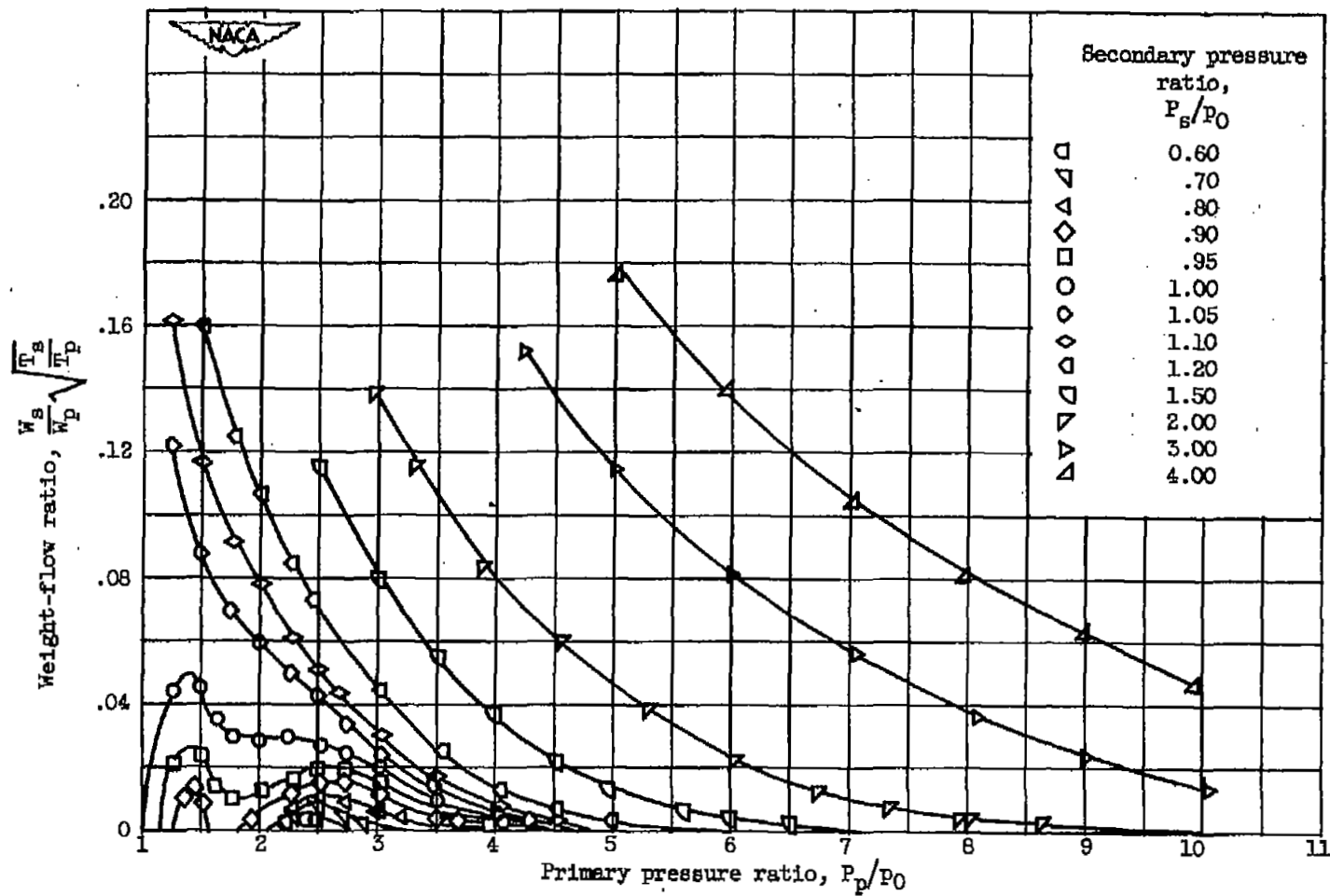
(d) Spacing ratio, 0.78.

Figure 6. - Continued. Effect of primary pressure ratio on ejector weight-flow ratio at diameter ratio of 1.06.



(e) Spacing ratio, 0.98.

Figure 6. - Concluded. Effect of primary pressure ratio on ejector weight-flow ratio at diameter ratio of 1.06.



(a) Spacing ratio, 0.41.

Figure 7. - Effect of primary pressure ratio on ejector weight-flow ratio at diameter ratio of 1.11.

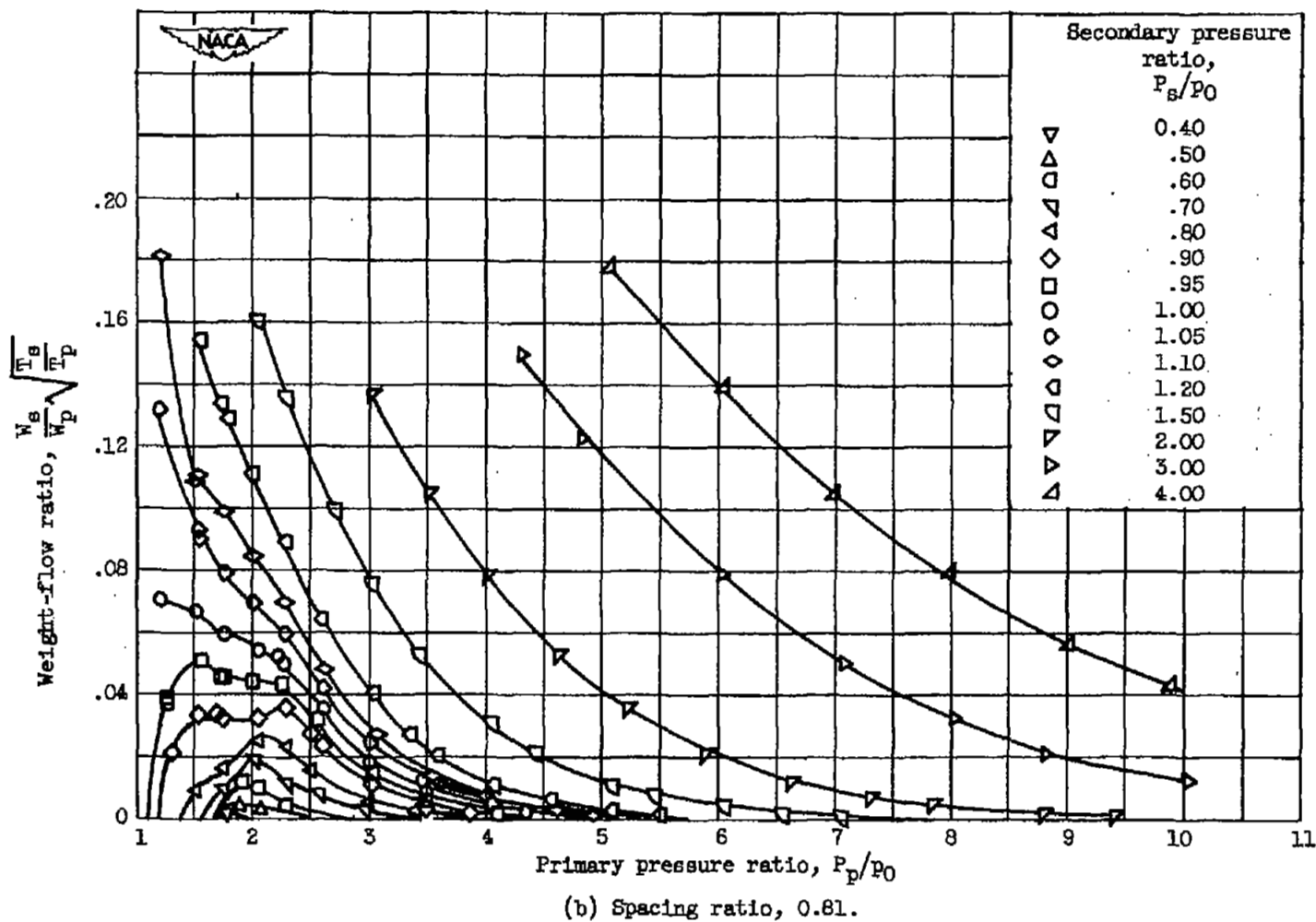
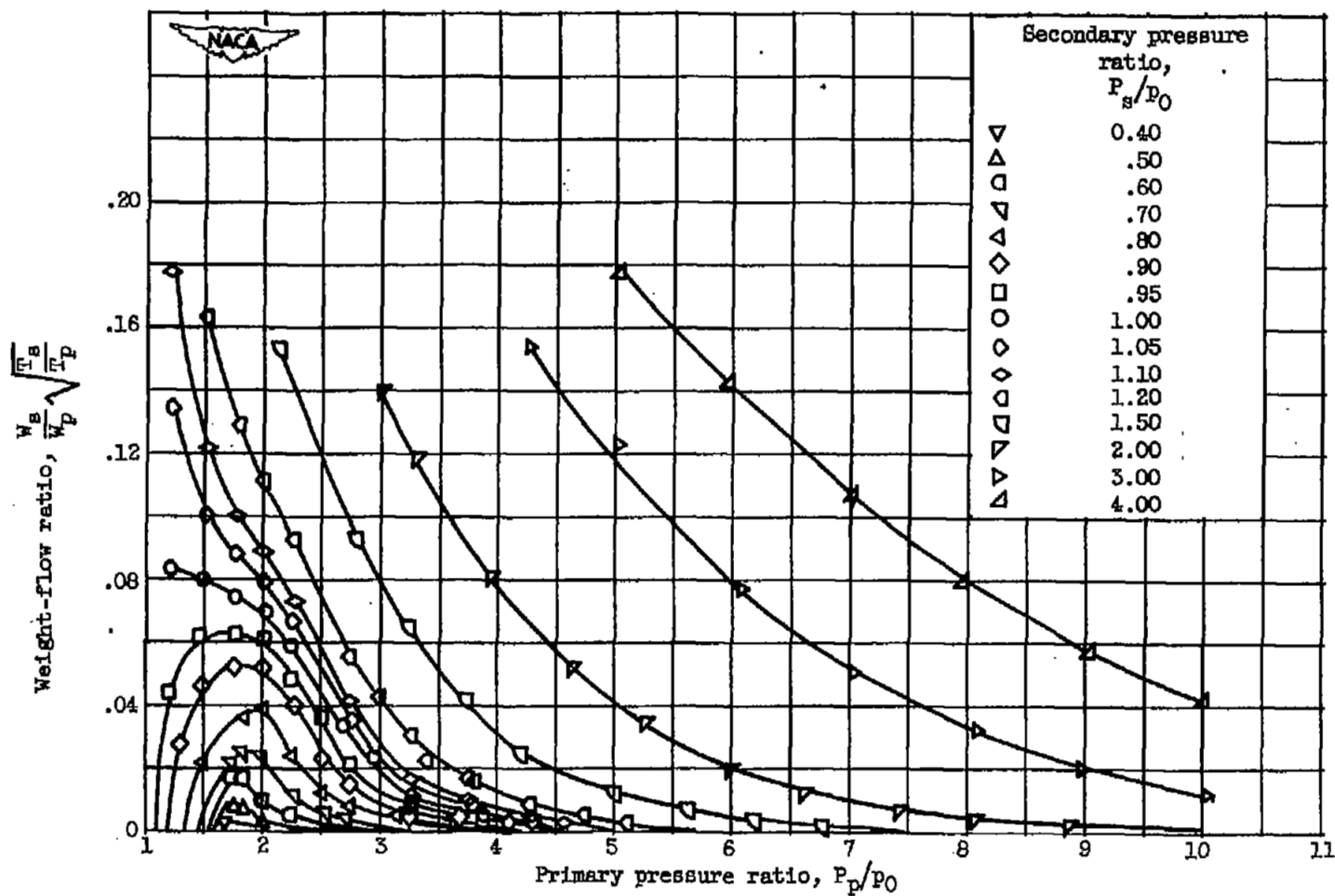


Figure 7. - Continued. Effect of primary pressure ratio on ejector weight-flow ratio at diameter ratio of 1.11.



(c) Spacing ratio, 1.22.

Figure 7. - Continued. Effect of primary pressure ratio on ejector weight-flow ratio at diameter ratio of 1.11.

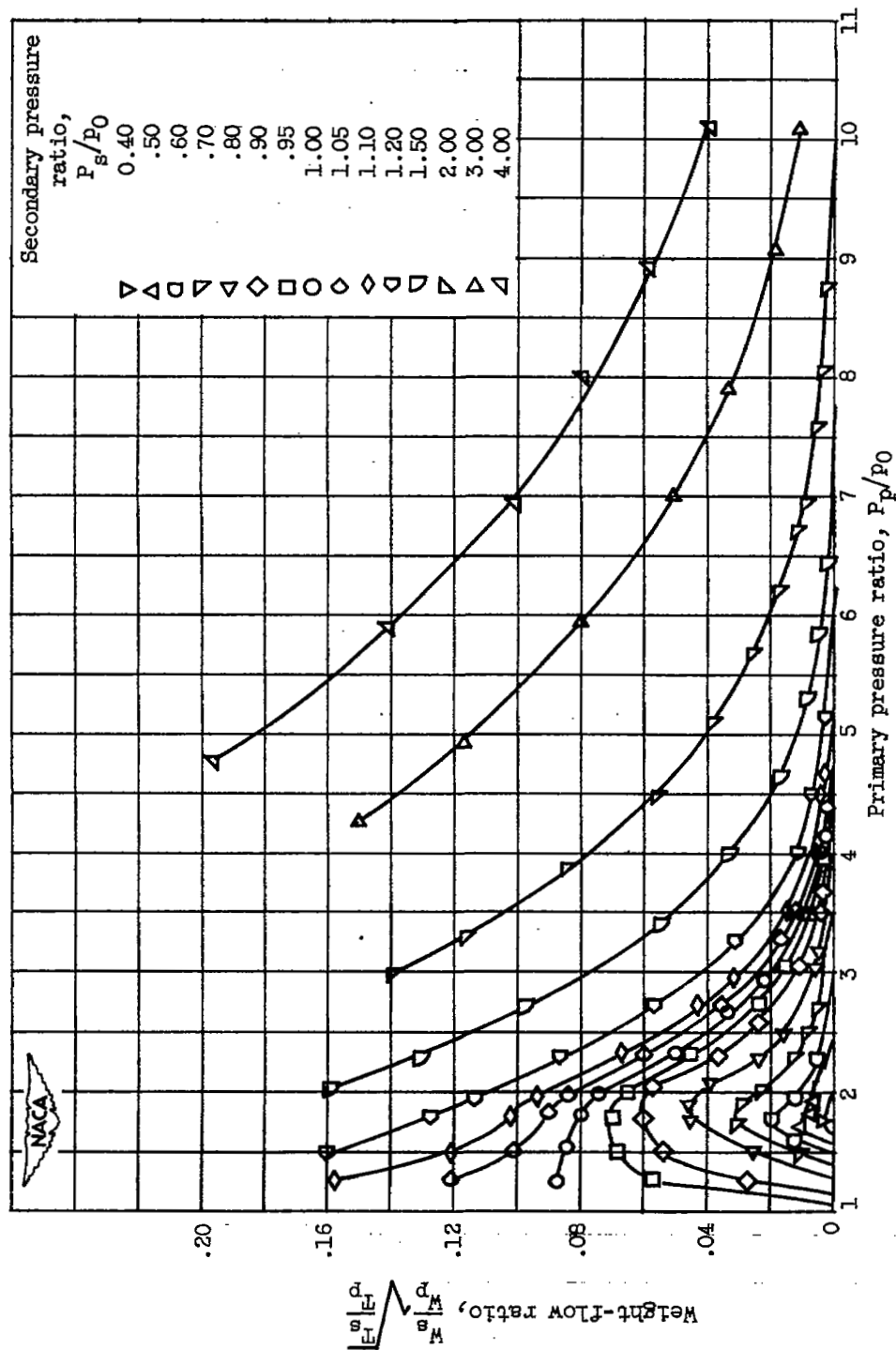


Figure 7. - Concluded. Effect of primary pressure ratio on ejector weight-flow ratio at diameter ratio of 1.11.

2799

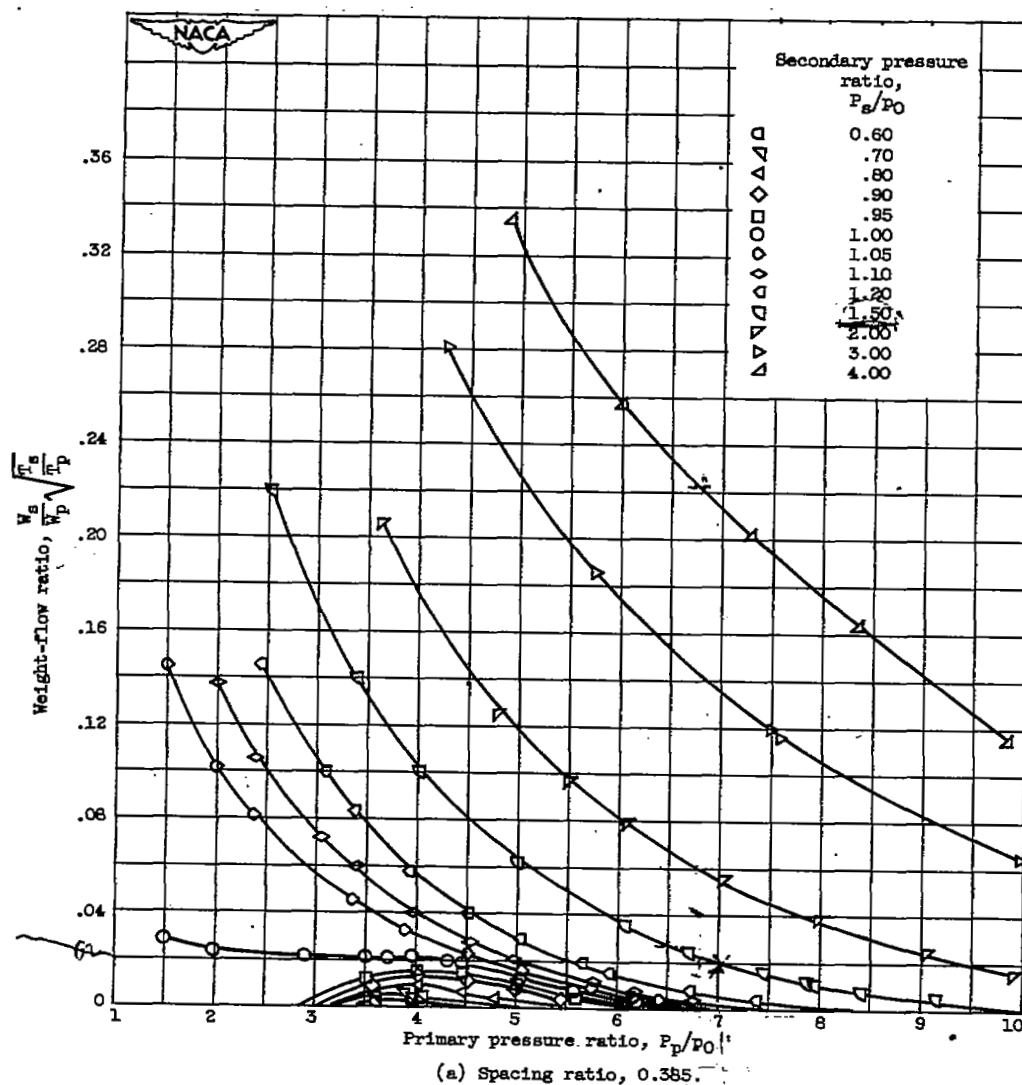


Figure 8. - Effect of primary pressure ratio on ejector weight-flow ratio at diameter ratio of 1.21.

$$\frac{H_2}{P_2} \times \frac{P_2}{H_2} = \frac{1.5}{7} = 0.214 \quad \frac{H_2}{P_2} \rightarrow 1.8$$

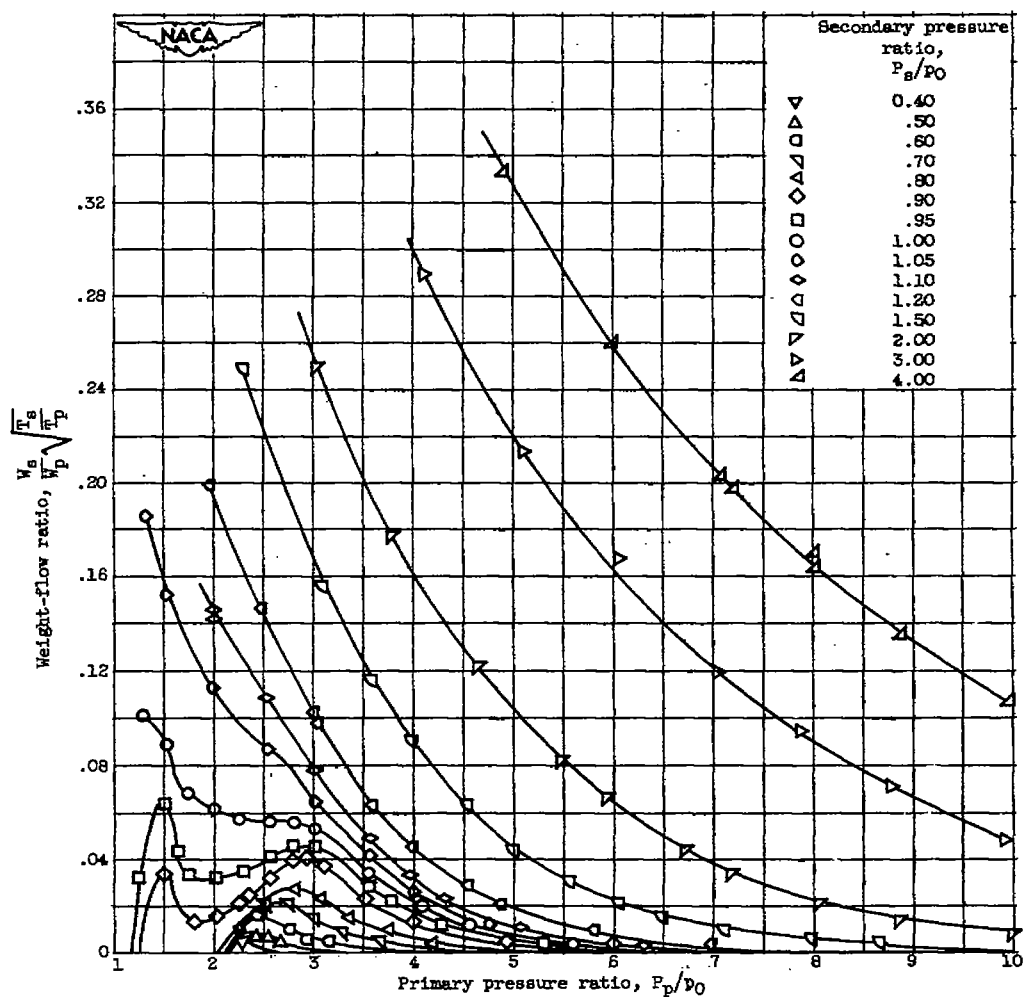


Figure 8. - Continued. Effect of primary pressure ratio on ejector weight-flow ratio at diameter ratio of 1.21.

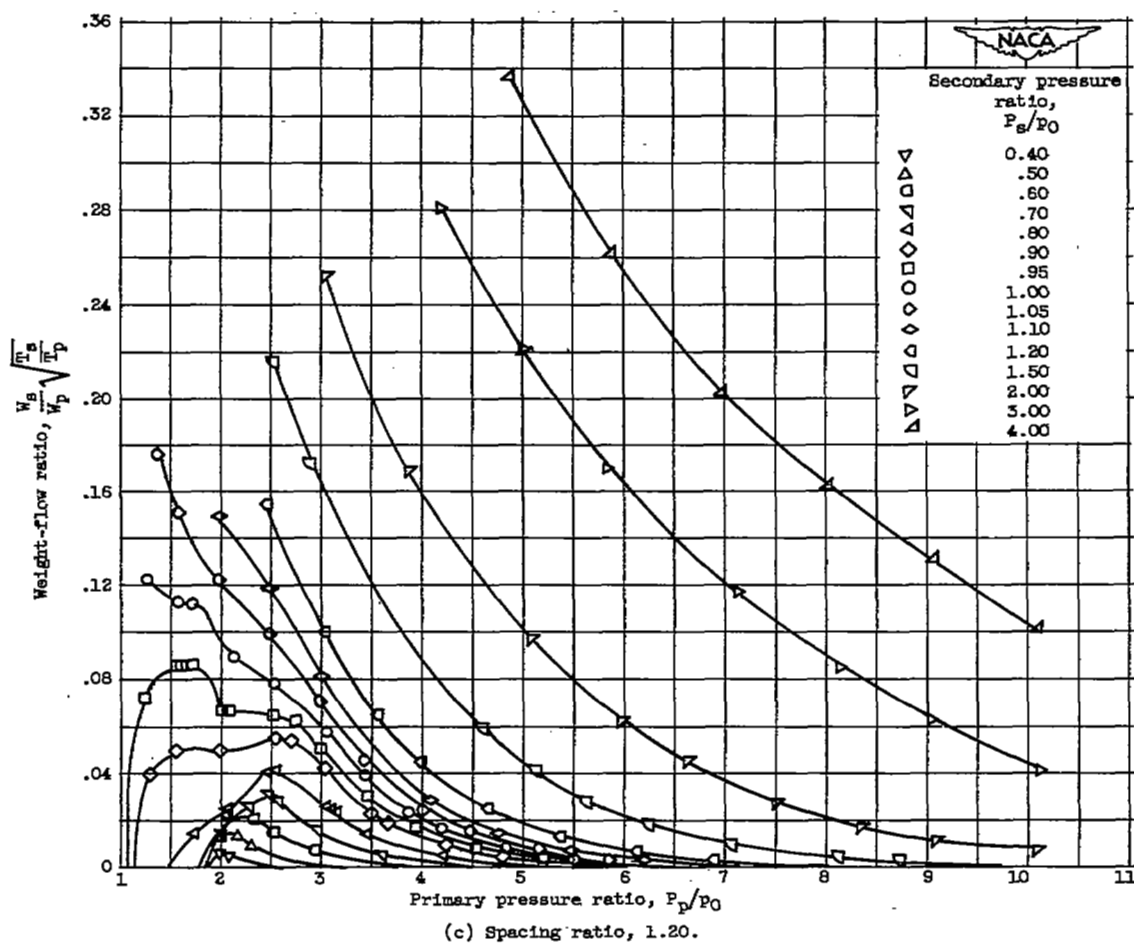


Figure 8. - Continued. Effect of primary pressure ratio on ejector weight-flow ratio at diameter ratio of 1.21.

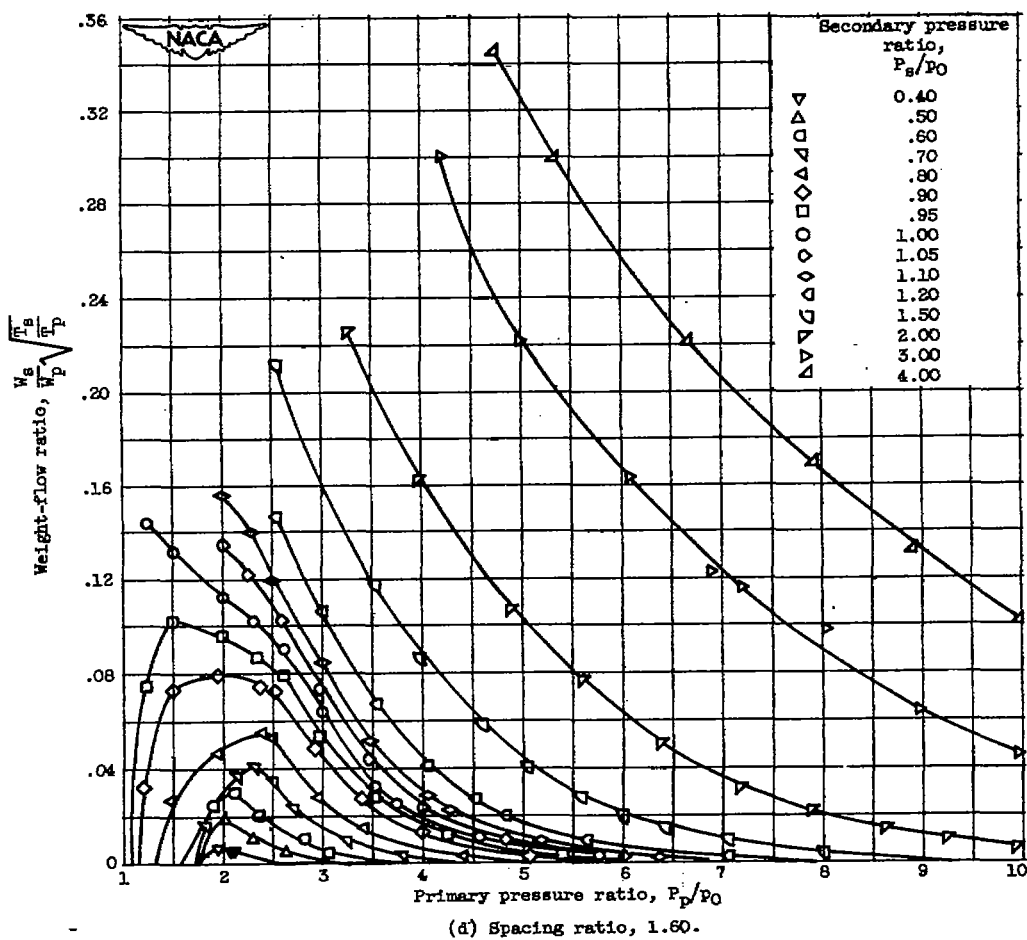


Figure 8. - Concluded. Effect of primary pressure ratio on ejector weight-flow ratio at diameter ratio of 1.21.

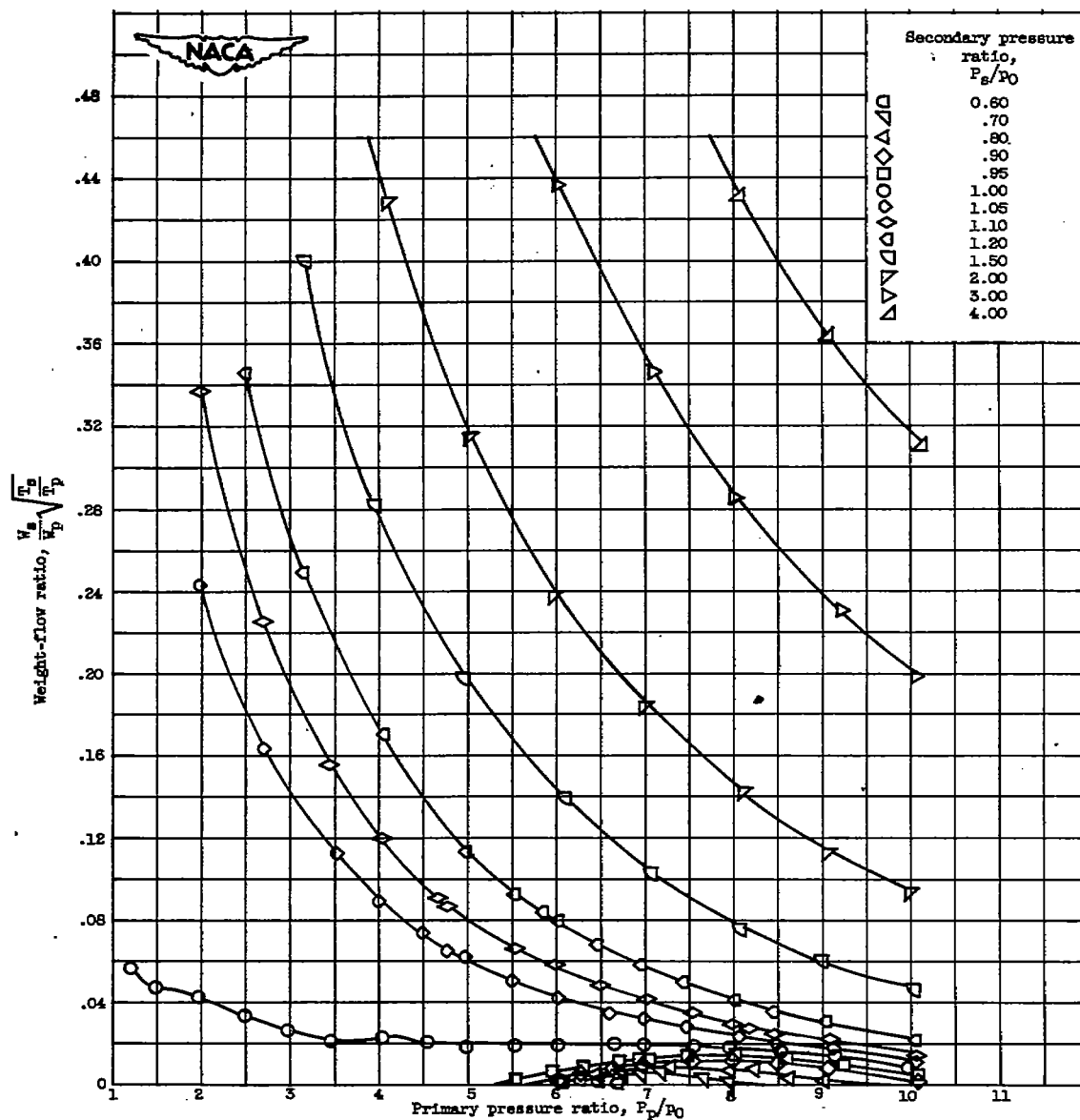


Figure 9. - Effect of primary pressure ratio on ejector weight-flow ratio at diameter ratio of 1.41.

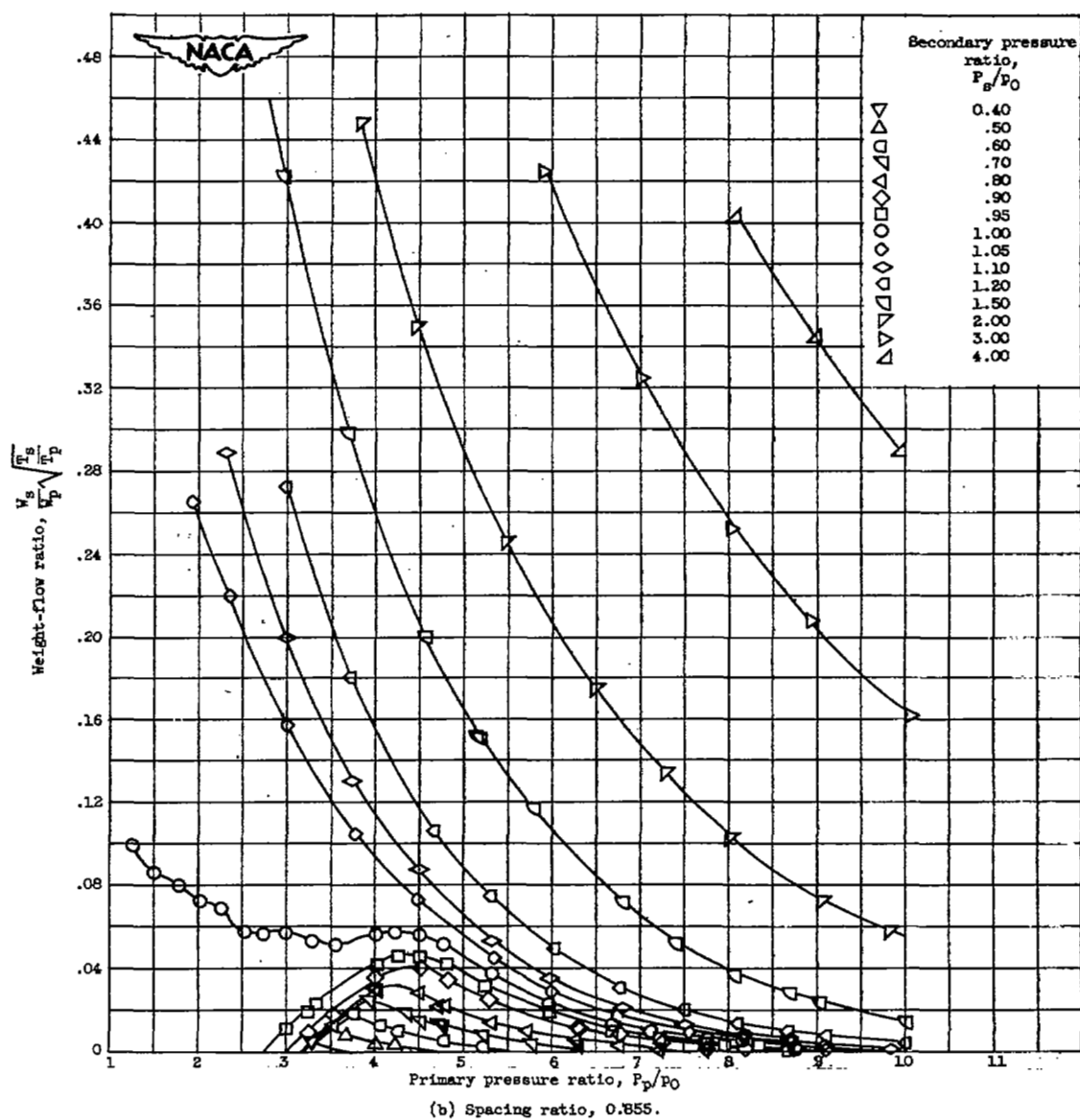


Figure 9. - Continued. Effect of primary pressure ratio on ejector weight-flow ratio at diameter ratio of 1.41.

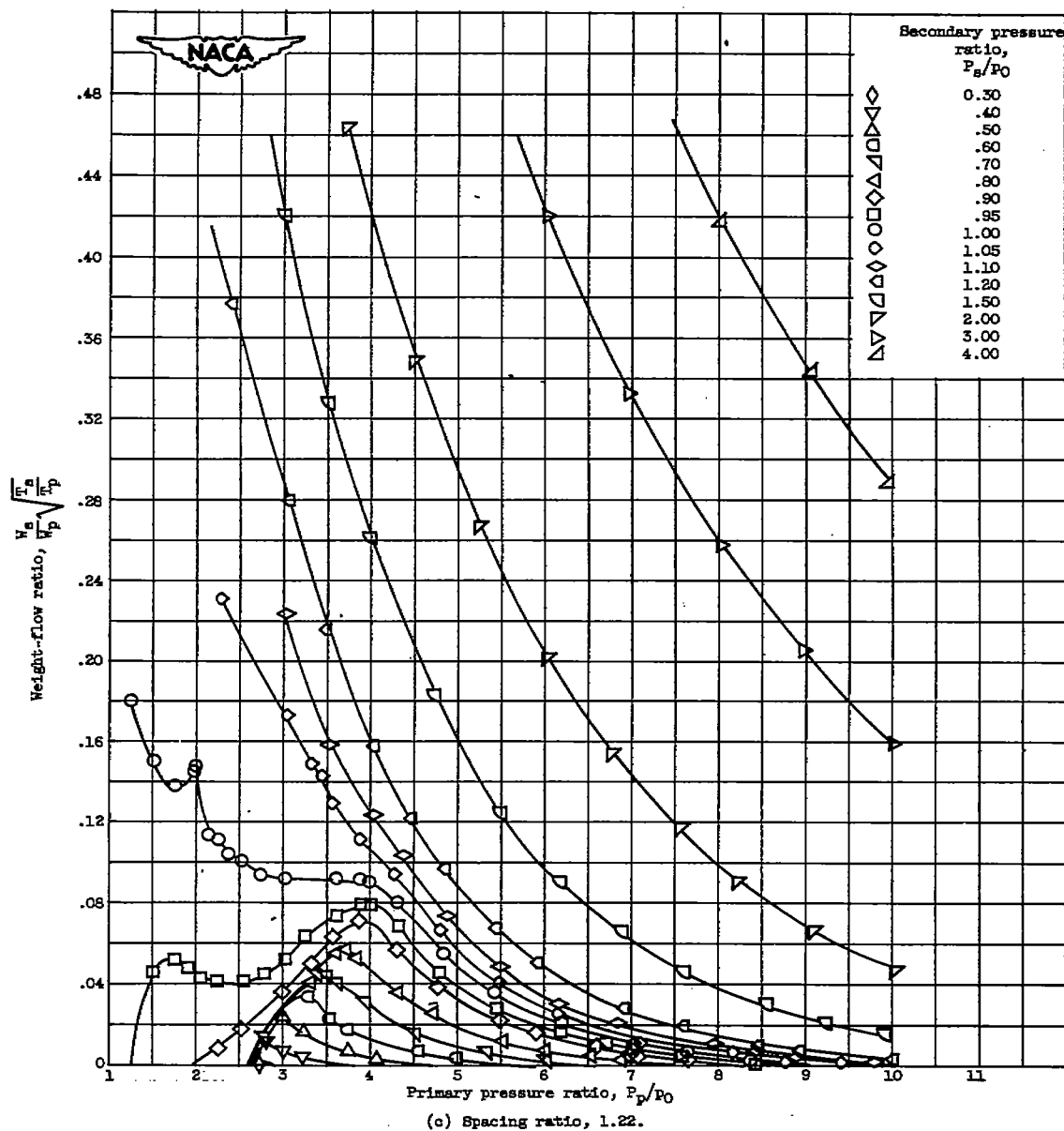


Figure 9. - Continued. Effect of primary pressure ratio on ejector weight-flow ratio at diameter ratio of 1.41.

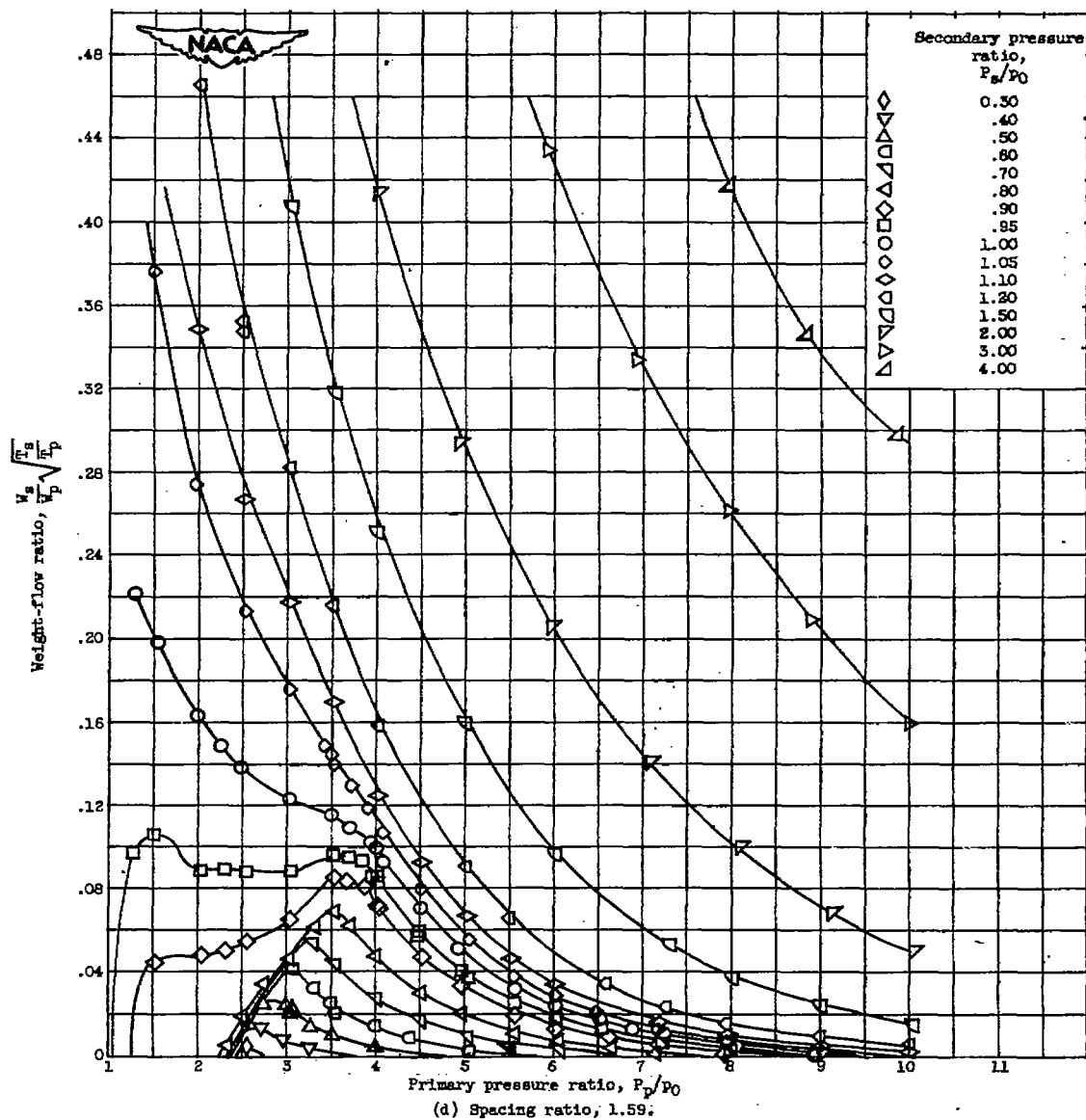


Figure 9. - Concluded. Effect of primary pressure ratio on ejector weight-flow ratio at diameter ratio of 1.41.

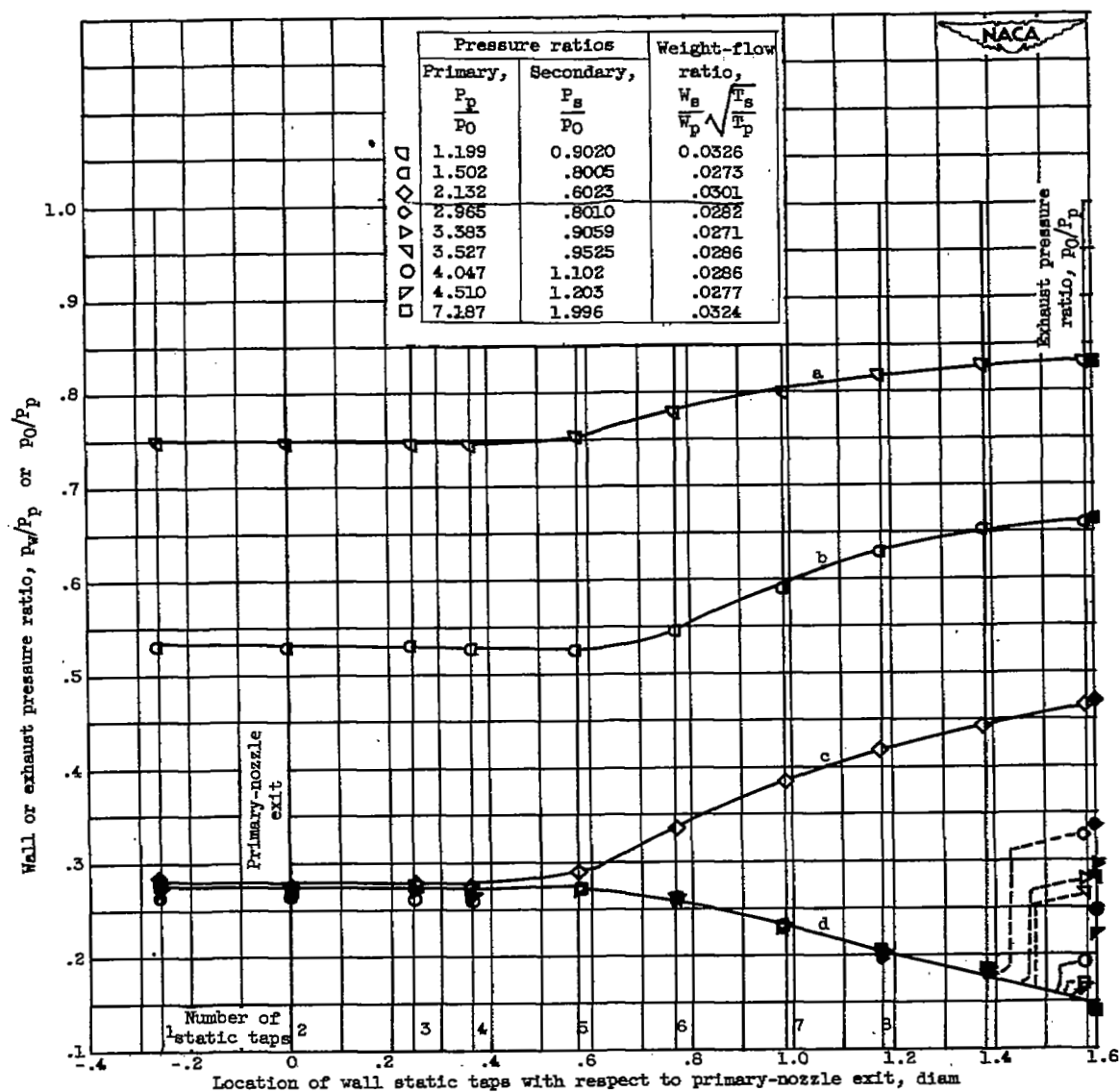


Figure 10. - Static-pressure profile along ejector shroud wall for constant weight-flow ratio of approximately 0.03. Cylindrical nozzle; diameter ratio, 1.21; spacing ratio, 1.60.

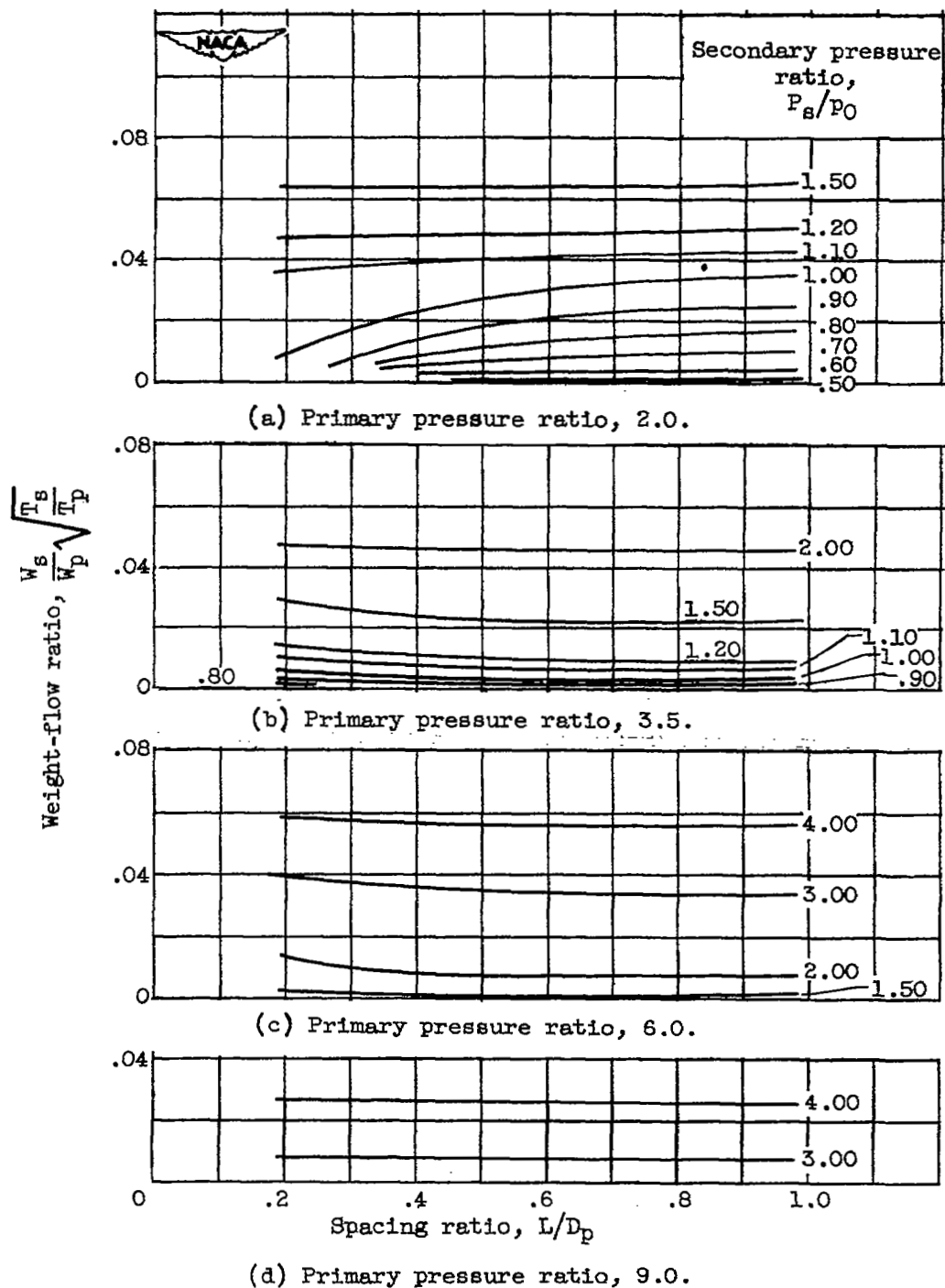


Figure 11. - Effect of spacing ratio on ejector weight-flow ratio for diameter ratio of 1.06.

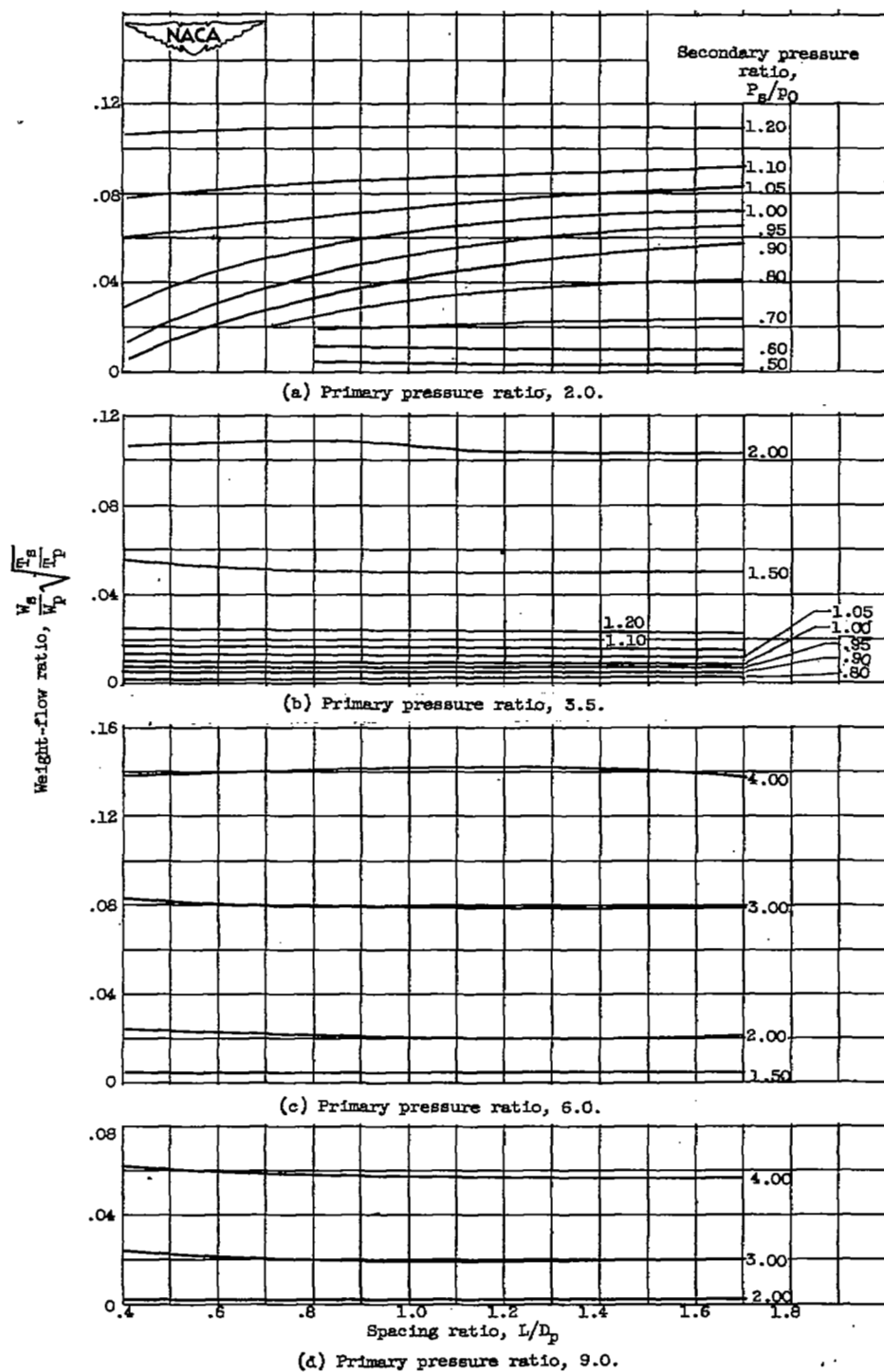


Figure 12. - Effect of spacing ratio on ejector weight-flow ratio for diameter ratio of 1.11.

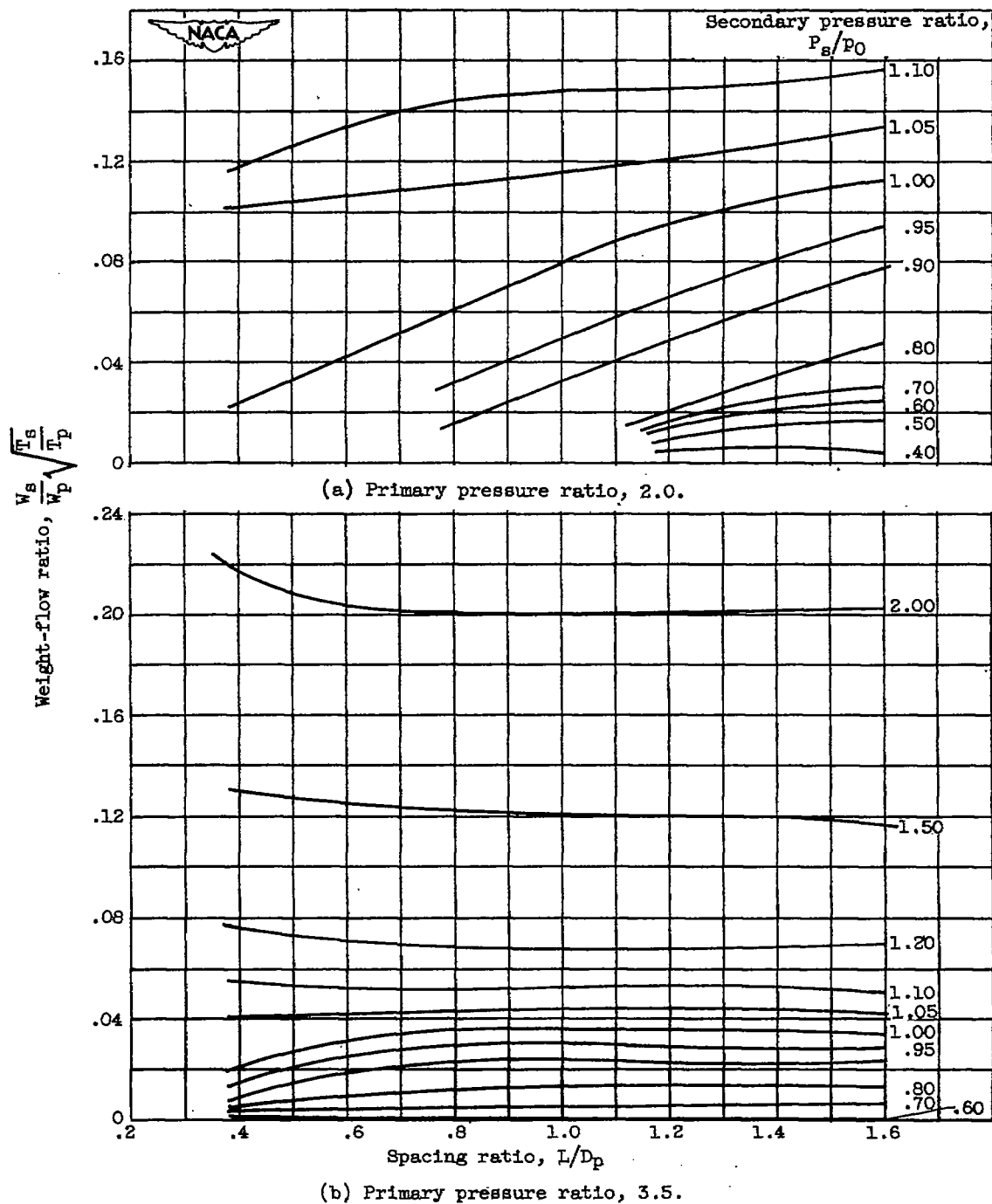


Figure 13. - Effect of spacing ratio on ejector weight-flow ratio for diameter ratio of 1.21.

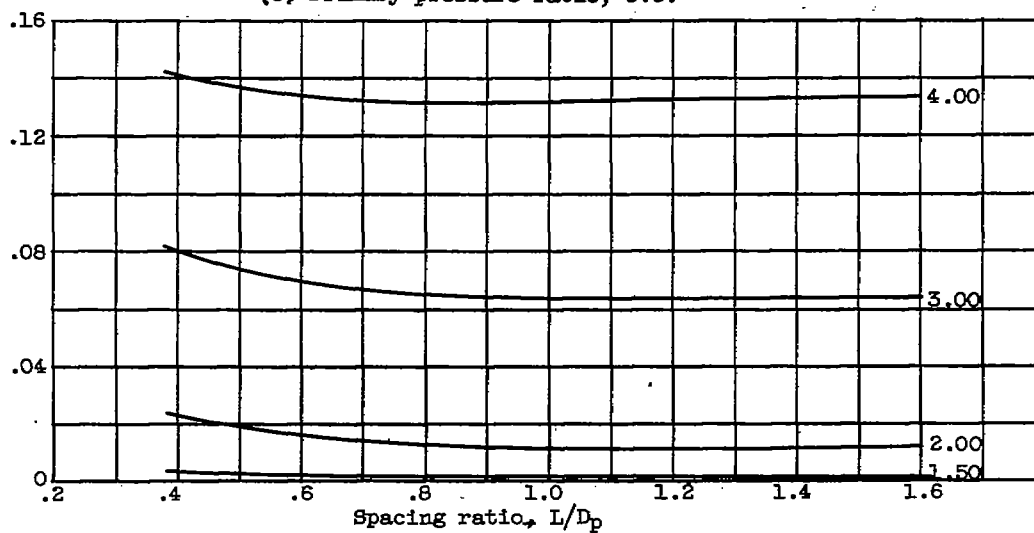
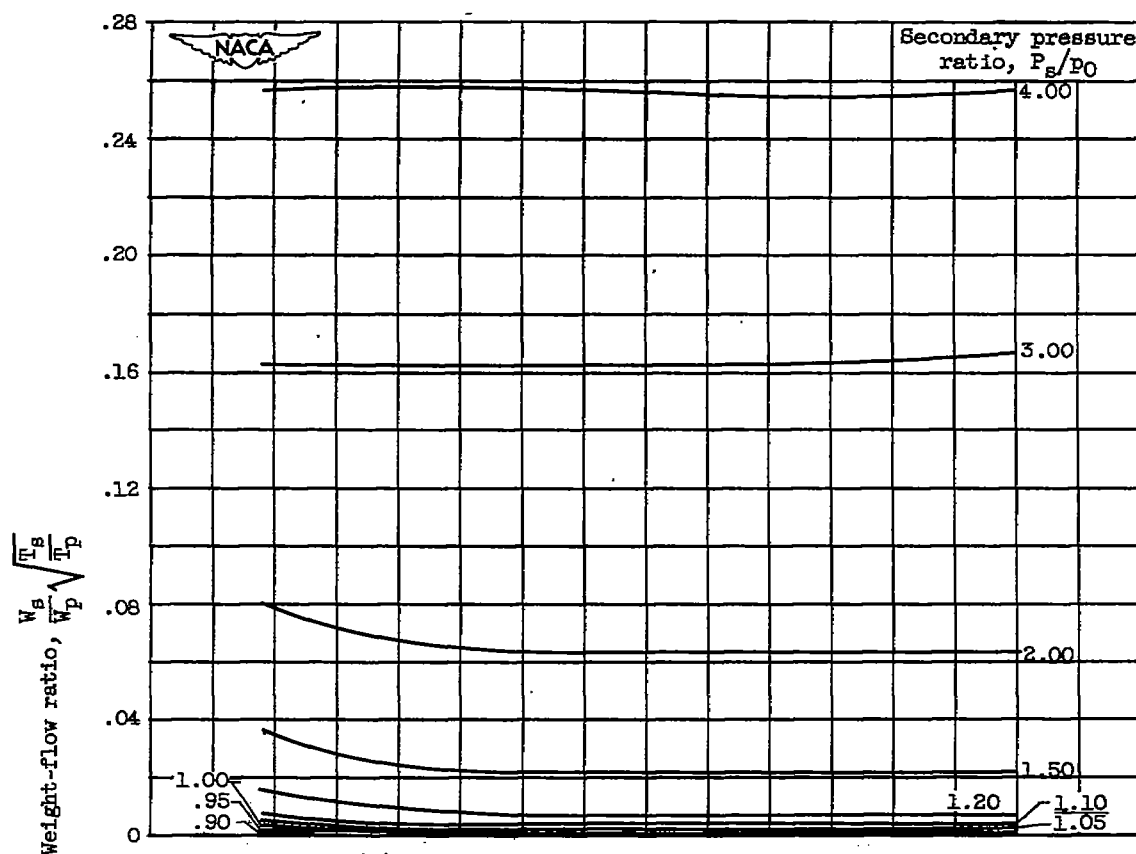
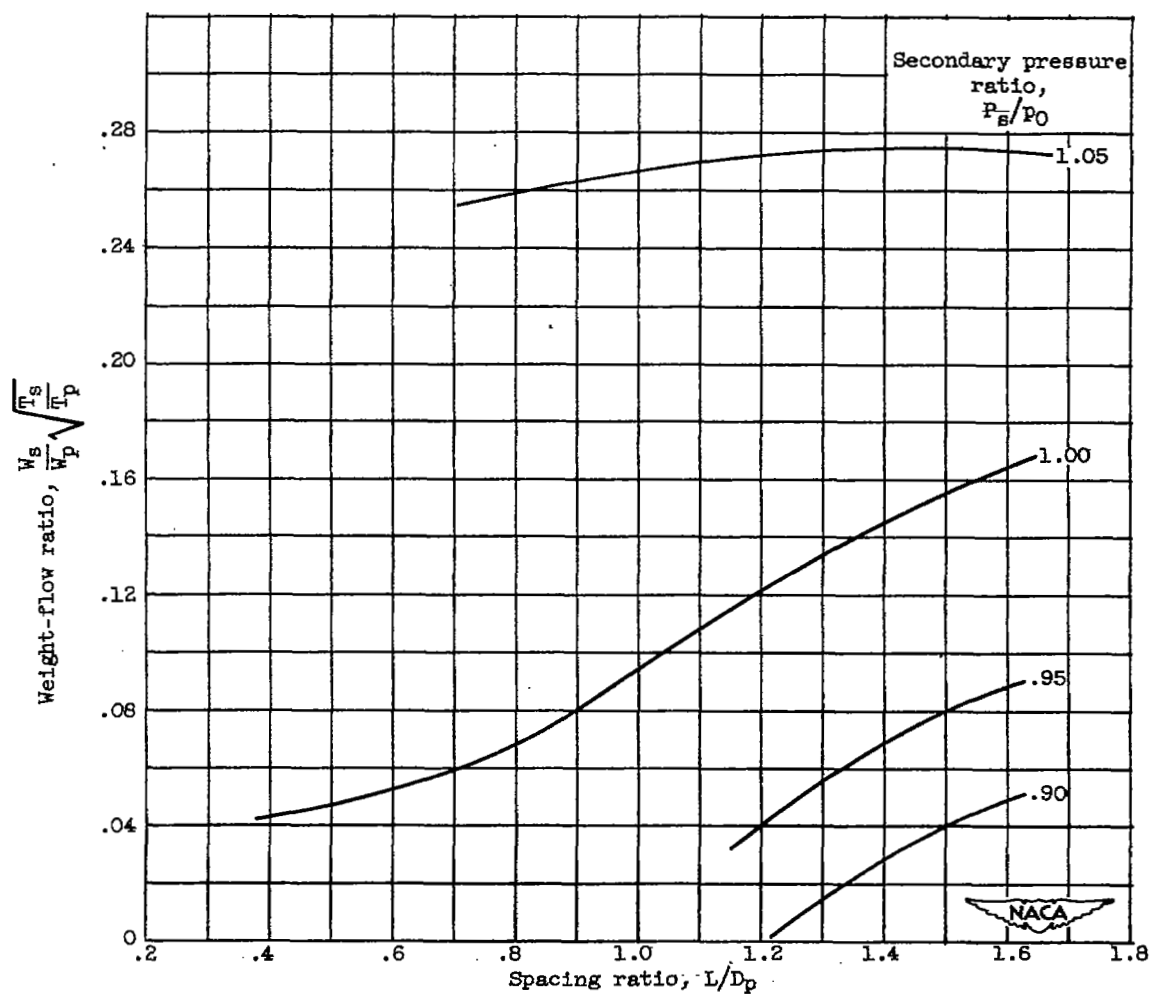
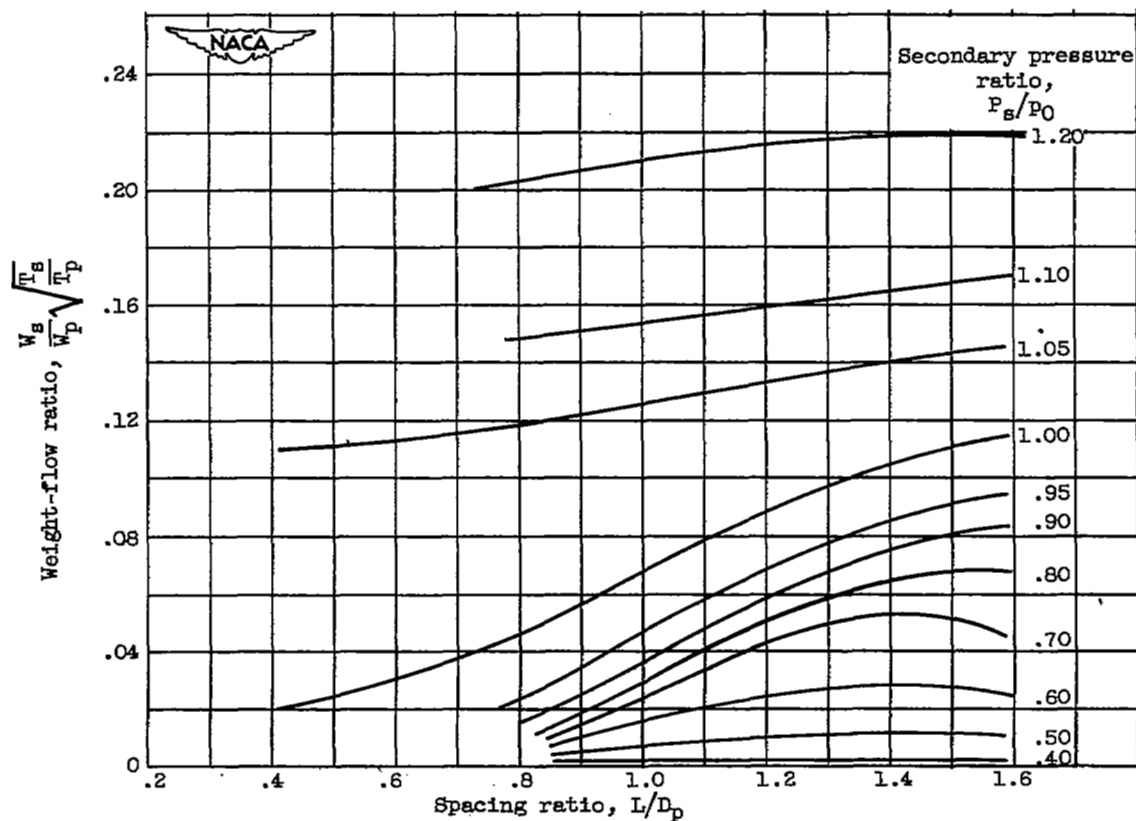


Figure 13. - Concluded. Effect of spacing ratio on ejector weight-flow ratio for diameter ratio of 1.21.



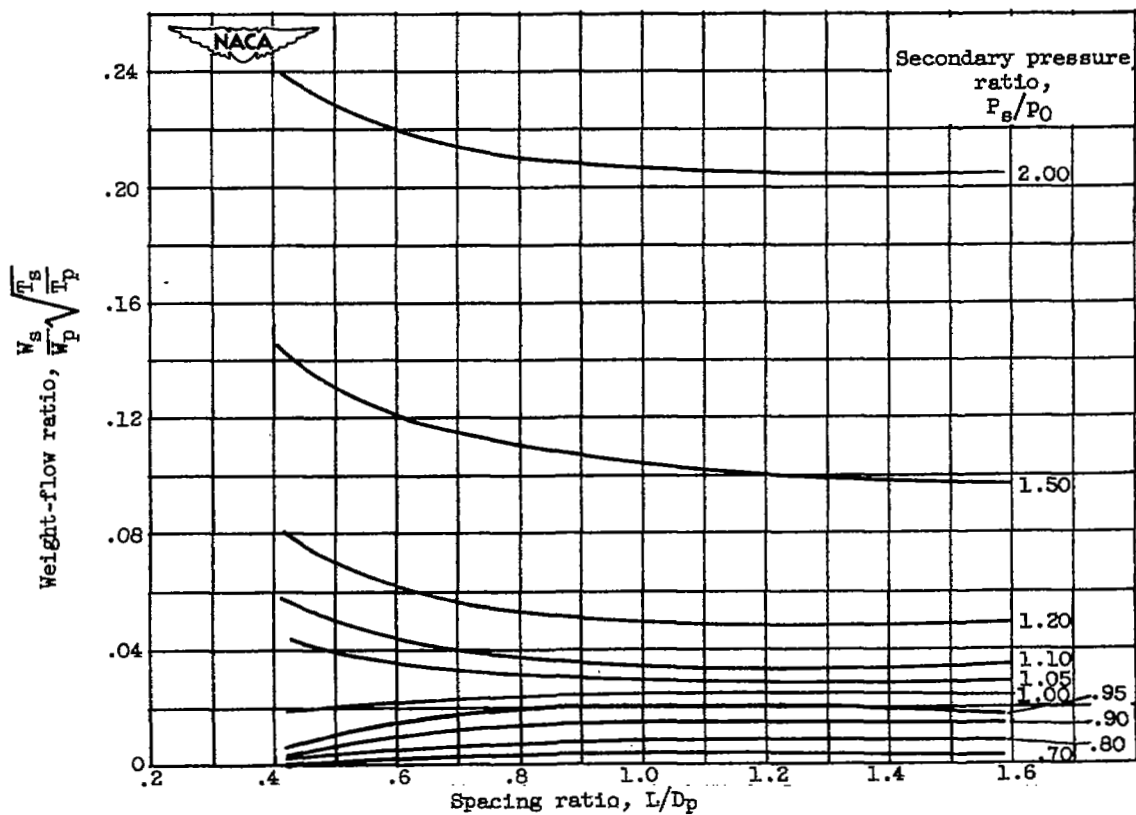
(a) Primary pressure ratio, 2.0.

Figure 14. - Effect of spacing ratio on ejector weight-flow ratio for diameter ratio of 1.41.



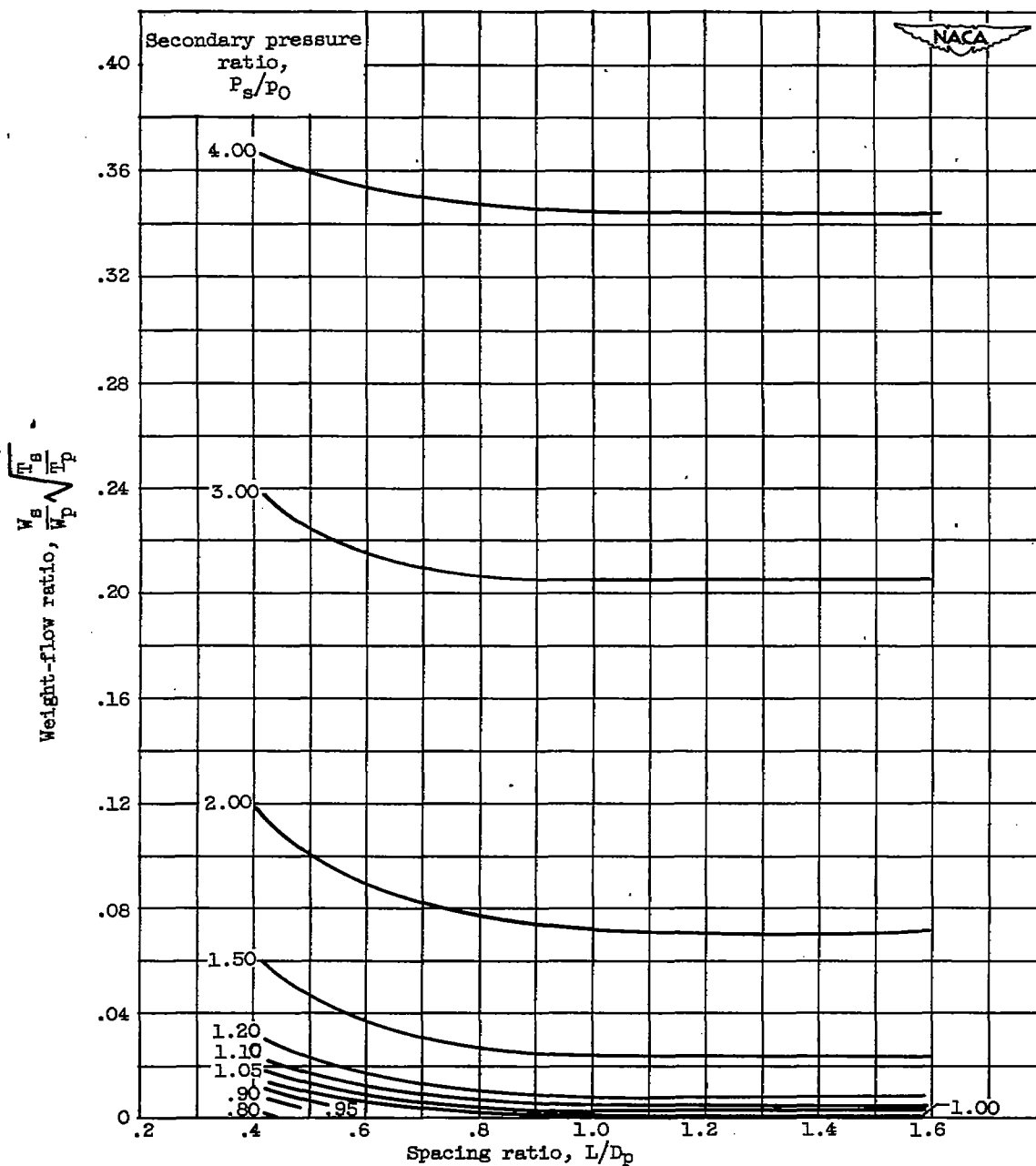
(b) Primary pressure ratio, 3.5.

Figure 14. - Continued. Effect of spacing ratio on ejector weight-flow ratio for diameter ratio of 1.41.



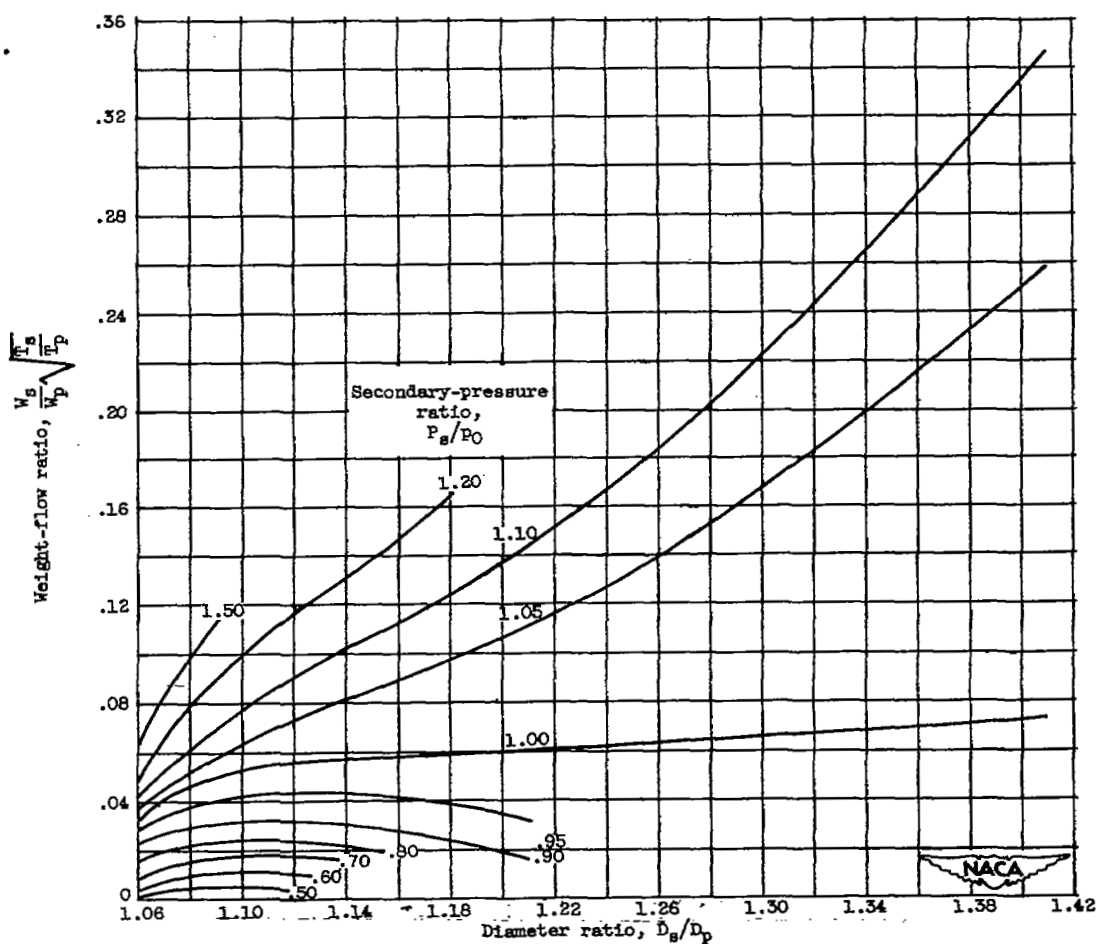
(c) Primary pressure ratio, 6.0.

Figure 14. - Continued. Effect of spacing ratio on ejector weight-flow ratio for diameter ratio of 1.41.



(d) Primary pressure ratio, 9.0.

Figure 14. - Concluded. Effect of spacing ratio on ejector weight-flow ratio for diameter ratio of 1.41.



(a) Primary pressure ratio, 2.0.

Figure 15. - Effect of diameter ratio on ejector weight-flow ratio for spacing ratio of 0.80.

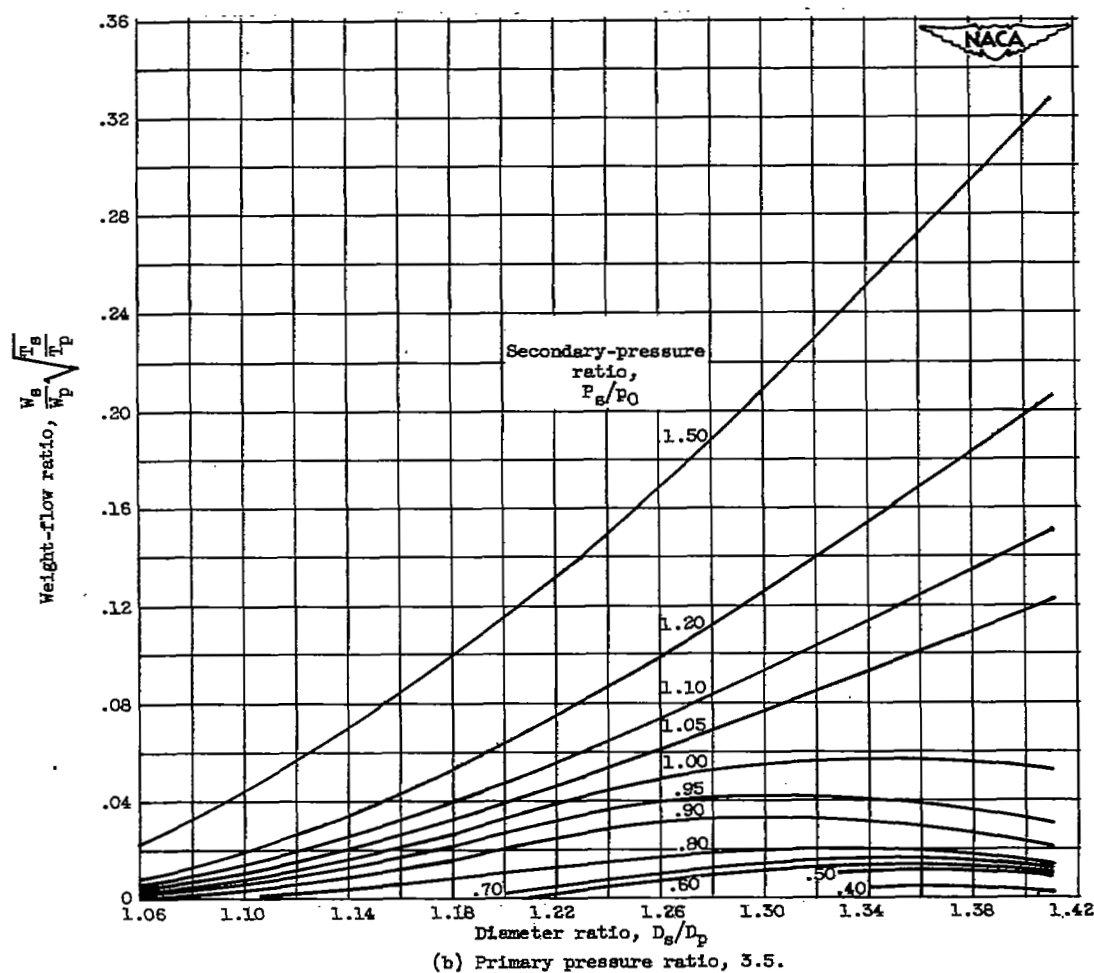
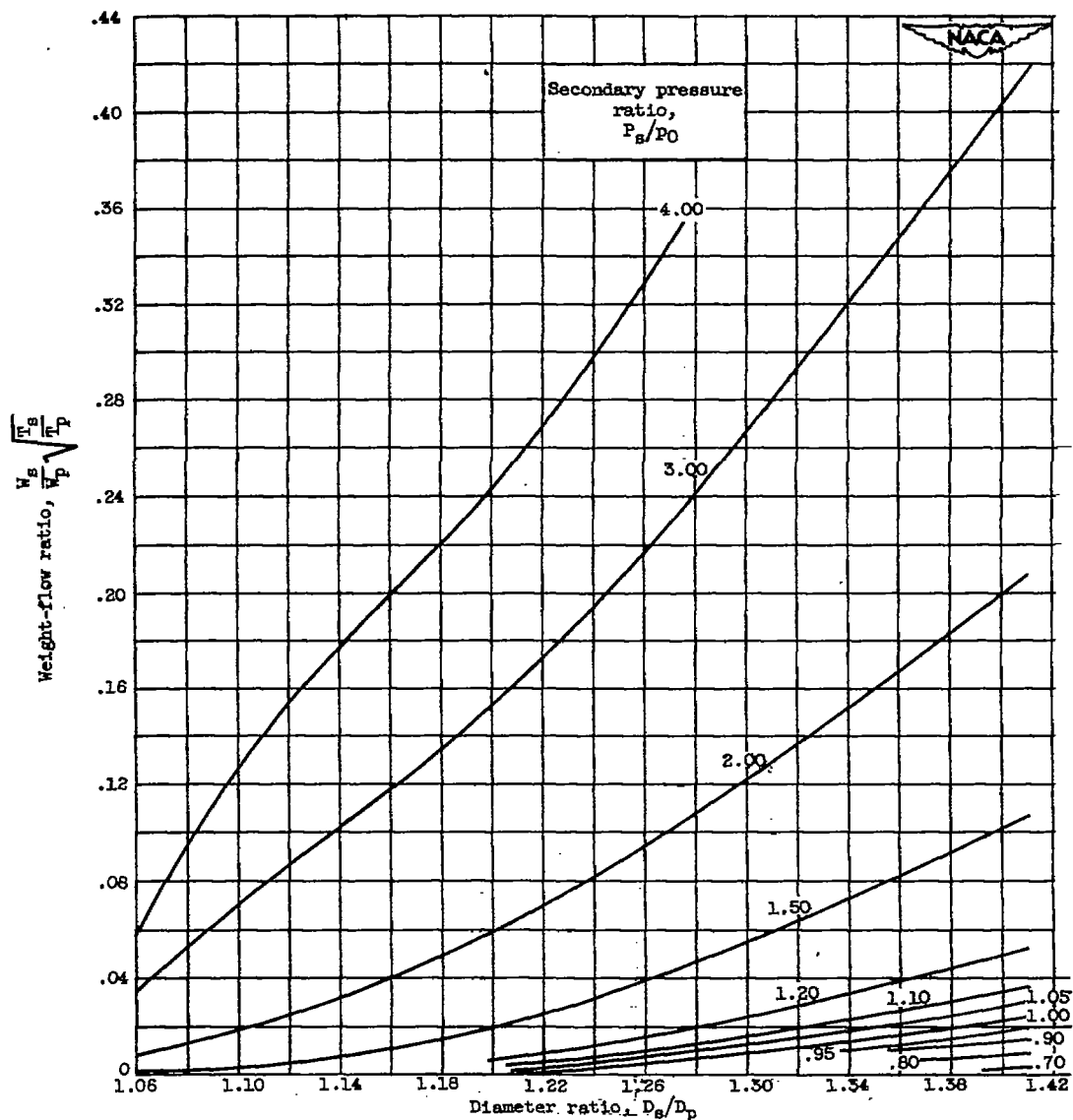


Figure 15. - Continued. Effect of diameter ratio on ejector weight-flow ratio for spacing ratio of 0.80.



(c) Primary pressure ratio, 6.0.

Figure 15. - Concluded. Effect of diameter ratio on ejector weight-flow ratio for a spacing ratio of 0.80.

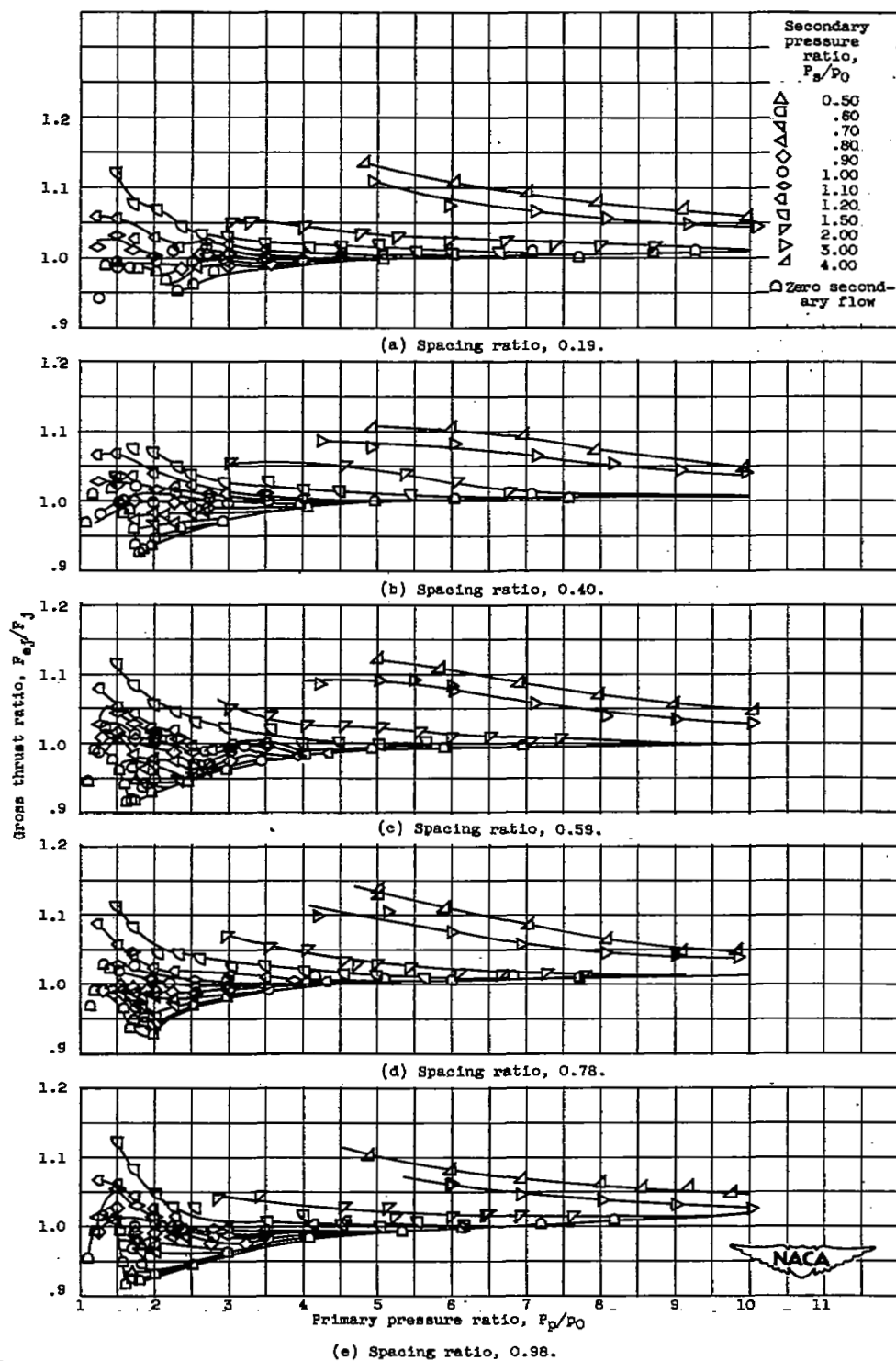


Figure 16. - Effect of primary pressure ratio on ejector gross thrust ratio at diameter ratio of 1.06.

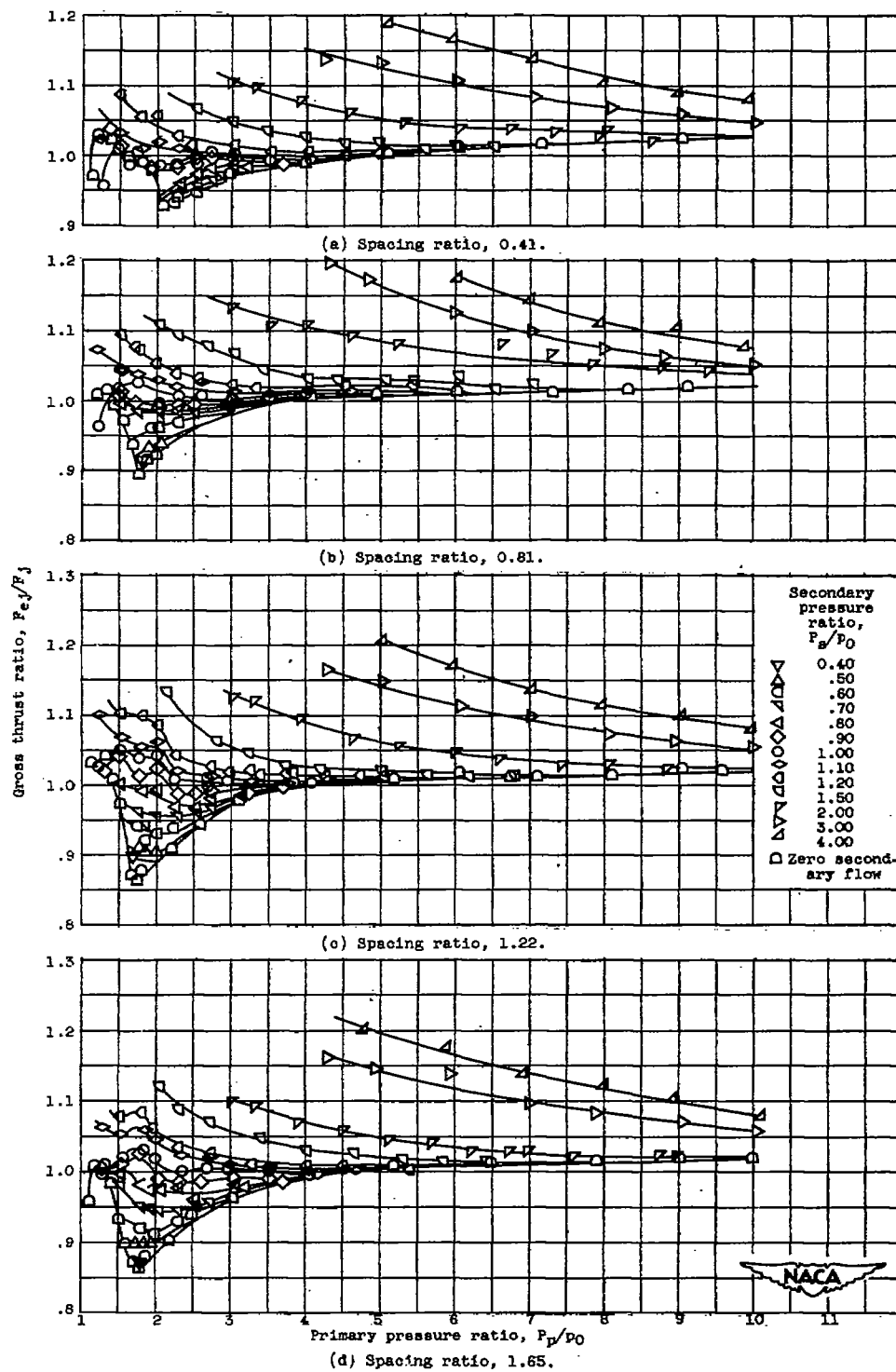


Figure 17. - Effect of primary pressure ratio on ejector gross thrust ratio at diameter ratio of 1.11.

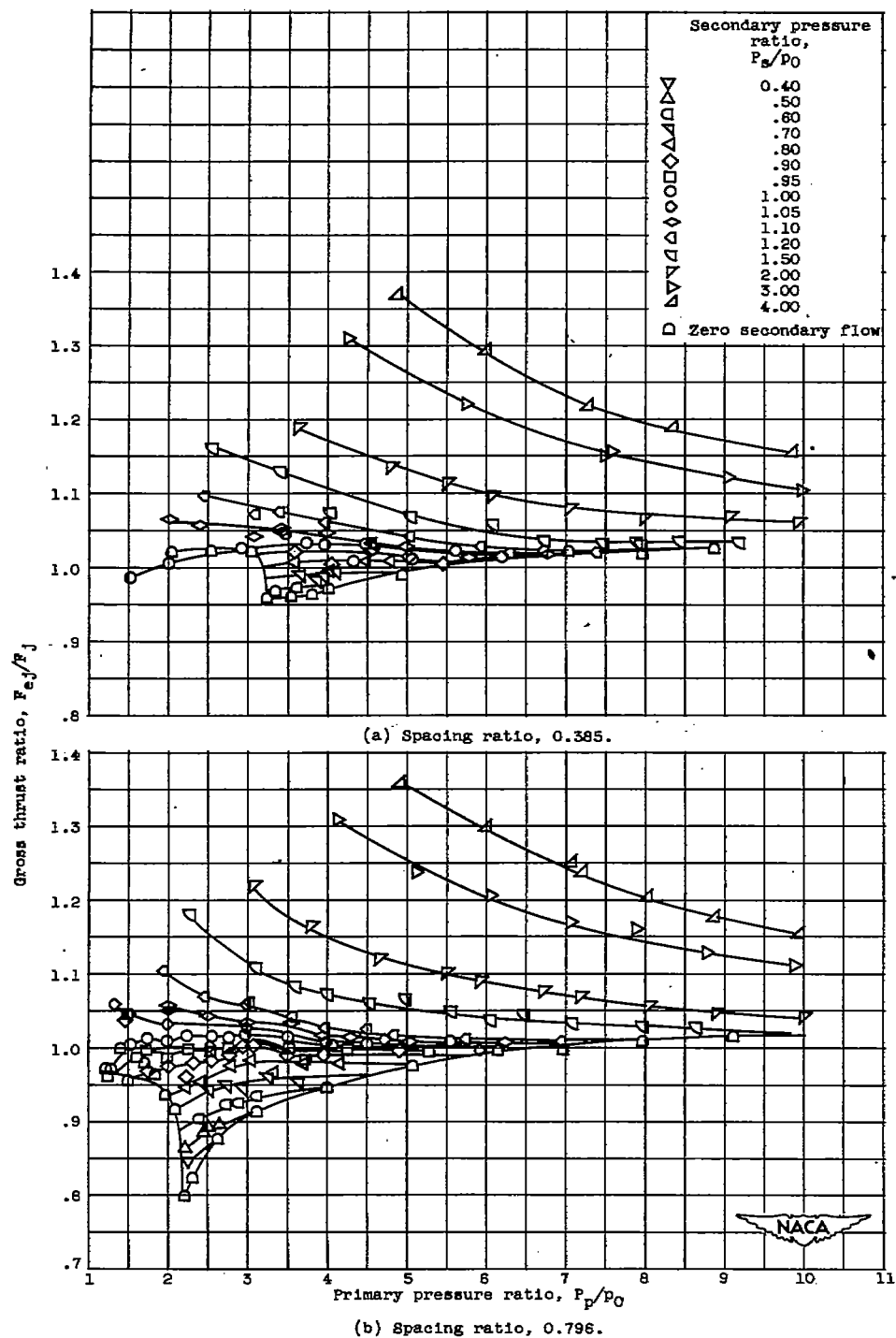


Figure 18. - Effect of primary pressure ratio on ejector gross thrust ratio at diameter ratio of 1.21.

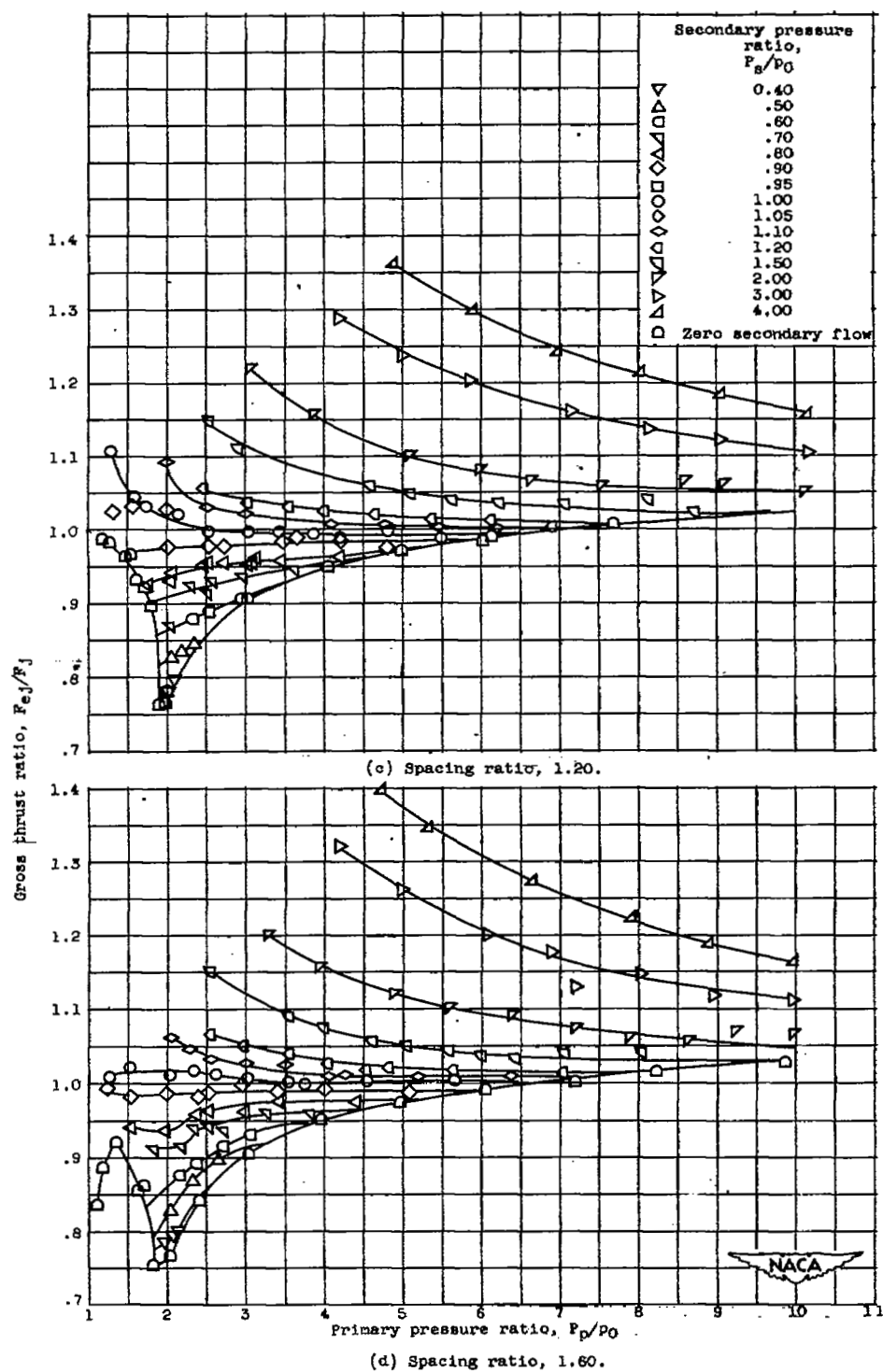


Figure 18. - Concluded. Effect of primary pressure ratio on ejector gross thrust ratio at diameter ratio of 1.21.

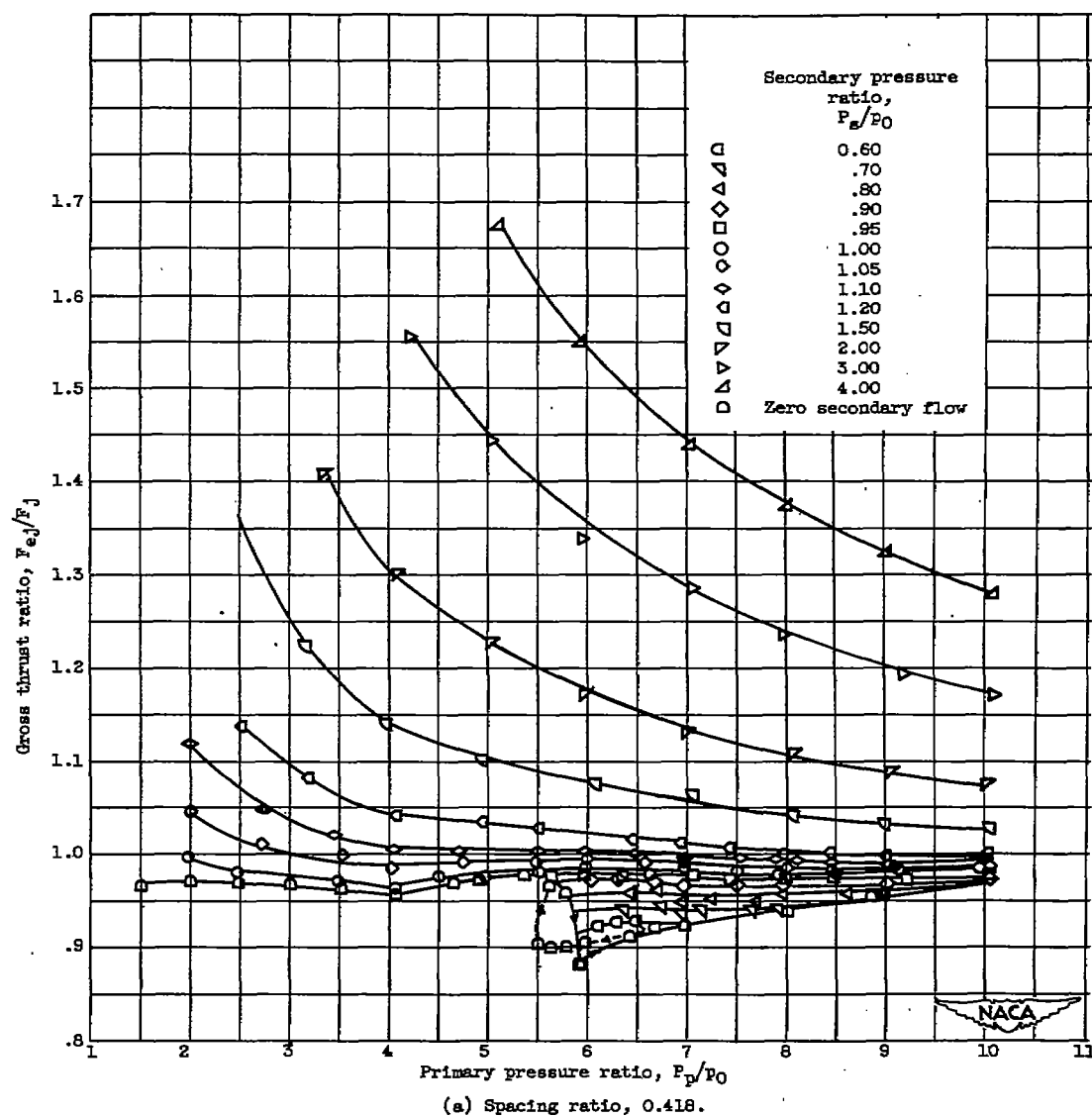


Figure 19. - Effect of primary pressure ratio on ejector gross thrust ratio at diameter ratio of 1.41.

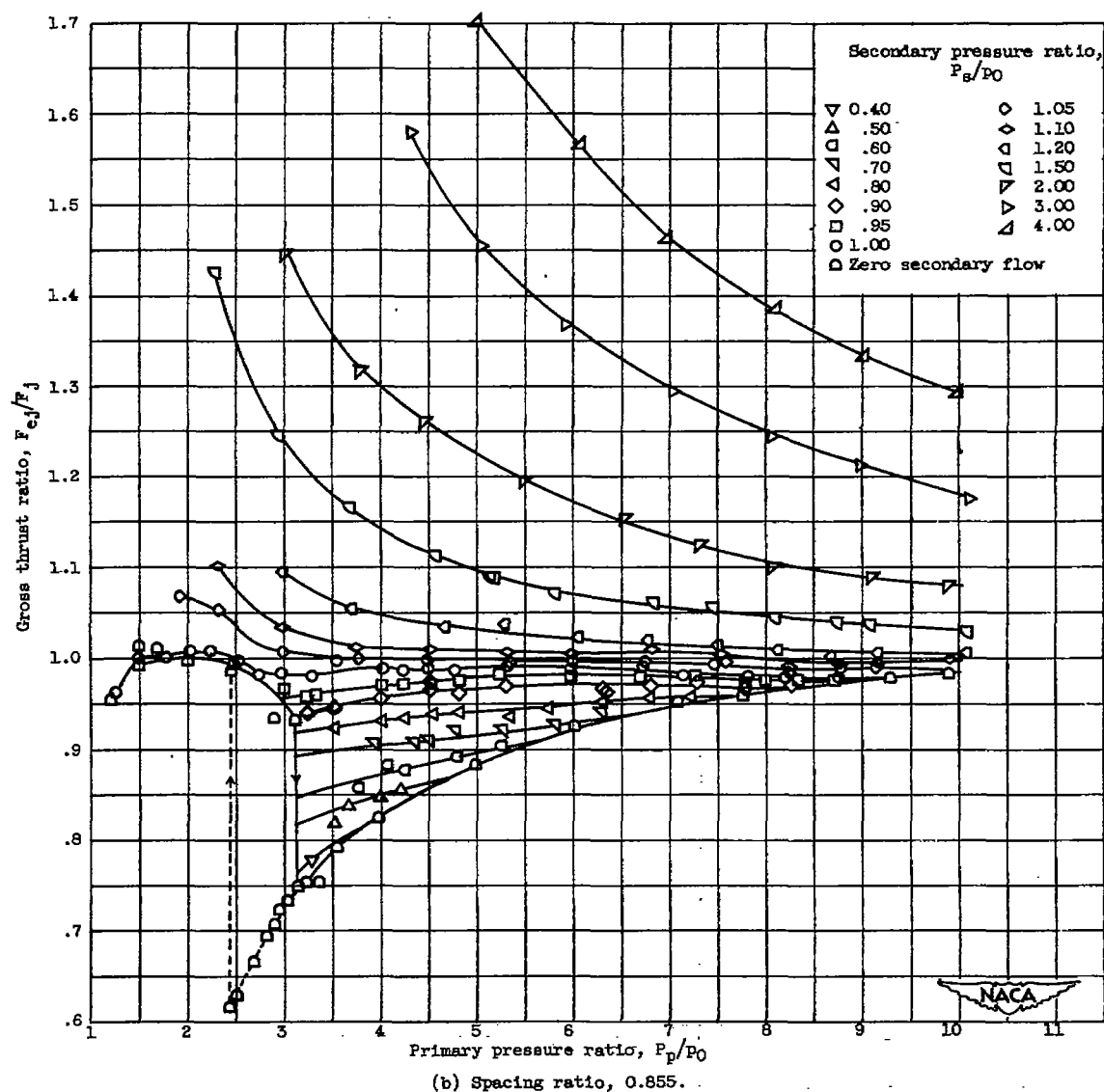
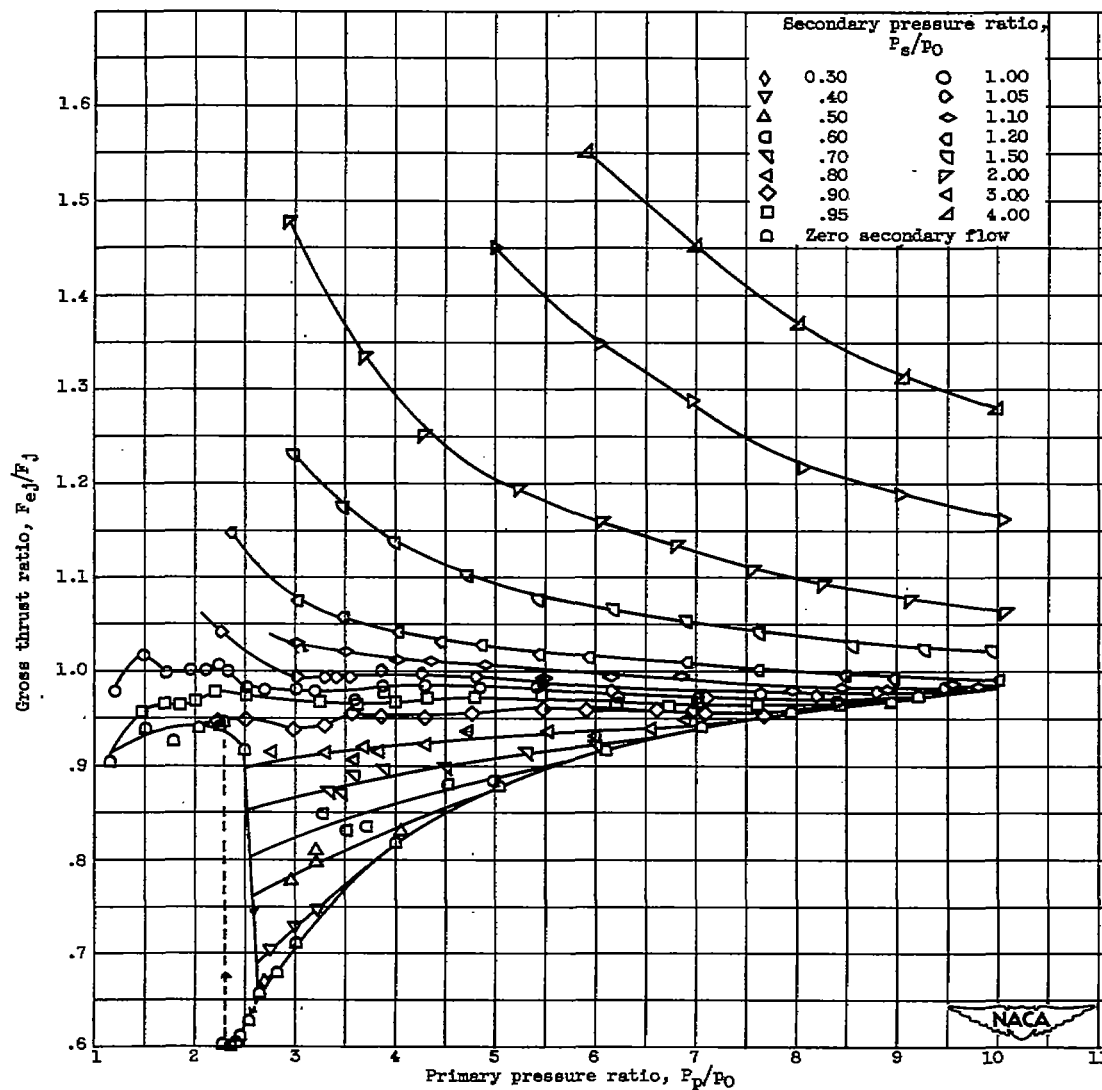


Figure 19. - Continued. Effect of primary pressure ratio on ejector gross thrust ratio at diameter ratio of 1.41.



(c) Spacing ratio, 1.22.

Figure 19, - Effect of primary pressure ratio on ejector gross thrust ratio at diameter ratio of 1.41.

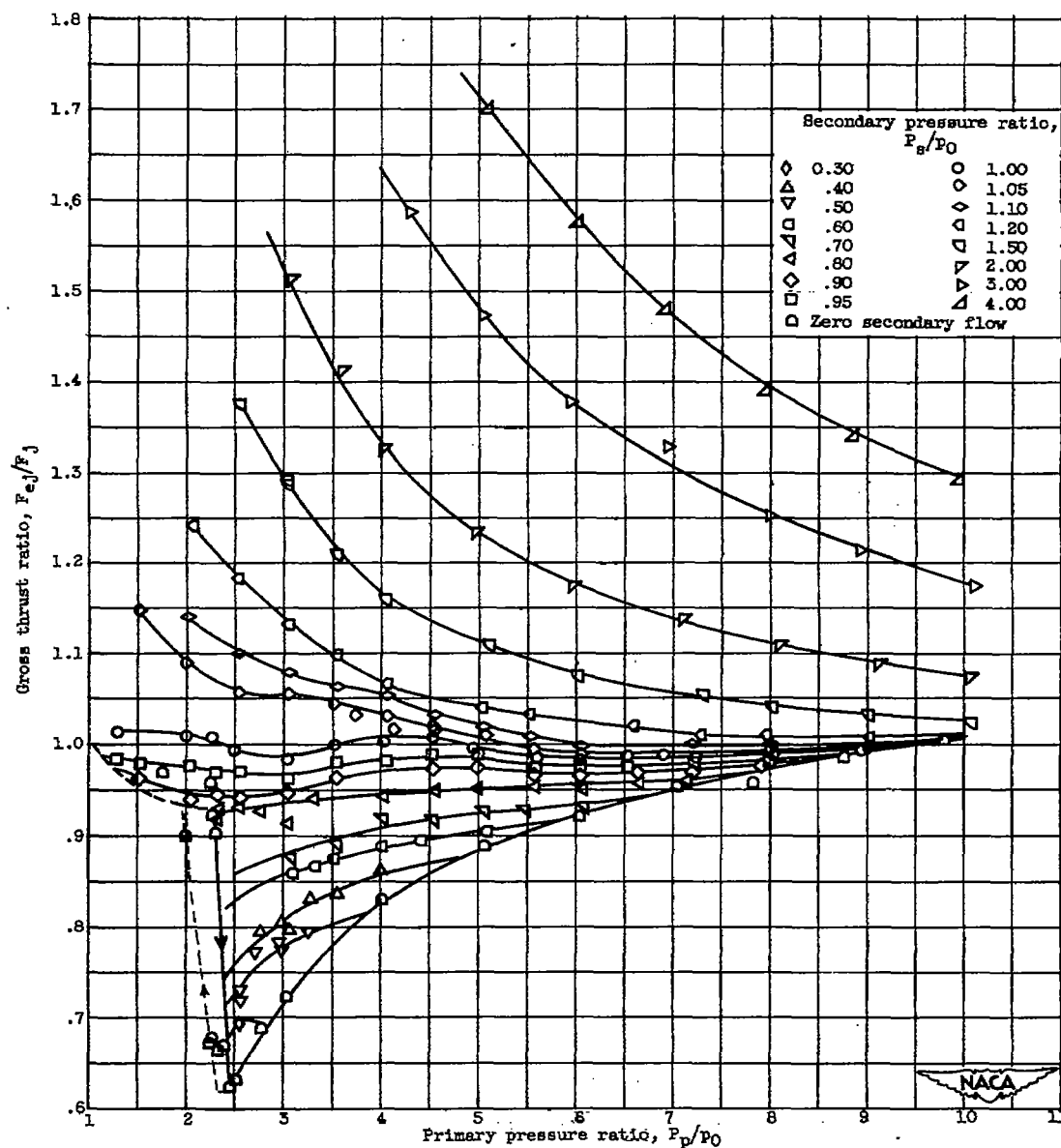


Figure 19. - Concluded. Effect of primary pressure ratio on ejector gross thrust ratio at diameter ratio of 1.41.

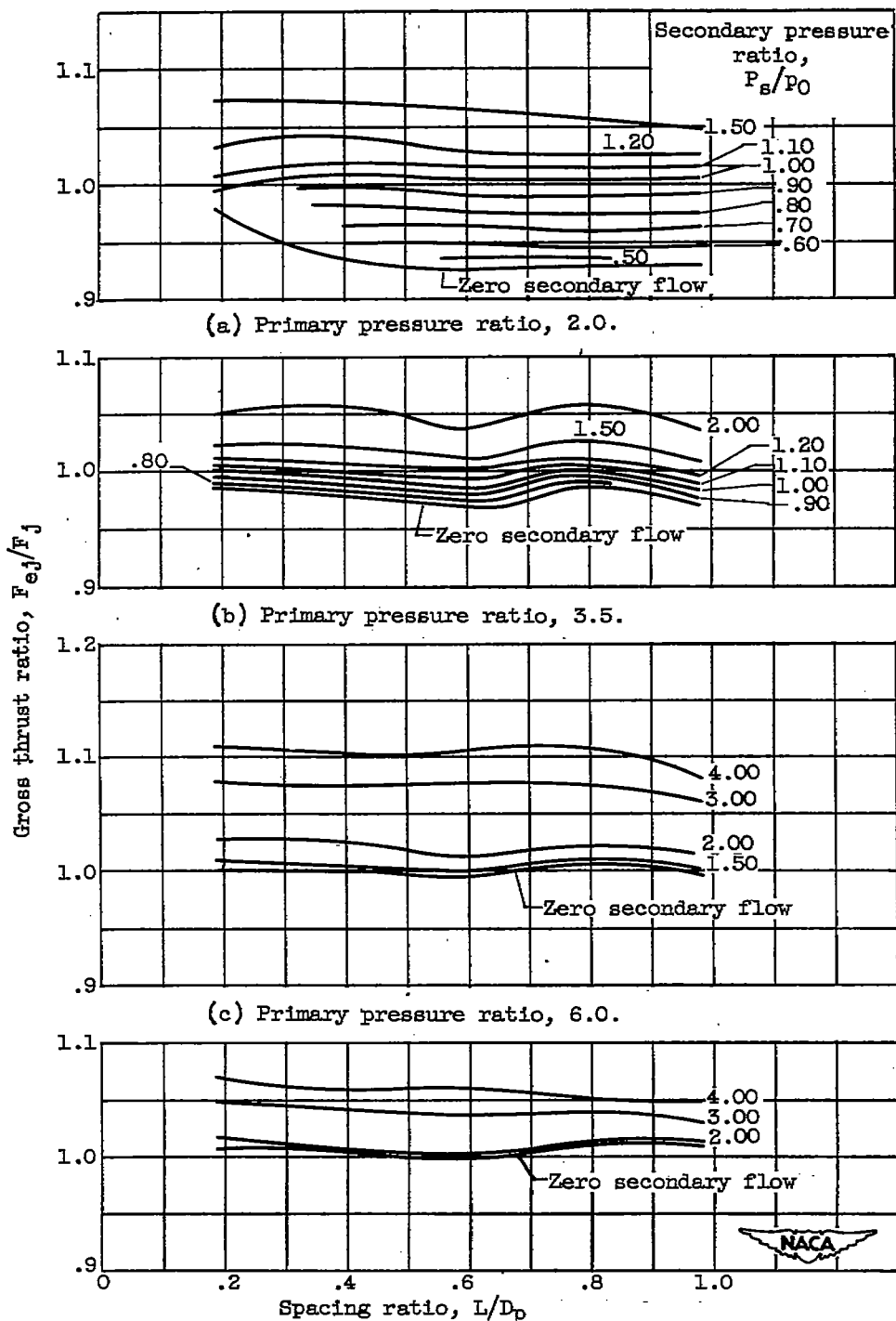


Figure 20. - Effect of spacing ratio on ejector gross thrust ratio for diameter ratio of 1.06.

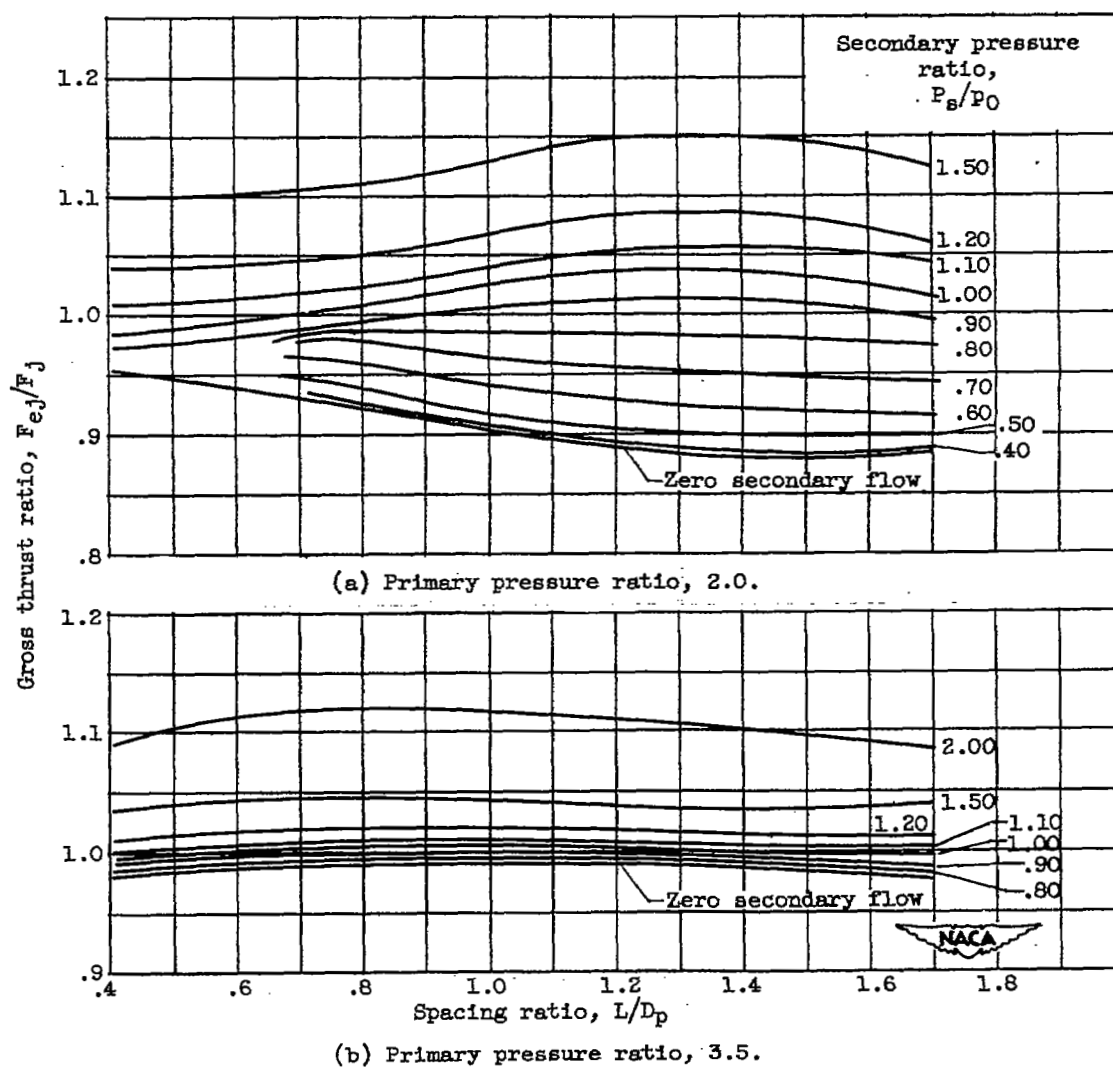
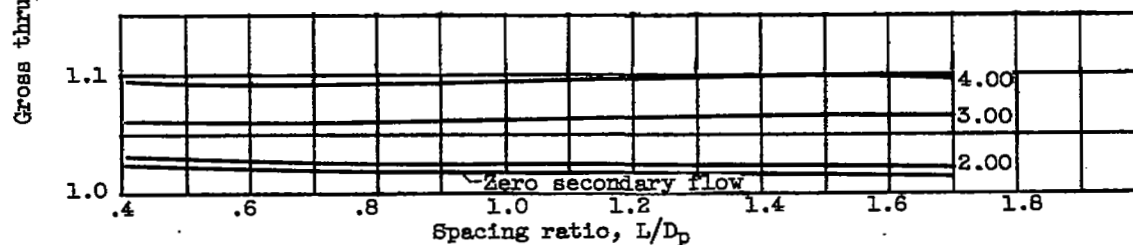


Figure 21. - Effect of spacing ratio on ejector gross thrust ratio for diameter ratio of 1.11.



(c) Primary pressure ratio, 6.0.



(d) Primary pressure ratio, 9.0.

Figure 21. - Concluded. Effect of spacing ratio on ejector gross thrust ratio for diameter ratio of 1.11.

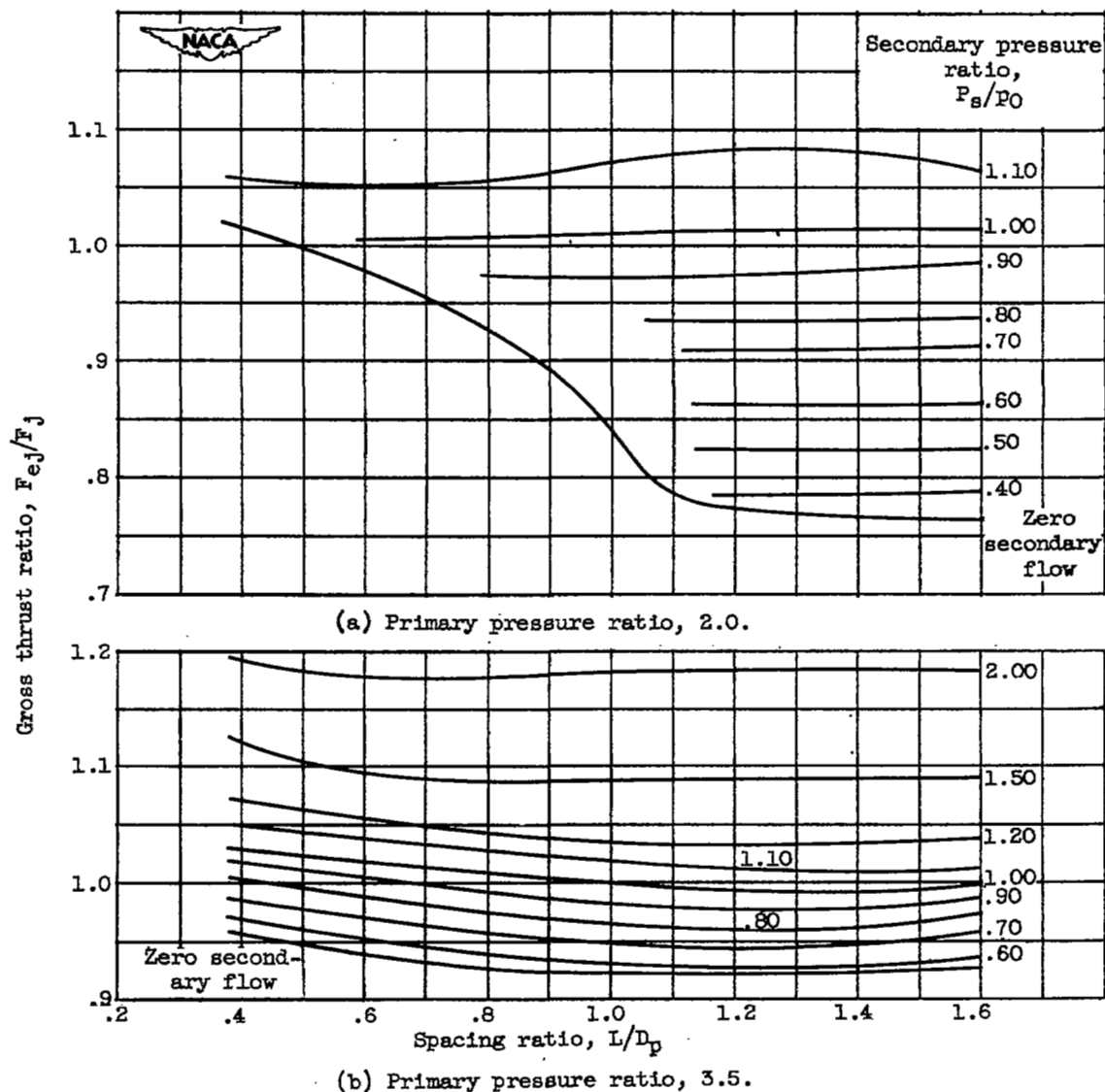


Figure 22. - Effect of spacing ratio on ejector gross thrust ratio for diameter ratio of 1.21.

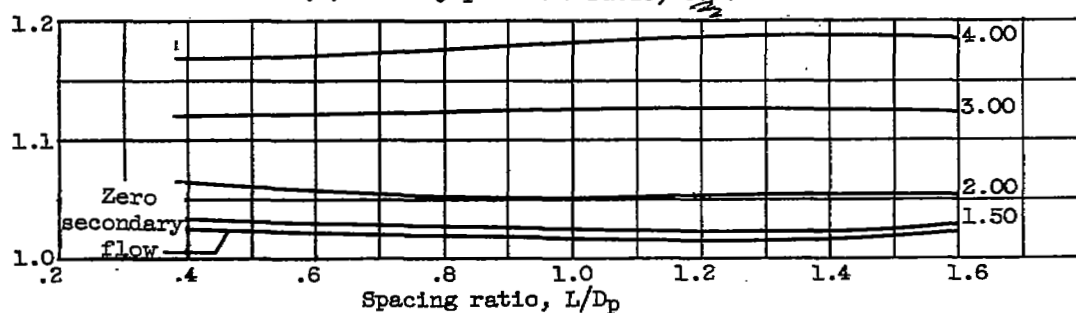
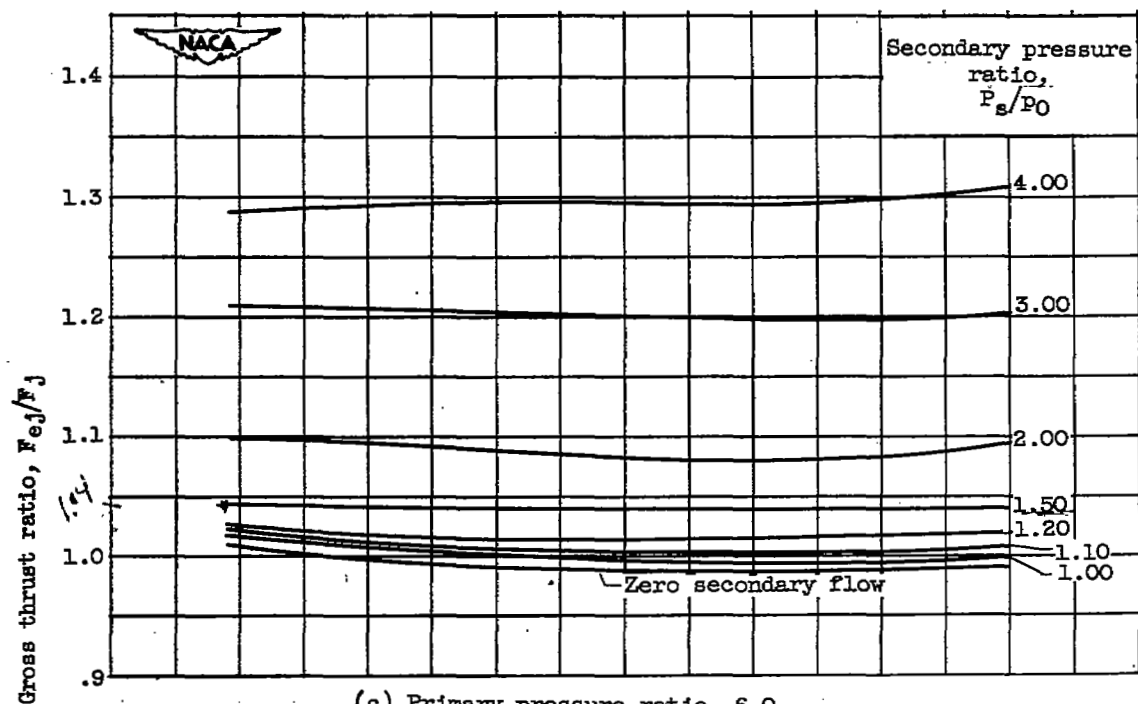
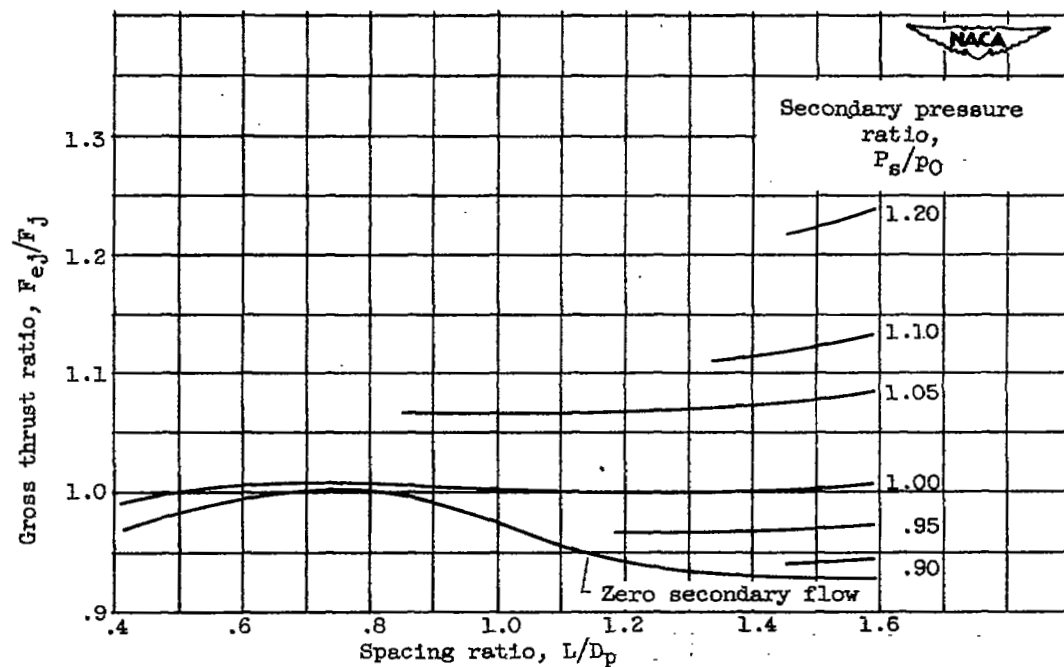


Figure 22. - Concluded. Effect of spacing ratio on ejector gross thrust ratio for diameter ratio of 1.21.

$$\frac{F_{ej}}{F_j} = 1.04$$

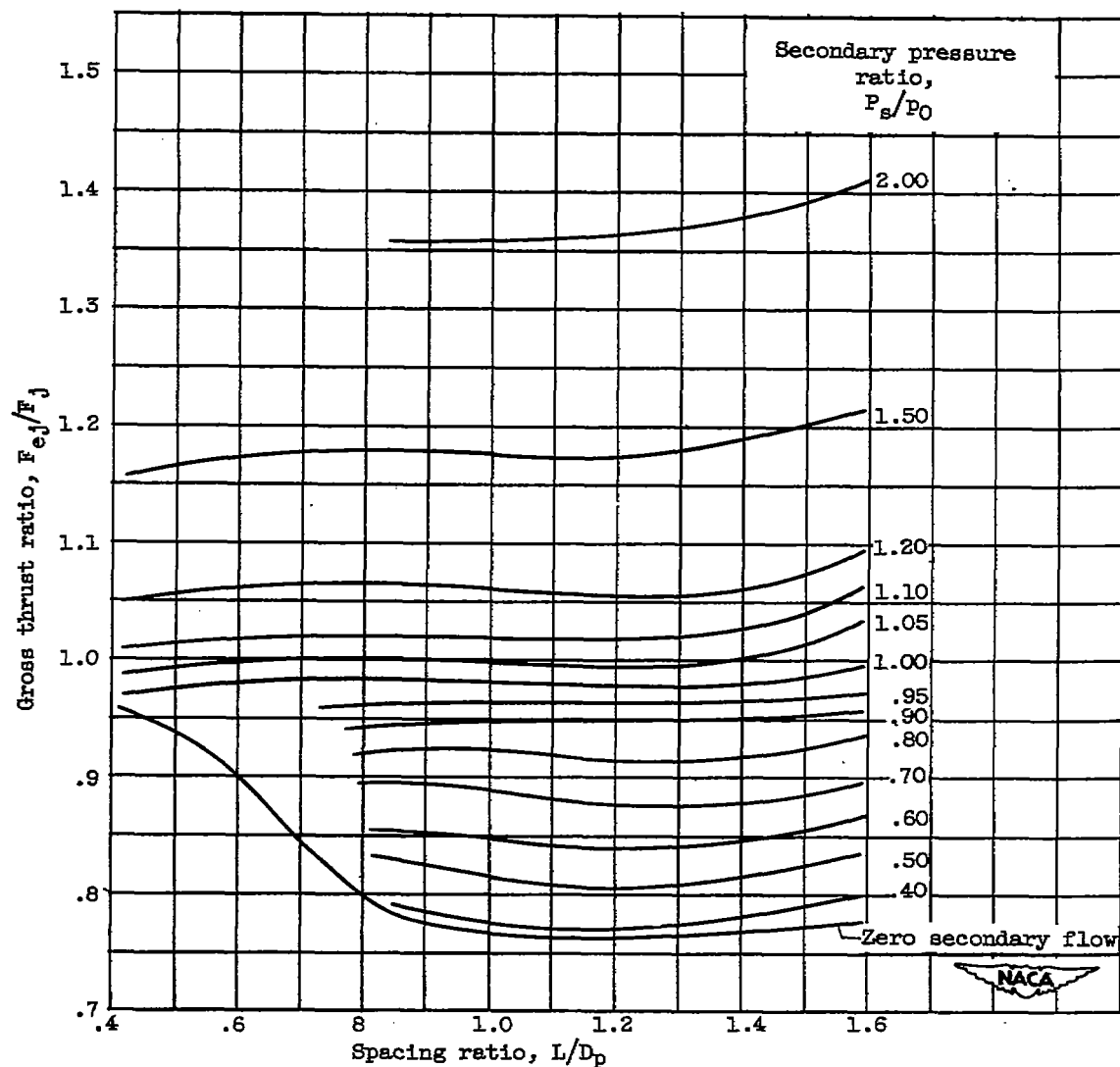
$$F_{ej} = 1.04 F_j$$

$$C_{Dm} = \frac{T}{\dot{m} V}$$



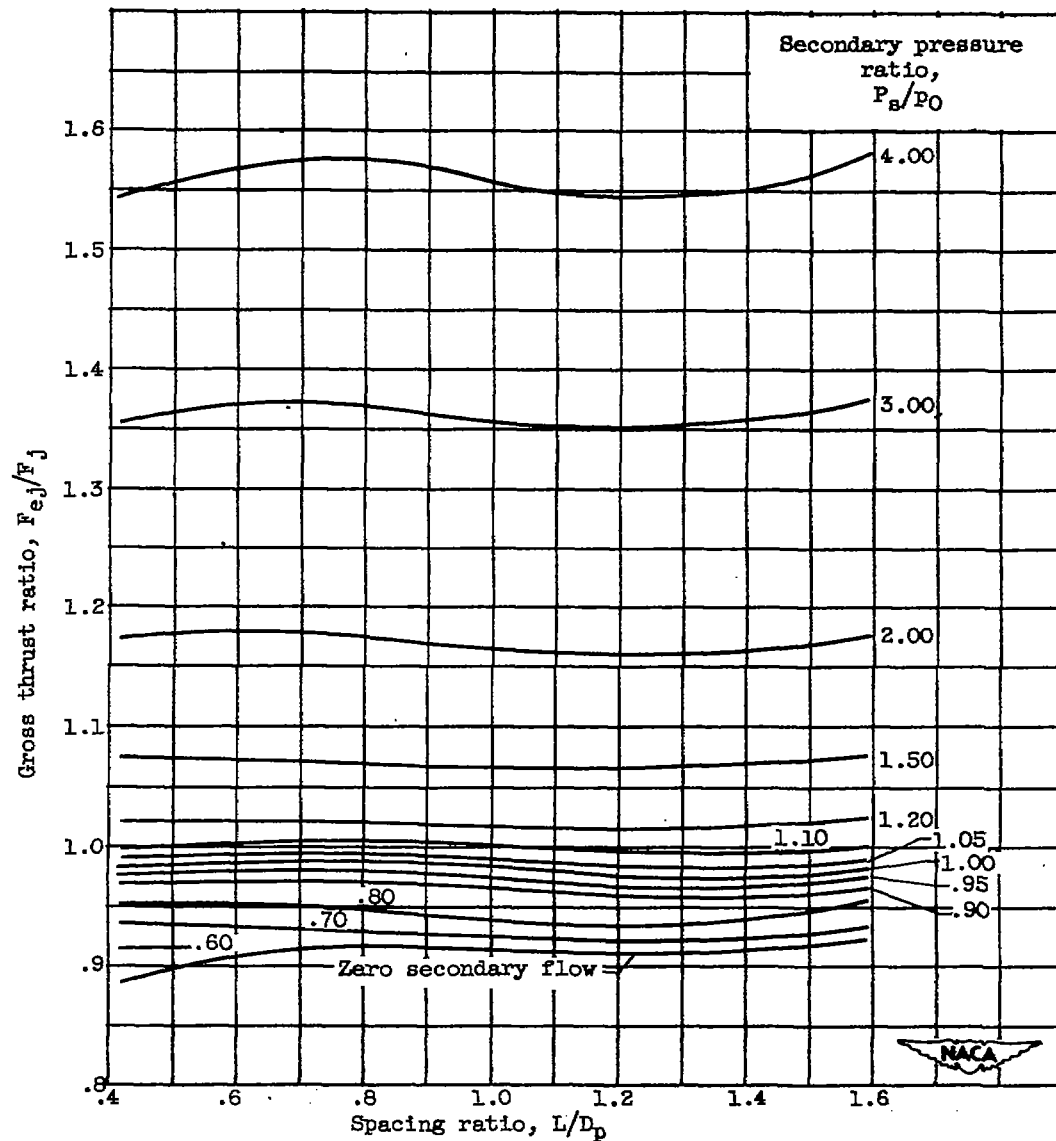
(a) Primary pressure ratio, 2.0.

Figure 23. - Effect of spacing ratio on ejector gross thrust ratio for diameter ratio of 1.41.



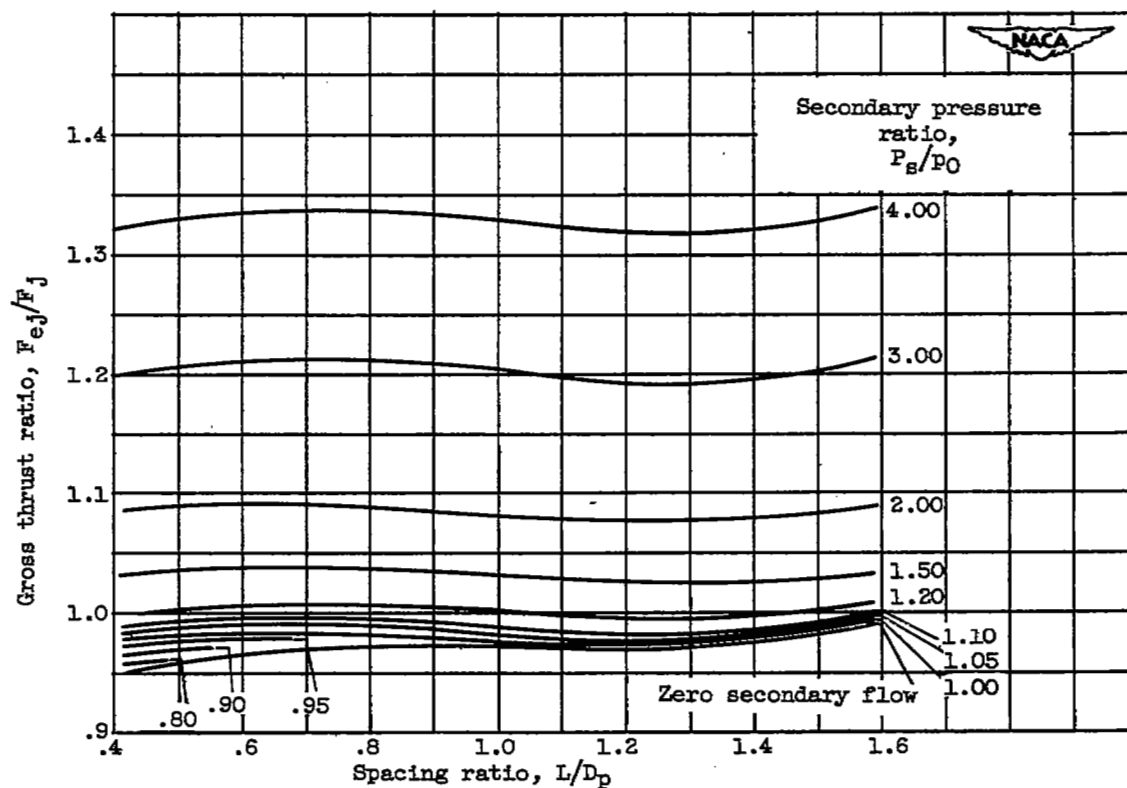
(b) Primary pressure ratio, 3.5.

Figure 23. - Continued. Effect of spacing ratio on ejector gross thrust ratio for diameter ratio of 1.41.



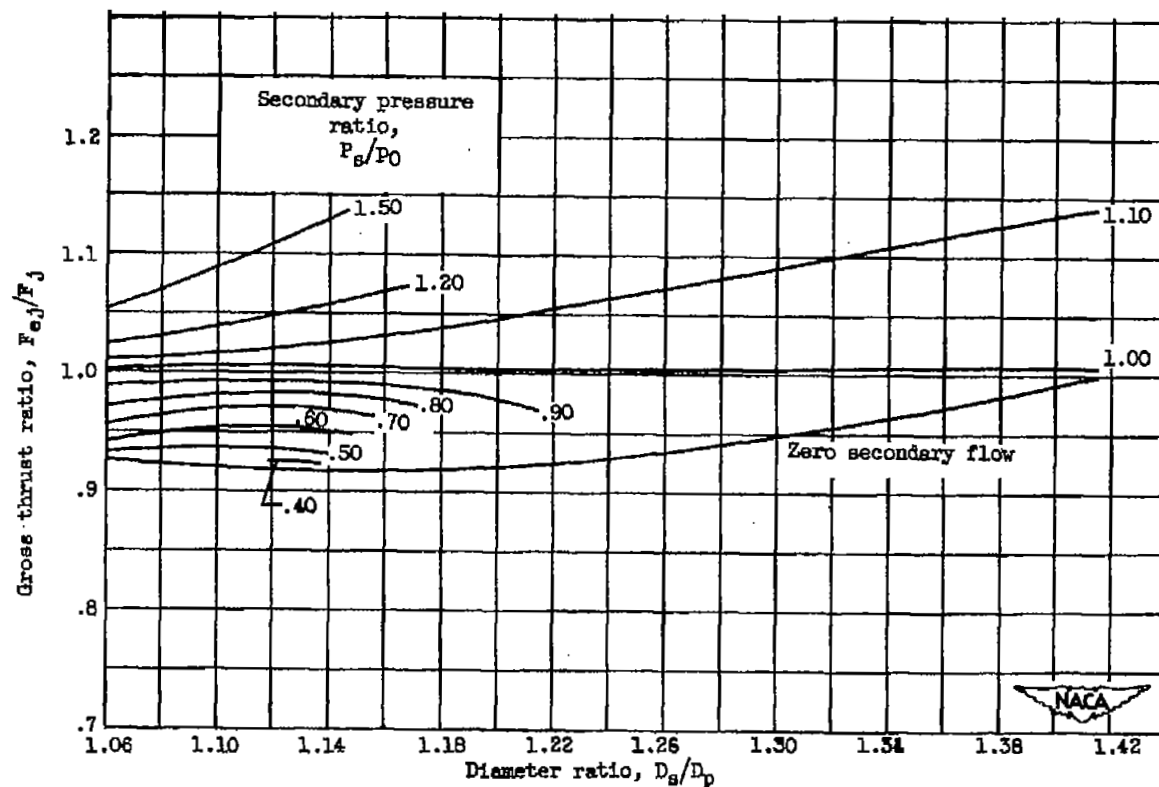
(c) Primary pressure ratio, 6.0.

Figure 23. - Continued. Effect of spacing ratio on ejector gross thrust ratio for diameter ratio of 1.41.



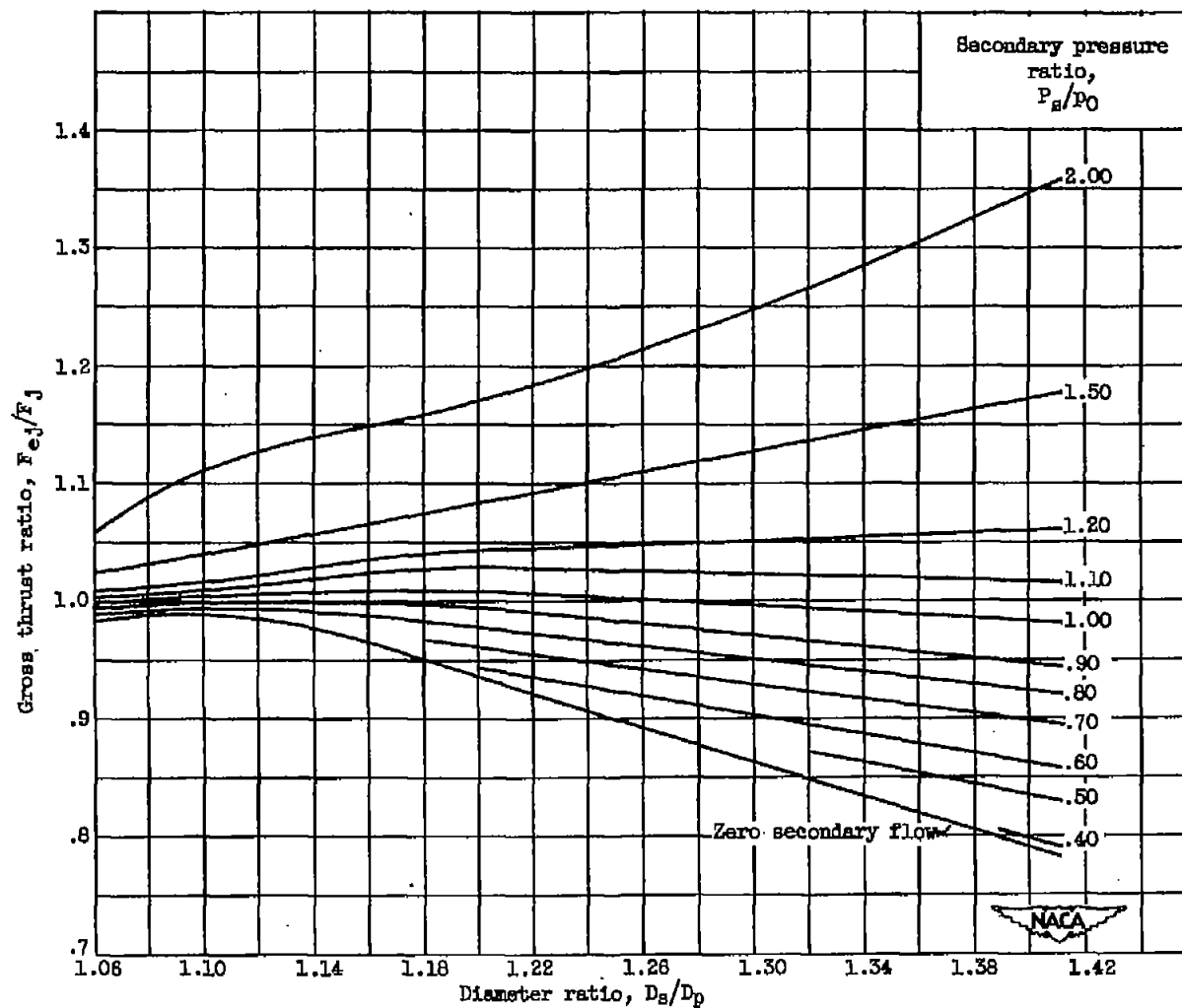
(d) Primary pressure ratio, 9.0.

Figure 23. - Concluded. Effect of spacing ratio on ejector gross thrust ratio for diameter ratio of 1.41.



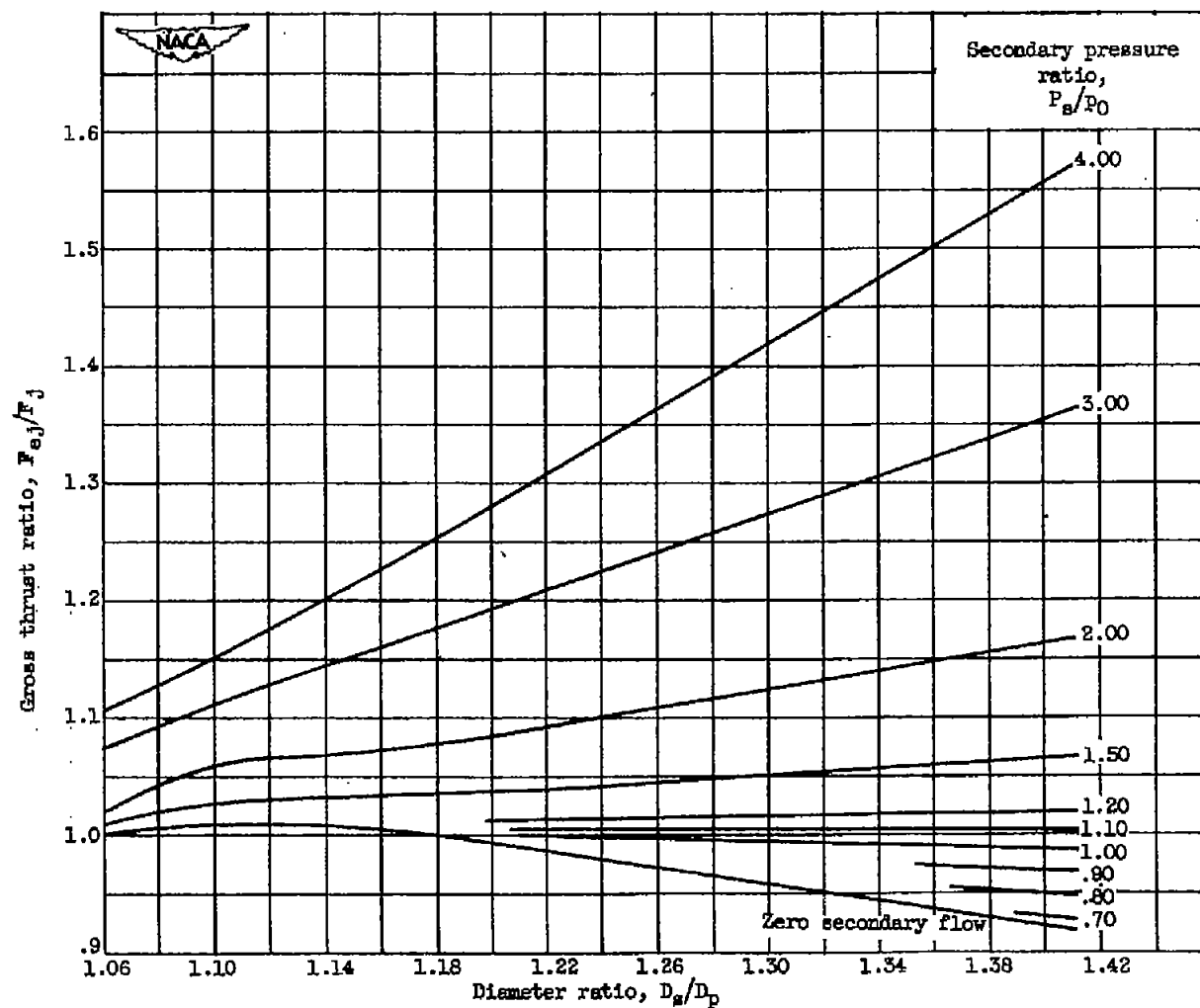
(a) Primary pressure ratio, 2.0.

Figure 24. - Effect of diameter ratio on ejector gross thrust ratio for spacing ratio of 0.80.



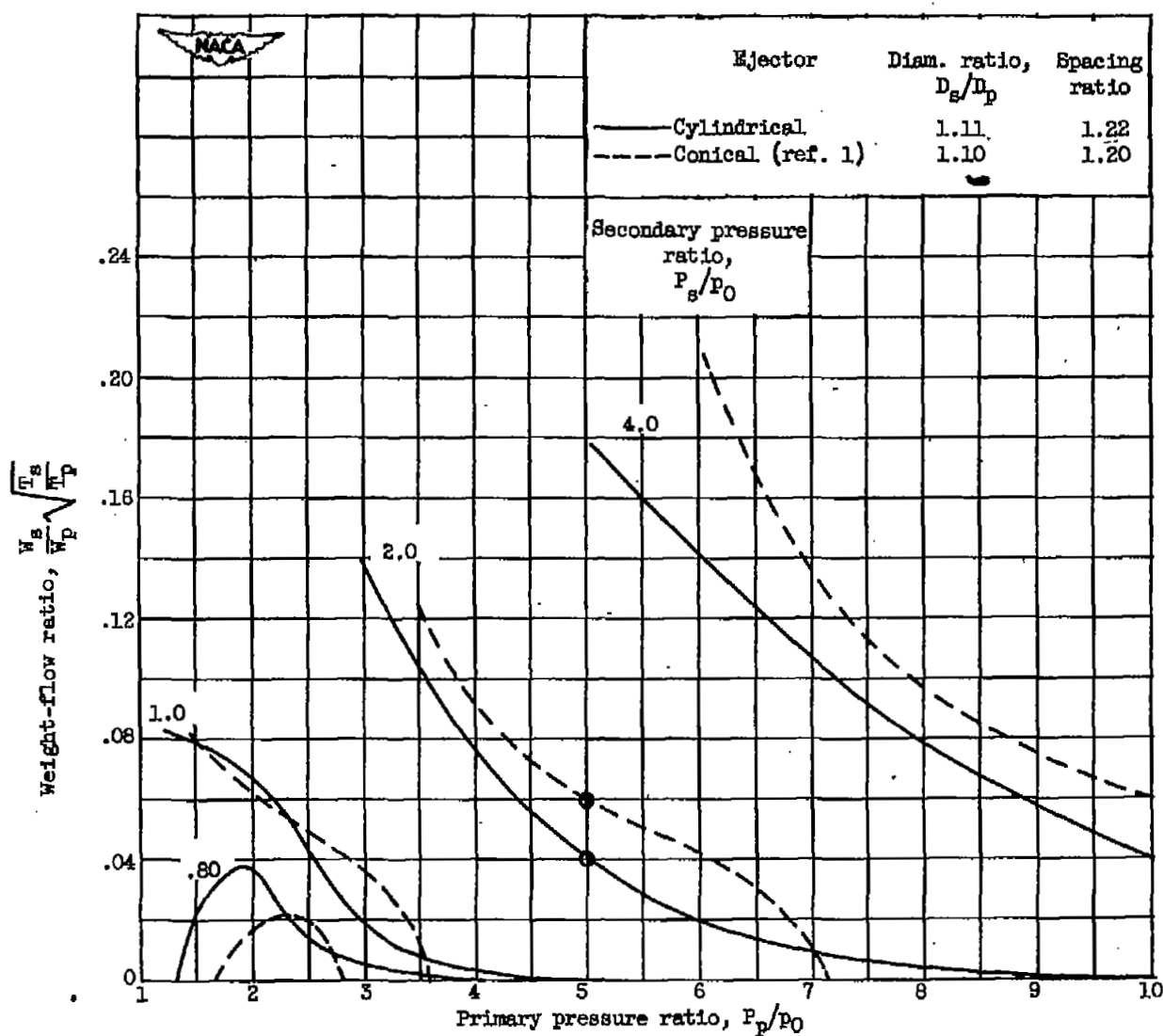
(b) Primary pressure ratio, 3.5.

Figure 24. - Continued. Effect of diameter ratio on ejector gross thrust ratio for spacing ratio of 0.80.



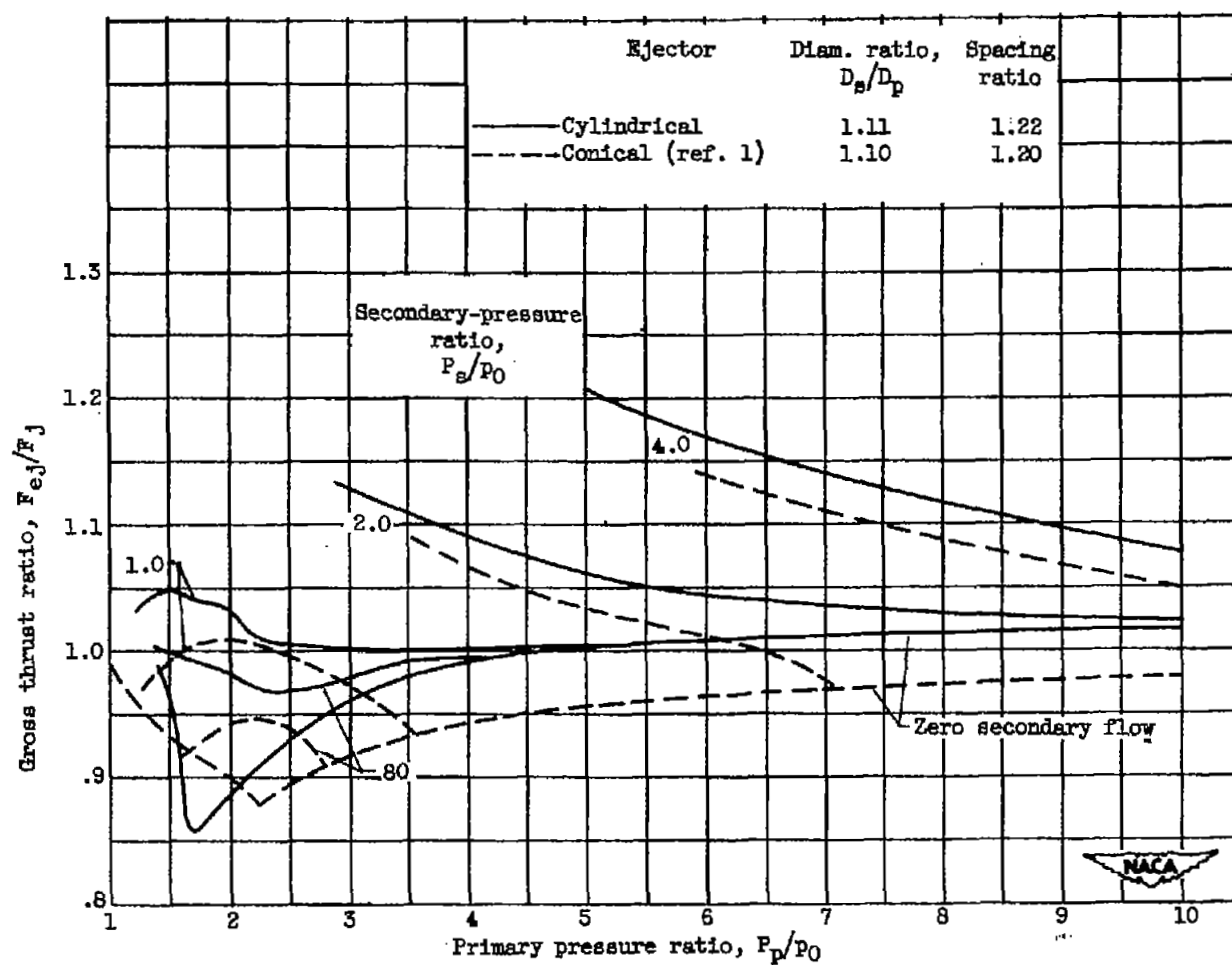
(c) Primary pressure ratio, 8.0.

Figure 24. - Concluded. Effect of diameter ratio on ejector gross thrust ratio for spacing ratio of 0.80.



(a) Pumping characteristics.

Figure 25. - Comparison of cylindrical and conical ejectors.



(b) Thrust characteristics.

Figure 25. - Concluded. Comparison of cylindrical and conical ejectors.

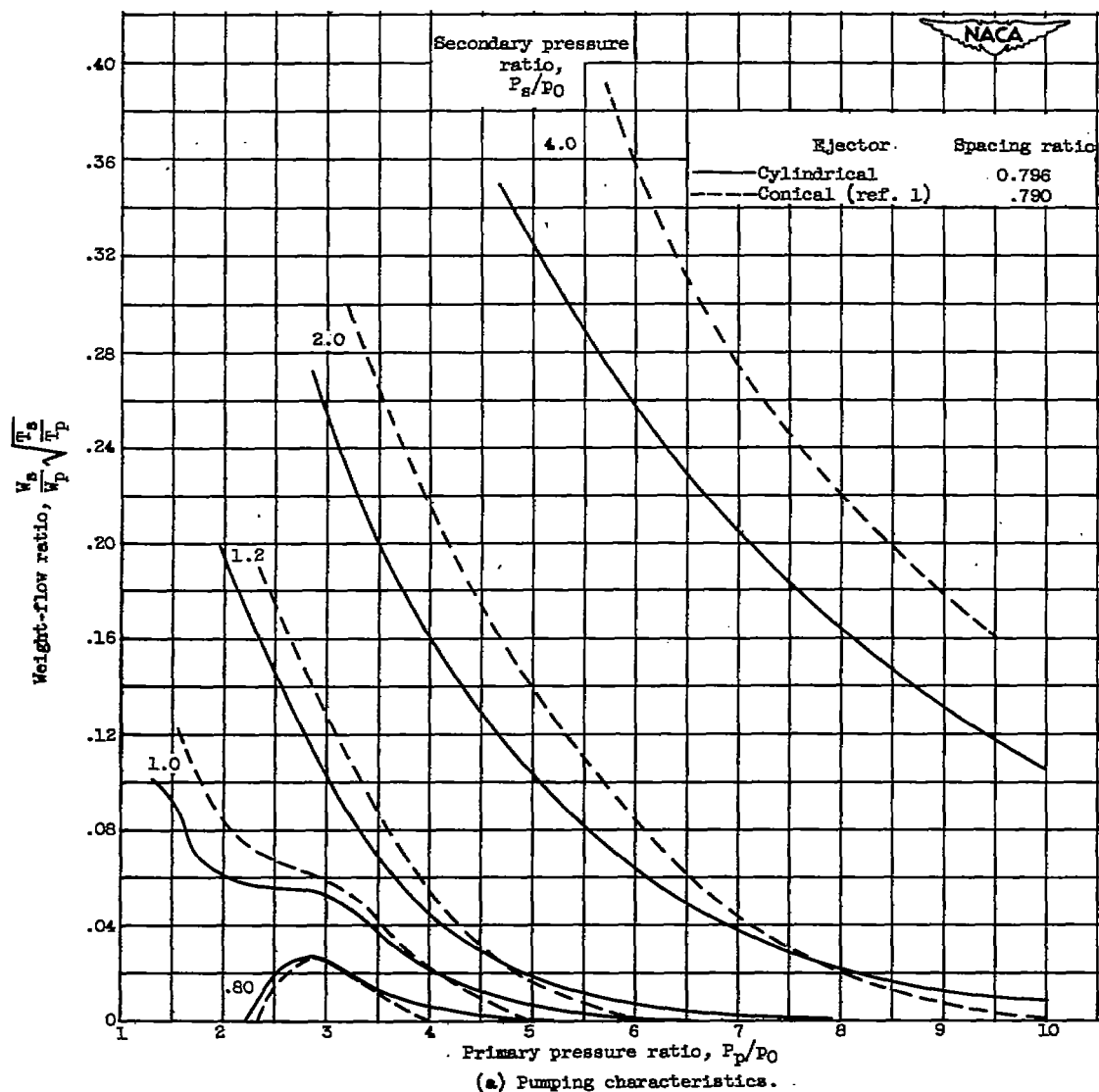
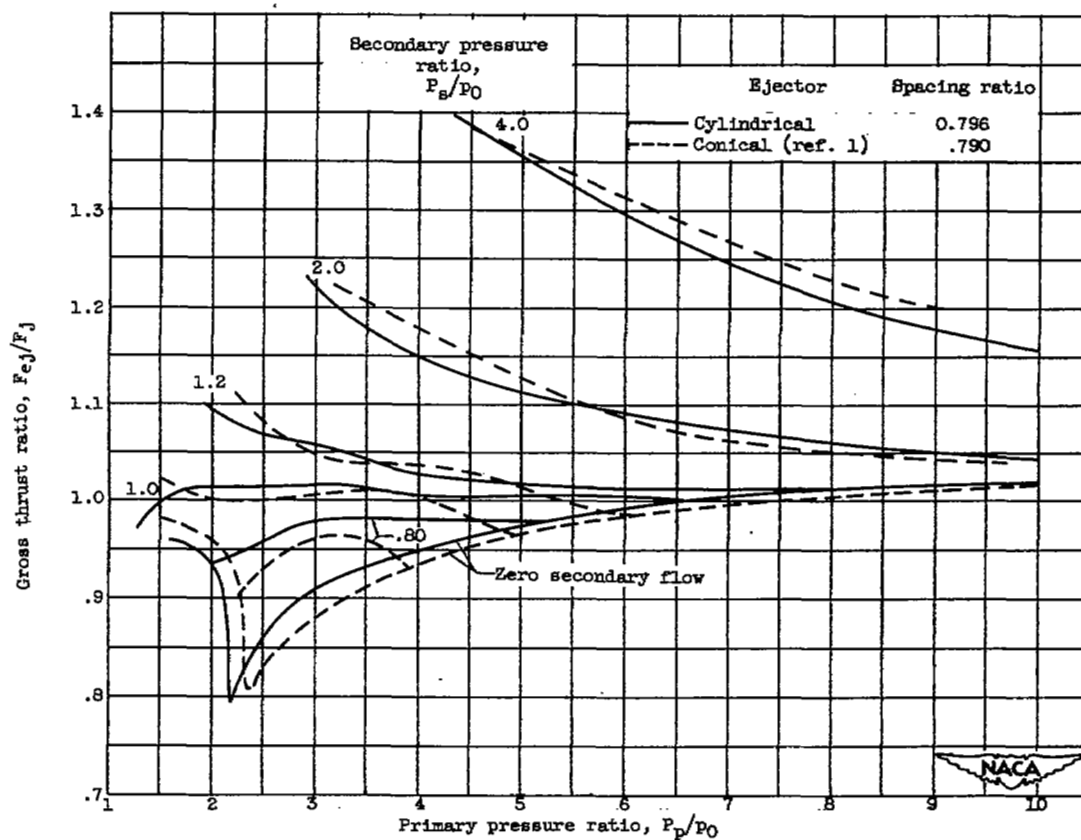
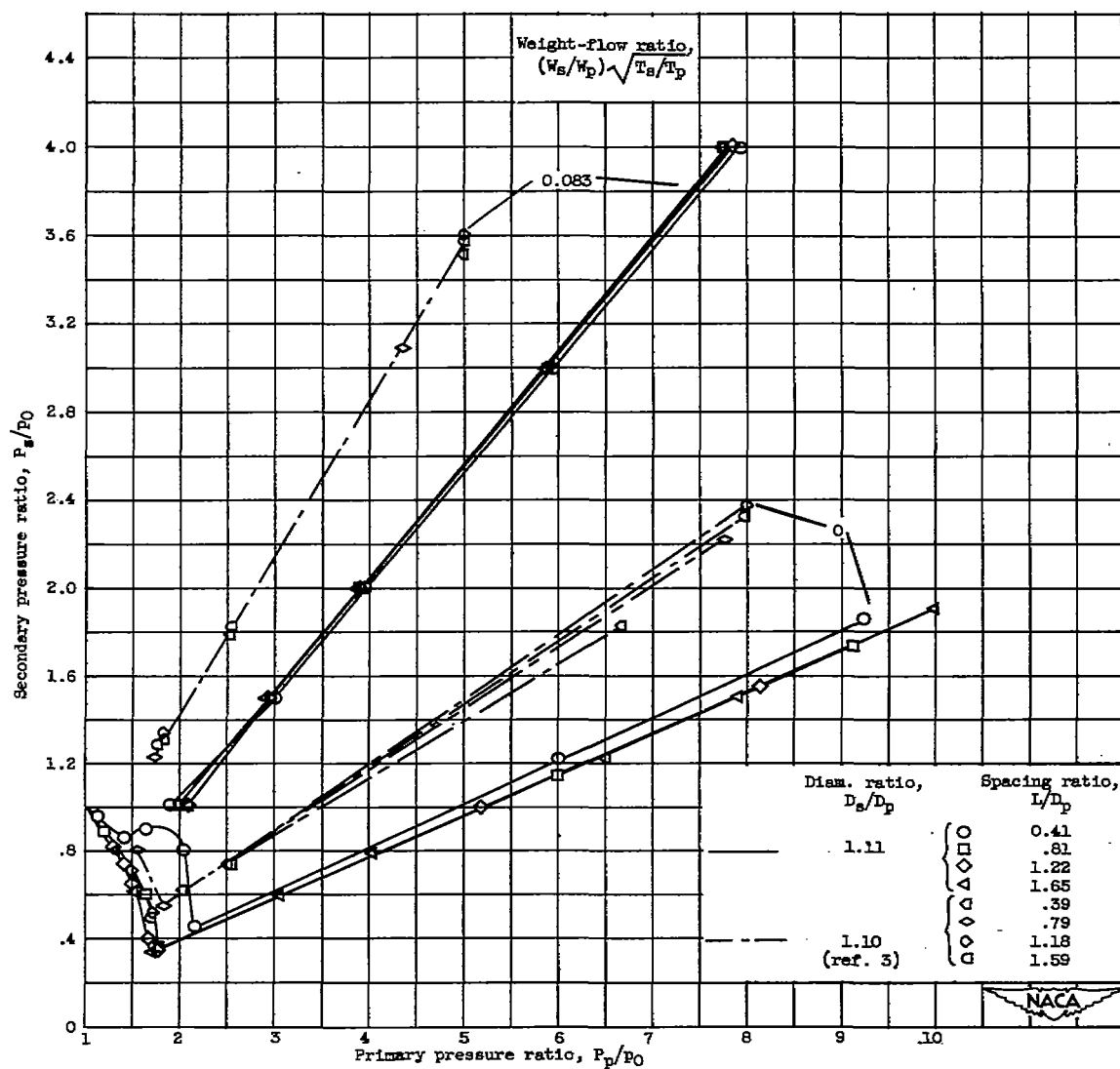


Figure 26. - Comparison of cylindrical and conical ejectors with diameter ratios of 1.21.



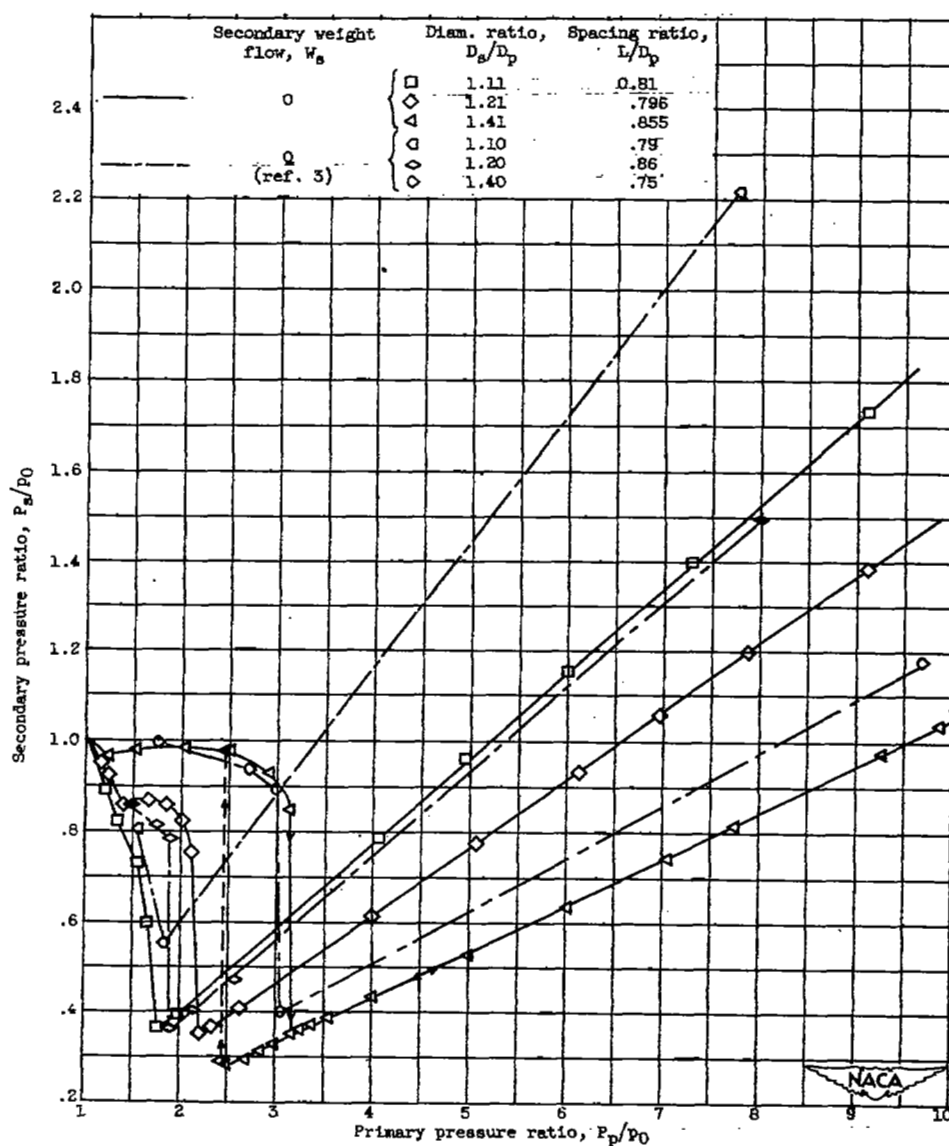
(b) Thrust characteristics.

Figure 26. - Concluded. Comparison of cylindrical and conical ejectors with diameter ratios of 1.21.



(a) Similar diameter ratios.

Figure 27. - Cylindrical-ejector data compared with data from reference 3.



(b) Similar spacing ratios; zero secondary-flow conditions.

Figure 27. - Concluded. Cylindrical-ejector data compared with data from reference 3.

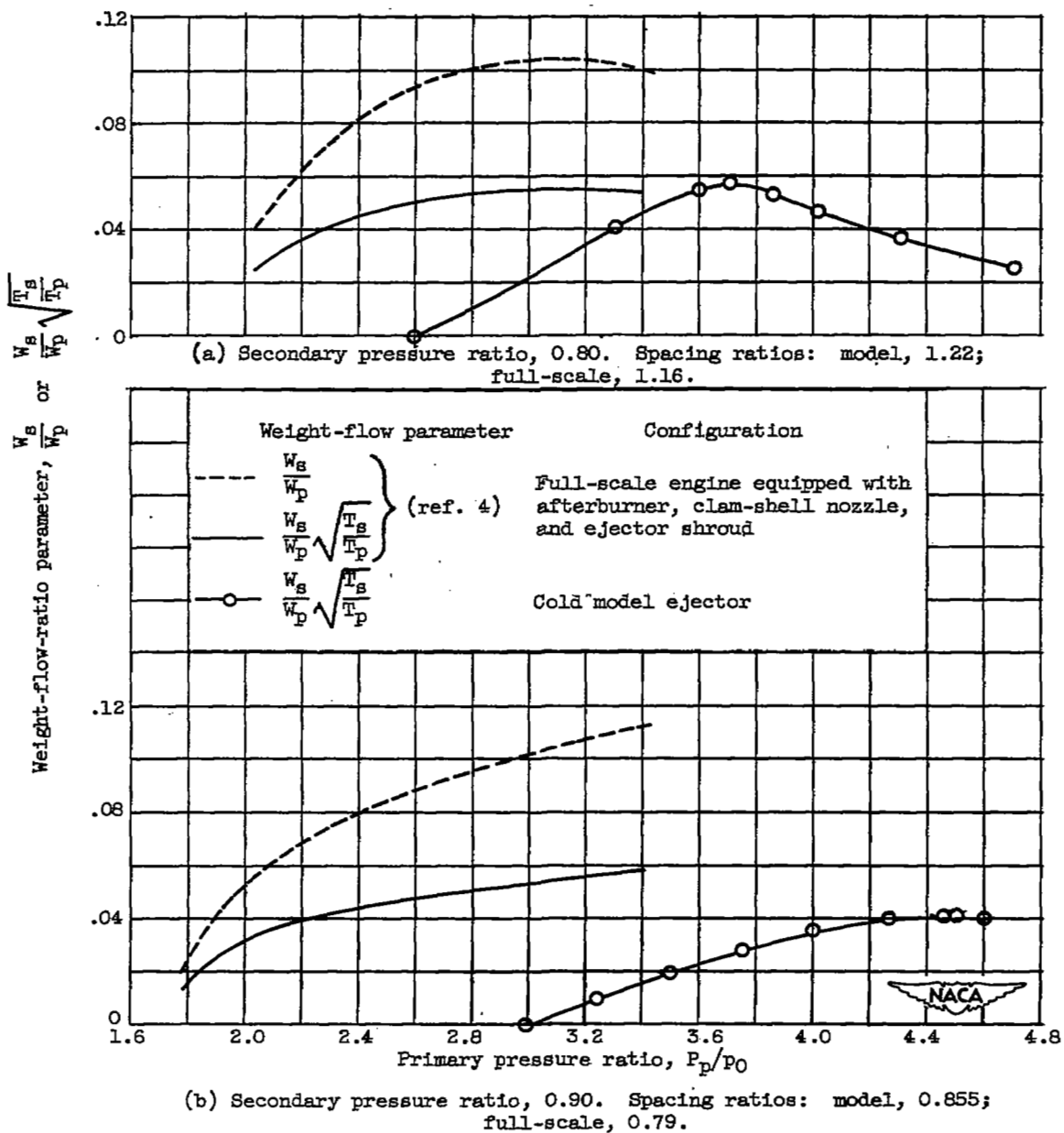
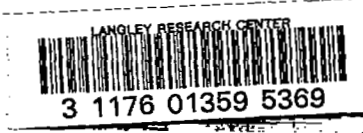


Figure 28. - Model cylindrical-ejector data compared with full-scale cylindrical-ejector data. Diameter ratios: model, 1.41; full-scale, 1.42.

SECURITY INFORMATION

~~CONFIDENTIAL~~



DO NOT REMOVE SLIP FROM MATERIAL	
Delete your name from this slip when returning material to the library.	
NAME	MS
Phillips	280
M. Lamb	280

~~CONFIDENTIAL~~